12-1-2010

Role of hypoxia-inducible factor-1 alpha in neural stem/progenitor cell function following hypoxia

Kate M. Candelario

Follow this and additional works at: https://digitalrepository.unm.edu/biom_etds
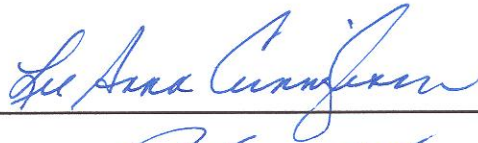
Kate M. Harms Candelario

Candidate

Biomedical Sciences

Department

This dissertation is approved, and it is acceptable in quality
and form for publication:
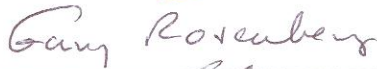
Approved by the Dissertation Committee:
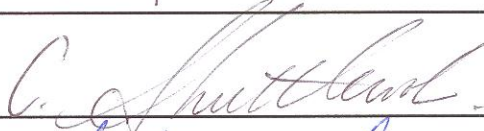
Lee Anna Cunningham, PhD,
Chairperson
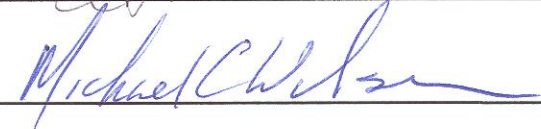
Paul McGuire, PhD

Gary Rosenberg, MD

C.W. Shuttleworth, PhD

Michael Wilson, PhD

**ROLE OF HYPOXIA-INDUCIBLE FACTOR-1 ALPHA
IN NEURAL STEM/PROGENITOR CELL FUNCTION
FOLLOWING HYPOXIA**

BY

KATE M. CANDELARIO

B.S. Neurobiology, Physiology, and Behavior

University of California, Davis, 2001

DISSERTATION

Submitted in Partial Fulfillment of the
Requirements for the Degree of

**Doctor of Philosophy
Biomedical Sciences**

The University of New Mexico
Albuquerque, New Mexico

December 2010

Acknowledgments

I would like to express my sincerest gratitude to the faculty, staff, and students of the Biomedical Sciences Graduate Program and the Department of Neurosciences. I am particularly grateful to my graduate advisor, Dr. Lee Anna Cunningham, for her help, support, and encouragement throughout my graduate career. I would like to thank the other members of my dissertation committee for their support of my project and helpful discussion regarding my dissertation: Dr. Bill Shuttleworth, Dr. Michael Wilson, Dr. Gary Rosenberg, and Dr. Paul McGuire. I would like to acknowledge the support of Buz Tyler and Mandara Devine for assistance regarding manuscript and grant submissions. I would like to thank the members of my lab for offering a supportive and fun place to work: Dr. Lu Li, Dr. Tamara Roitbak, Dr. Monica Wetzel, Dr. Erszi Kokovay-Cearley, Brit Ventura, Ashleigh Miele, Kelsey Thomas, Kenta Kajimoto, and Carrie Wright.

I would like to acknowledge my previous advisors who led me to become interested in a career in research, including Dr. Michael Croft, Dr. Jan Dvorak, and Dr. Jim Millam.

I would like to thank my family for their love and encouragement throughout my education and graduate career. I would like to thank my mother, Karen Fahrner, for her support of my interest in science, valuing my accomplishments, and for encouraging me to do what I love. I would like to thank my father, Leon Harms, for his support of my education and whose passion for math sparked mine. I would like to thank my sister, Alison Miller, for her friendship and moral support. I am grateful to my husband, Eduardo Candelario-Jalil, for his support, encouragement, enthusiasm, discussions, sacrifices, and understanding.

**ROLE OF HYPOXIA-INDUCIBLE FACTOR-1 ALPHA
IN NEURAL STEM/PROGENITOR CELL FUNCTION
FOLLOWING HYPOXIA**

BY

KATE M. CANDELARIO

ABSTRACT OF DISSERTATION

Submitted in Partial Fulfillment of the
Requirements for the Degree of

**Doctor of Philosophy
Biomedical Sciences**

The University of New Mexico
Albuquerque, New Mexico

December 2010

ROLE OF HYPOXIA-INDUCIBLE FACTOR 1-ALPHA IN NEURAL STEM/PROGENITOR CELL FUNCTION FOLLOWING HYPOXIA

by

Kate M. Candelario

B.S. Neurobiology, Physiology, and Behavior, University of California, Davis, 2001

Ph.D. Biomedical Sciences, University of New Mexico, 2010

ABSTRACT

Stroke can be caused by focal ischemia due to cerebral artery occlusion or by global ischemia that occurs when global blood supply to the brain is interrupted. The acute phase of ischemic brain injury is followed by a more prolonged period of revascularization and repair that can last for several months. One hallmark of this repair phase includes an endogenous neural stem/progenitor cell (NSPC) regenerative response that occurs concomitant with angiogenesis. Several studies suggest that the cytogenic response is beneficial for recovery following stroke, however, more studies need to be done to determine whether the beneficial effects are due to functional replacement of lost neurons and/or due to nutritive functions of the NSPCs for penumbral tissue.

Therapeutic targeting of regeneration and repair phases of stroke will require an understanding of NSPC function, particularly under conditions of hypoxia/ischemia.

This dissertation is focused on elucidating the metabolic properties of NSPCs that allow them to withstand sudden onset and prolonged hypoxia, and the mechanisms by which NSPCs may provide neuroprotection against ischemic damage. We found that NSPCs express stabilized hypoxia-inducible factor-1α (HIF-1α) under normoxic conditions, a transcription factor that has been shown to regulate a variety of genes including those involved in angiogenesis, neuroprotection, and glycolytic metabolism. In this dissertation, we show that, *in vitro*, HIF-1α expression in NSPCs mediates the ability of NSPCs to provide protection to neurons that undergo oxygen-glucose deprivation through regulation of vascular endothelial growth factor. We also show that HIF-1α is required for NSPCs to survive 24 h anoxia in culture. We determined that NSPCs appear to produce most of their ATP via glycolysis, although the metabolic phenotype of NSPCs under normoxic conditions does not appear to be regulated by HIF-1α. To determine whether NSPCs display similar properties *in vivo*, we created a *nestin*-CreER^{T2}/R26R-YFP/*Hif1a*$^{fl/fl}$ mouse that could simultaneously express yellow fluorescent protein and delete *Hif1a* specifically in nestin-positive NSPCs following tamoxifen administration. The results of these experiments increase our understanding of endogenous NSPC properties under hypoxic conditions and form the basis for future studies that aim to therapeutically manipulate NSPC function for facilitating brain repair.

Table of Contents

List of Figures

1. Introduction

1.1 Clinical impact of ischemic stroke

Stroke is the third cause of death and first cause of debilitation in first-world countries (Feigin et al., 2003). Approximately 80% of strokes are ischemic, rather than hemorrhagic, and cause a significant social burden(Feigin et al., 2003). Ischemic stroke results from a transient or permanent reduction of cerebral blood flow, usually caused by the occlusion of a major cerebral artery by local thrombosis (blood clot) or an embolus (free-moving blood clot) (Dirnagl et al., 1999). Blood carries the two main substrates required for energy production in the brain, oxygen and glucose. Glucose is metabolized for the production of the main cellular energy source, adenosine triphosphate (ATP), via glycolysis, alone or in combination with mitochondrial metabolism. Oxygen is required to produce ATP within the mitochondria, but not for ATP production via glycolysis.

Following artery occlusion, lack of blood flow to the surrounding tissue results in immediate acute injury followed by more prolonged inflammatory and repair processes that persist for months. At the core of the ischemic infarct, ATP depletion results in edema and death of endothelial and neuronal cells by necrosis (Krupinski et al., 1994; Dirnagl et al., 1999). In the penumbral region surrounding the infarct, neurons undergo programmed cell death (apoptosis). A few hours following stroke, the blood-brain barrier begins to break-down, microglial cells are activated, and astrocytes become reactive (Dirnagl et al., 1999). Within one to two days, the brain becomes infiltrated by blood-borne inflammatory cells including neutrophils, monocytes, and lymphocytes (Dirnagl et al., 1999; Moskowitz et al., 2010). Initial efforts by the brain to repair the vasculature and infarcted cortical tissue are seen approximately one week following the initial stroke

and can last for many months (Thored et al., 2007). Thus, ischemic stroke stimulates an evolving continuum of events that transition from acute injury to chronic phases of brain repair.

Therapeutic targets of ischemic stroke have been aimed at altering the endogenous injury and repair processes. However, numerous clinical trials targeting mechanisms of injury have failed to improve post-stroke outcome (Moskowitz et al., 2010). Currently, the only FDA-approved therapy to treat ischemic stroke is the use of a thrombolytic agent involved in the breakdown of blood clots, known as recombinant tissue plasminogen activator (tPA). However, less that 10% of patients receive tPA treatment due to a small therapeutic window (3 hours) and increased risk of hemorrhage if administered once the blood-brain barrier opens (Moskowitz et al., 2010). With limited treatment options, it is critical that researchers develop ways to extend the therapeutic window for ischemic stroke and improve post-stroke rehabilitation. Whether the endogenous repair processes can be therapeutically targeted remains to be determined.

To study post-stroke events in the laboratory, various models can be employed including the use of animals as well as cell culture. Ischemic stroke is modeled by occluding blood flow to the animal brain transiently, followed by reperfusion (reintroduction of blood flow). Focal cerebral ischemia can be induced in the mouse by occluding the middle cerebral artery (MCA) using a nylon filament. In culture, the effects of ischemia are modeled by transiently depriving cells of oxygen and glucose, the substrates carried by blood that are necessary for ATP production. Transient oxygen and glucose deprivation (OGD) is a well-characterized *in vitro* model that has been used to mimic ischemia-induced programmed cell death in neurons (Goldberg and Choi, 1993; Martin-Villalba et

al., 2001; Plesnila et al., 2001; Wetzel et al., 2008). The *in vitro* OGD cell culture model is useful to investigate isolated cellular responses to ischemic injury. In this dissertation, we employ both *in vivo* and *in vitro* models of ischemic stroke to study endogenous repair mechanisms, to specifically understand how murine neural stem/progenitor cells survive severe hypoxia as well as protect neurons. The overarching hypothesis of this dissertation is that hypoxia-inducible factor-1 alpha (HIF-1α) plays an essential role in the regulation of neural stem/progenitor cell function *in vitro* and *in vivo* under both normal and hypoxic conditions.

1.2 Adult Neural Stem/Progenitor Cells

1.2.1 Stem cell definition

The term "stem cell" refers to phenotypically uncommitted cells with the ability to self-renew and give rise to specialized cells that make up the tissues and organs of the body. These uncommitted cells can undergo asymmetric cell division to give rise to a new stem cell and a cell of more restricted lineage fate. Stem cells can be isolated from embryos (embryonic stem cells; ESCs), adult organs (adult stem cells), and can be artificially induced from fully differentiated cell types through genetic manipulation (induced pluripotent stem cells; iPSCs). Stem cells represent key research tools for understanding embryonic development and mechanisms of disease. In addition, stem cells have a wide array of potential therapeutic applications for functional replacement of differentiated cells that are lost to injury or disease (e.g., diabetes, cardiovascular disease, neurodegeneration). Thus, unraveling the mysteries of stem cell biology is important for advancing basic medical science and for therapeutic applications in regenerative medicine.

1.2.2 Neural stem/progenitor cells in the adult brain

The adult mammalian brain harbors two germinal centers in which neural stem/progenitor cells reside and give rise to new neurons and glia throughout adulthood. These include the subgranular zone (SGZ) of the dentate gyrus of the hippocampus, which gives rise to new dentate granule neurons, and the subventricular zone (SVZ) surrounding the lateral ventricles, which gives rise to new neurons within the adult olfactory bulb (Eriksson et al., 1998; Gage, 2000; Doetsch, 2003a; Alvarez-Buylla and Lim, 2004). The production of new neurons throughout adulthood is conserved across many species including human (Eriksson et al., 1998; Macas et al., 2006; Curtis et al., 2007). Neural stem/progenitor cells that reside in the germinal centers of the adult brain are self-renewing, multipotent cells that give rise to neuronal, astrocyte and oligodendrocyte lineages (Martino and Pluchino, 2006).

The terminology defining mitotically active multipotent cells in the adult brain has been argued. Many investigators refer to these cells collectively as neural stem cells, recognizing that they are restricted to a CNS phenotype yet acknowledging their self-renewal and multipotentiality. Other investigators prefer the term neural stem/progenitor cell to indicate their restriction to neural cell fates. Throughout this dissertation, we utilize the term neural stem/progenitor cells (NSPCs) to define this population.

1.2.3 SVZ and Adult Olfactory Neurogenesis

Within the SVZ, radial glial-derived astrocytic stem cells are termed type B cells. These cells are slowly proliferating cells, but give rise to rapidly dividing transient amplifying progenitor cells (type C cells). Transient amplifying progenitors within the SVZ have the potential to give rise to both neurons and glial cell types. *In vivo*, under non-pathological

4

conditions, most stem cells give rise to doublecortin (Dcx)-positive migrating neuroblasts which form a rostral migratory stream to the olfactory bulb to become mature interneurons that integrate into the olfactory bulb circuitry (Riquelme et al., 2008) (Figure 1.1).
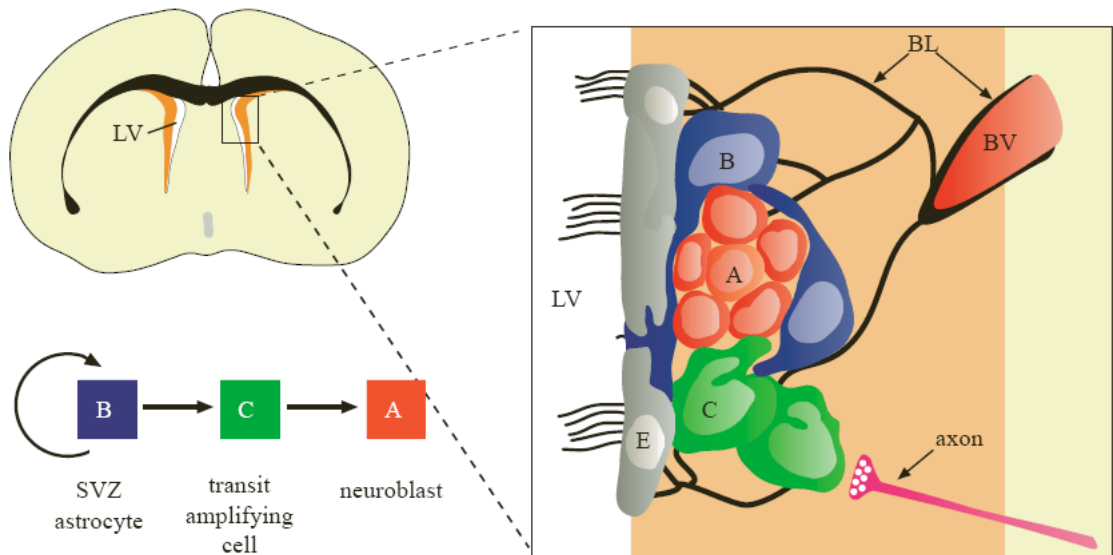
Figure 1.1: Cytoarchitecture of the subventricular zone (SVZ). The adult mouse SVZ is located adjacent to the lateral ventricle (LV). Type B cells (SVZ astrocytes) divide slowly and have the ability to divide symmetrically to give rise to another stem cell, or divide asymmetrically to give rise to Type C transient amplifying progenitor cells. Type A doublecortin-positive neuroblasts differentiate from Type C cells. The wall of the lateral ventricle is lined with ependymal cells (E) that directly contact SVZ progenitors. Blood vessels (BV) and basal lamina (BL) also directly contact the cells of the SVZ. Figure adapted from(Riquelme et al., 2008).

1.2.4 SGZ and Hippocampal Neurogenesis

In addition to the SVZ, radial glial-like neural stem cells also persist within the adult SGZ. The cytoarchitecture of the SGZ differs from that of the SVZ. Within the SGZ, radial glial-derived stem cells give rise to transient amplifying progenitor cells that migrate only a short distance into the granule cell layer of the dentate gyrus, where they

give rise to newborn dentate granule neurons (Figure 1.2). Adult hippocampal neurogenesis is thought to be important for learning and memory processes, since ablation of adult hippocampal neurogenesis attenuates spatial learning, whereas stimulation of hippocampal neurogenesis improves learning ability (Zhao et al., 2008). Radial glial-like stem cells within the SVZ and SGZ express the glial marker, glial fibrillary acidic protein (GFAP) as well as the stem cell markers nestin and prominin.
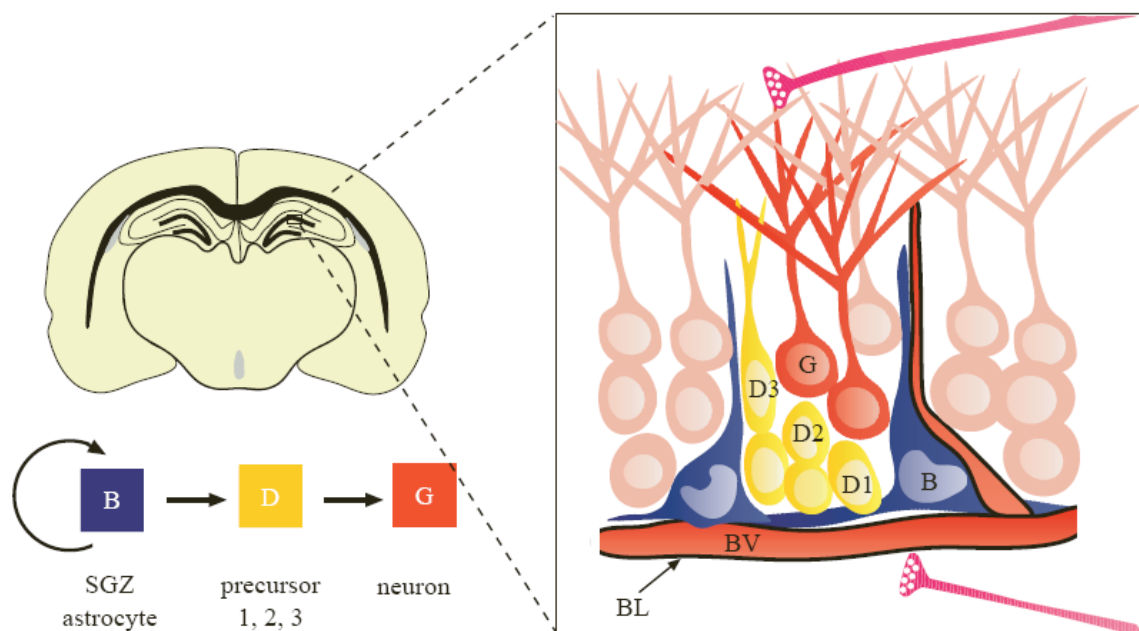
Figure 1.2: Cytoarchitecture of the subgranular zone (SGZ). In the adult mouse brain, type B SGZ astrocytes proliferate and give rise to intermediate precursors which progressively generate more differentiated progeny (D1, D2, D3) including immature neurons. Immature neurons migrate a short distance into the granule cell layer of the dentate gyrus, where mature granule neurons (G) integrate into the circuitry of the dentate gyrus through extension of dendrites into the molecular layer and an axon along the mossy fiber pathway. Blood vessels (BV) and basal lamina (BL) directly contact the cells of the SGZ. Figure adapted from (Riquelme et al., 2008).

<u>1.2.5 NSPC lineage fate</u>

In the adult brain, neural stem/progenitor cells give rise primarily to neurons (neurogenesis) under non-pathological conditions, but can also give rise to a small number of astrocytes and oligodendrocytes (gliogenesis). Injury, expansion in culture, or transplantation of NSPCs into non-neurogenic regions (outside the SVZ or SGZ) results in a predominant gliogenic differentiation fate (Herrera et al., 1999; Li et al., 2010). Lineage fate is most-likely determined by extrinsic factors within the local environment, such as growth factors and cytokines (Kokovay et al., 2008). Interestingly, transplantation of stem cells from spinal cord, a non-neurogenic region, into the hippocampus generates neurons (Shihabuddin et al., 2000). That some regions of the brain promote neuronal *vs.* glial differentiation suggests that the stem cell microenvironment determines lineage fate. Differences in lineage fate of the injured brain may contribute to repair processes.

1.3 Neural stem/progenitor cell (NSPC) response to stroke

NSPCs within the SVZ and SGZ mount regenerative responses following many types of metabolic and traumatic brain injuries, making them an attractive therapeutic target for promoting structural and functional brain repair. Stroke-induced neurogenesis was first described following transient global cerebral ischemia in gerbils, which stimulated increased neurogenesis in the dentate gyrus (Liu et al., 1998). Later studies demonstrated that focal cerebral ischemia induced by middle cerebral artery occlusion (MCAO) in rats stimulated ectopic migration of hundreds of thousands of neuroblasts from the SVZ into the ischemic striatum (Arvidsson et al., 2002). MCAO has been shown to reduce the

partial pressure of oxygen in the SVZ to below 1.4%, yet cells in this region survive this hypoxic event and mount a proliferative and migratory response (Thored et al., 2007). The SVZ cytogenic response to focal ischemia is delayed and of long duration, such that peak proliferation in the SVZ occurs 7 days following MCAO, and migration out to the lesion continues for up to one year in rodents (Zhang et al., 2004; Thored et al., 2007). Our laboratory has recently demonstrated that the SVZ response to stroke encompasses multilineage cytogenesis whereby SVZ NSPCs generate new oligodendrocyte progenitors, astrocytes, and neuroblasts (Li et al., 2010) (and Appendix).

The endogenous SVZ cytogenic response may be important for structural and functional recovery following stroke. In rodents, spontaneous improvements in behavioral deficits and cognitive function following focal ischemia are temporally correlated with the onset of neurogenesis (Kondziolka et al., 2000; Zhang et al., 2003b). Maysami and colleagues demonstrated that depletion of NSPCs by mitotic inhibition (using methylazoxymethanol; MAM), or by inducible depletion of GFAP+ NSPCs (using ganciclovir in GFAP/HSV-TK mice), significantly attenuated ischemic tolerance, suggesting a role for endogenous progenitors in the protective effect of ischemic tolerance (Maysami et al., 2008). More recently, Jin and colleagues demonstrated that depletion of migrating neuroblasts in ganciclovir-treated Dcx/HSV-TK mice results in exacerbated motor deficits and expansion of infarct size (Jin et al., 2010a).

Much evidence suggests a functional link between the SVZ regenerative response and angiogenesis that occurs during the repair phase of stroke injury. Following MCAO and bilateral common carotid artery occlusion, reactive astrocytes and blood vessels appear to provide the physical substrate for neuroblast migration (Ohab et al., 2006; Yamashita et

al., 2006). Endothelial cells have been shown to produce factors that promote neural stem/progenitor cell proliferation, neuroblast migration, and neuronal differentiation (Shen et al., 2004). These include brain derived neurotrophic factor (BDNF) (Leventhal et al., 1999), stromal-derived factor 1 (SDF-1) (Kokovay et al., 2010), and angiopoietin 1 (Ang1) (Ohab et al., 2006), and other as yet undefined factors. Thus, angiogenesis and neurogenesis appear to be inextricably linked, and this has led to the concept of a "neurovascular niche" important for maintaining neural stem cell function under both normal physiological and pathological conditions.

While rodent models of stroke allow researchers to study the mechanisms involved in pathological processes, it is important to understand if these models translate to human disease. To study the cytogenic response in post-mortem tissue, antibodies can be utilized that are directed against proteins known to be expressed in neural stem/progenitor cells and their progeny. To study proliferation, the marker Ki67 can be used to detect all active phases of the cell cycle. Because NSPCs proliferate in response to injury, and most other cells in the brain are post-mitotic, Ki67 is a popular marker to study the NSPC response to stroke. Antibodies can also be used to determine lineage fate (Figure 1.3), including a marker for immature neuronal committed progenitors known as polysialylated neural cell adhesion molecule (PSA-NCAM), as well as the immature neuronal marker neuron-specific class III beta-tubulin (Tuj1).
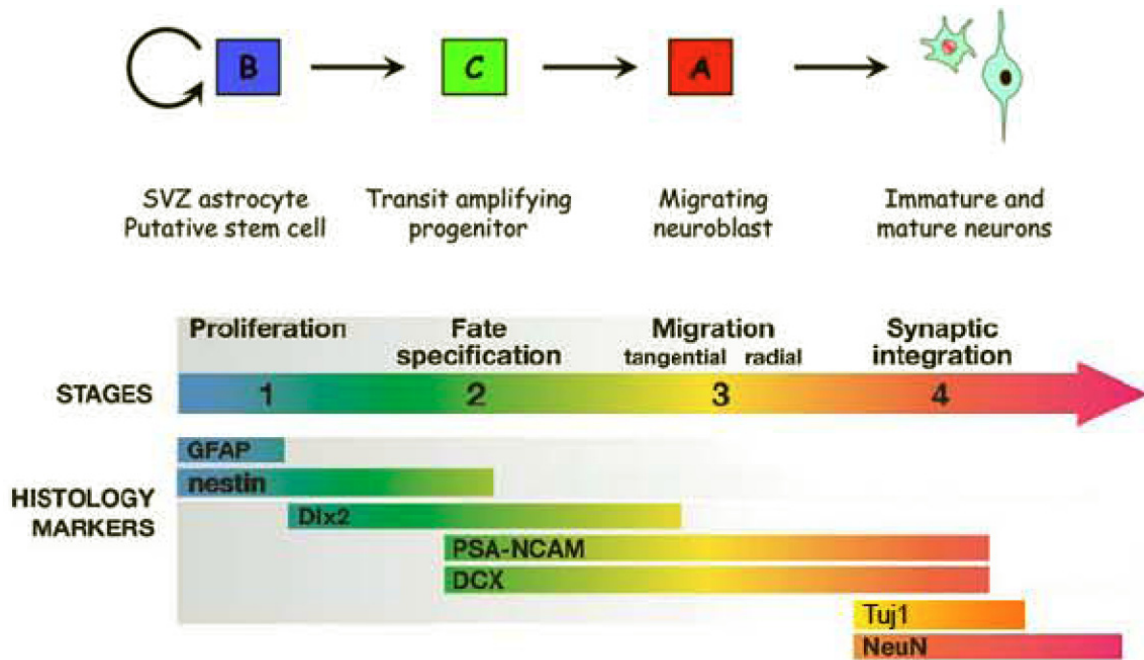
Figure 1.3: Markers used to identify cell types in the SVZ. SVZ astrocytic stem cells (Type B cells) express the markers GFAP and nestin. Nestin expression is retained in transient amplifying progenitor cells (Type C cells), which also express Dlx2. Migrating Type A neuroblasts express PSA-NCAM and Dcx, markers which are retained into immature neurons. Immature neurons express Tuj1 and mature neurons express NeuN. Each of these markers can detected using antibodies against these proteins. Adapted from (Ming and Song, 2005) and(Abrous et al., 2005).

To investigate whether humans exhibit an NSPC response to stroke, Jin and colleagues compared Ki67 staining of post-mortem tissue from the cerebral cortices of stroke patients versus patients who died without brain pathology. They reported increased Ki67-immunoreactive cells in the tissue of stroke patients (Jin et al., 2006). Later that year, Macas and colleagues reported that following stroke, patients exhibited increased Ki67-immunoreactive cells in the ipsilateral SVZ, as well as increased PSA-NCAM, near the walls of the lateral ventricle (Macas et al., 2006). Recently, Marti-Fabregas and colleagues confirmed increased Ki67-immunoreactive cells, and also discovered an

increase in the number of Tuj1- or PSA-NCAM-positive cells, in the ipsilateral SVZ following stroke (Marti-Fabregas et al.). Therefore, there is evidence of a neurogenic response to stroke in humans. Understanding the role of the endogenous NSPC response to stroke is important for understanding brain repair mechanisms. Ultimately, NSPC survival and directed lineage fate may be important therapeutic goals to improve recovery from brain injury in humans (Zhang et al., 2005; Lichtenwalner and Parent, 2006; Taupin, 2006).

1.4 Hypoxia-inducible factor-1α (HIF-1α)

Our interest in the mechanisms that support NSPC survival and replenishment of damaged cells within the ischemic brain led us to explore the role of hypoxia-inducible factor-1α (HIF-1α). HIF-1α is a well-known mediator of adaptive cellular responses to hypoxia through direct transcriptional regulation of cellular metabolism (Semenza, 2010b). Evidence also points to a novel role of HIF-1α in maintainance of the neural stem/progenitor cell phenotype (Gustafsson et al., 2005).

HIF-1α is most widely recognized for its role in the adaptive response to hypoxia through transcriptional regulation of metabolism. In most cell types, the level of HIF-1α is post-translationally regulated in an oxygen-dependent manner. Under normoxic conditions, prolyl hydroxylase domains (PHD) use molecular oxygen (O_2), 2-oxoglutarate, and iron (II) to drive hydroxylation of proline residues on HIF-1α protein, as well as the production of carbon dioxide (CO_2) and succinate(Freeman et al., 2003). HIF-1α protein is constitutively produced, but has a cellular half-life of less than 5 minutes due to
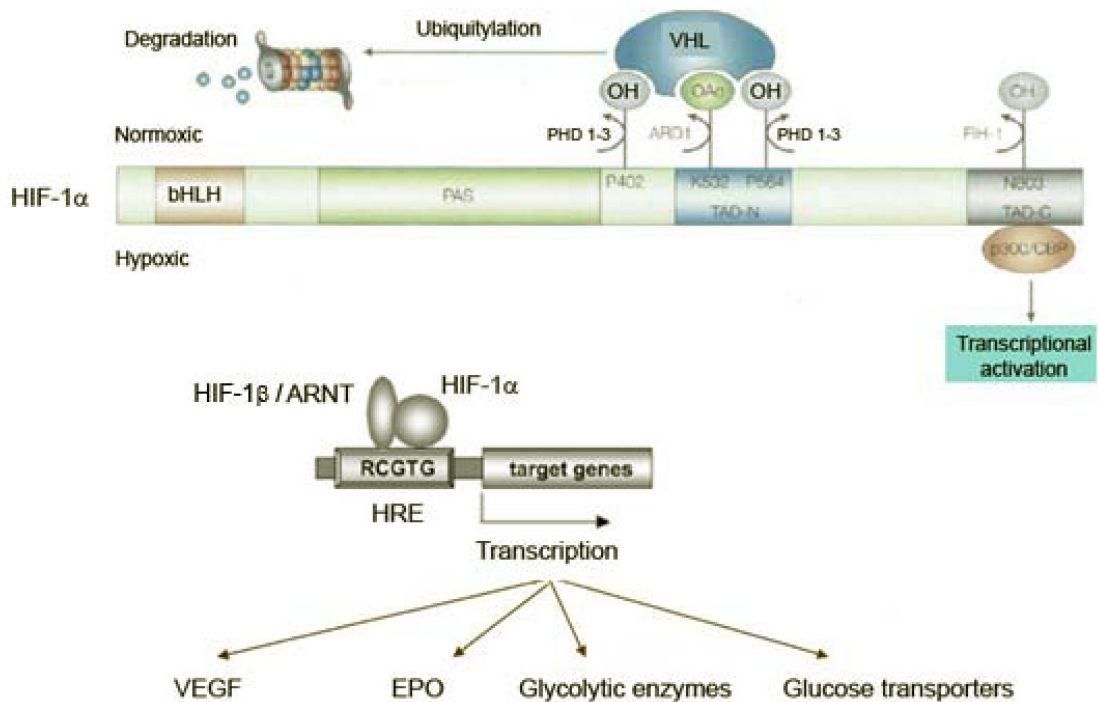
Figure 1.4: Stabilization and transcriptional targets of HIF-1α. HIF-1α is targeted for proteasomal degradation under normoxic conditions. Under hypoxia, HIF-1α is stabilized due to decreased prolyl hydroxylase domain (PHD) activity and can enter the nucleus to interact with HIF-1β/ARNT and drive transcription of target genes. Examples of HIF-1α regulated genes include vascular endothelial growth factor (VEGF), erythropoietin (EPO), glycolytic enzymes, and glucose transporters. Figure adapted from the following publications: (Sharp et al., 2000; Semenza, 2003; Yeo et al., 2004).

rapid proteosomal degradation promoted by prolyl hydroxylation and association with the

von Hippel Lindau protein (VHL) (Semenza, 2003; Weidemann and Johnson, 2008).

Under conditions of hypoxia, prolyl hydroxylase activity decreases and unhydroxylated

HIF-1α rapidly accumulates within the nucleus. There, HIF-1α dimerizes with the

oxygen-independent HIF-1β subunit (ARNT [aryl hydrocarbon receptor nuclear

translocator]), forming the HIF-1 transcriptional complex that regulates target genes

through cis-acting hypoxia response elements (HREs) (Semenza, 2003). Well-known

HIF-1 target genes include those that promote glycolysis and angiogenesis (Figure 1.4) (Yeo et al., 2004).

1.4.1 HIF-1α-regulated genes

In cancer cells, HIF-1α has been shown to regulate the transcription of hundreds of target genes, including those involved in angiogenesis, growth factor signaling, glucose and energy metabolism, metastasis, and stem cell maintenance (Semenza, 2010a). HIF-1α has been well-characterized in cancer models due to its expression under hypoxia and its influence on tumor vascularization.

1.4.1.1 HIF-1α regulation of angiogenesis and neurogenesis

HIF-1α was first described for its ability to mediate transcription of hypoxia-inducible erythropoietin (EPO) (Semenza and Wang, 1992). At the time, EPO was known as a glycoprotein hormone with the ability to stimulate erythrocyte production resulting in increased oxygen delivery to hypoxic tissue. Later, HIF-1α was described to regulate the transcription of the angiogenic protein vascular endothelial growth factor (VEGF) (Forsythe et al., 1996). In addition to their classical roles, current research reveals that both EPO and VEGF promote neurogenesis and act as neuroprotective factors (Ferriero, 2005).

1.4.1.2 HIF-1α regulation of cellular metabolism

Hypoxic cells, including cancer cells, shift their metabolism from mitochondrial respiration to glycolysis within the cytosol. This shift results in glycolytic production of ATP, the main cellular energy source. HIF-1α has been shown to regulate this shift from

oxidative phosphorylation in the mitochondria to substrate-level phosphorylation in the cytosol (Seagroves et al., 2001) and activate the transcription of genes that encode the glucose transporters GLUT1 and GLUT3, as well as all of the enzymes involved in glycolysis (Iyer et al., 1998; Seagroves et al., 2001; Lum et al., 2007; Semenza, 2010b). Pyruvate, a product of glycolysis, can either be converted by the enzyme lactate dehydrogenase A (LDHA) to lactate, or converted by pyruvate dehydrogenase (PDH) to acetyl coenzyme A for entry into the tricarboxylic acid (TCA) cycle (Citric acid/Krebs cycle). Conversion of pyruvate into lactate yields NAD^+, which reenters glycolyis at the level of glyceraldehyde-3-phosphate. HIF-1α upregulates the transcription of LDHA, and lactate can be transported out of the cell by monocarboxylate transporter 4 (MCT4), which is also transcriptionally upregulated by HIF-1α (Semenza, 2010b). In addition, HIF-1α transcriptionally upregulates pyruvate dehydrogenase kinase 1 (PDK1), which phosphorylates and inactivates PDH. Inactivation of PDH shunts pyruvate away from the mitochondria (Kim et al., 2006; Papandreou et al., 2006). Thus, HIF-1α has been shown in cancer cells to essentially promote glycolysis and suppress mitochondrial respiration.

HIF-1α activity itself can be regulated by metabolic products and enzymes. For example, loss-of-function of the TCA cycle enzymes succinate dehydrogenase, fumarate hydratase, or isocitrate dehydrogenase alter the levels of the substrates succinate, fumarate, and α-ketoglutarate, respectively (Semenza, 2010b), which impair hydroxylation of HIF-1α and stabilize it even under normoxic conditions. In addition, elevated levels of pyruvate and lactate have been shown to inactivate prolyl hydroxylase domains resulting in

stabilization of HIF-1α under normoxia, establishing a feed-forward mechanism for HIF-1α stabilization (McFate et al., 2008).

1.4.1.3   HIF-1α regulation of NSPC differentiation

Hypoxia has been shown to promote the survival and proliferation of NSPCs grown in culture (Morrison et al., 2000; Studer et al., 2000; Burgers et al., 2008; Santilli et al., 2010), as well as other stem cell types (Gustafsson et al., 2005).   In addition, hypoxia prevents the ability of neural stem cells to differentiate, an effect mediated by Notch signaling (Gustafsson et al., 2005).   Activation of a Notch receptor (Notch 1-4) by one of its ligands (Delta, Serrate, Lag-2) liberates the Notch intracellular domain (Notch ICD) which translocates to the nucleus and interacts with the DNA binding protein C-promoter-binding-factor (CSL).   HIF-1α acts in a non-canonical fashion by binding to the Notch ICD and promotes transcription of genes that regulate the undifferentiated phenotype, including Hes and Hey (Simon and Keith, 2008).

In other cell types, hypoxia has also been shown to disrupt Wnt/β-catenin signaling.   Wnt ligands are secreted glycoproteins that signal through Frizzled receptors to prevent proteosomal degradation of intracellular β-catenin.   Stabilized β-catenin translocates to the nucleus and interacts with transcription factors (Tcf/Lef) to drive transcription of Wnt target genes (Toledo et al., 2008).   Signaling through Wnt/β-catenin is required for hippocampal neurogenesis (Lie et al., 2005) and stimulates NSPC differentiation toward the neuronal lineage by upregulating the proneural transcription factor NeuroD1 (Kuwabara et al., 2009).   In non-neuronal cells, HIF-1α binds to β-catenin, thereby inhibiting its transcriptional activity (Kaidi et al., 2007).

1.5 Use of *Nestin*-CreER^{T2} mice for NSPC-specific *Hif1a* gene deletion

Systemic deletion of the *Hif1a* gene is embryonic lethal, associated with malformation of the heart and cardiovascular system (Iyer et al., 1998). Conditional deletion of *Hif1a* within nestin-positive stem cells of the developing nervous system results in hydrocephalus, massive neuronal apoptosis, and regression of vasculature (Tomita et al., 2003). Therefore, we have utilized a tamoxifen-inducible Cre/*lox*P approach to selectively knockout *Hif1a* gene expression in adult NSPCs within the context of the adult brain. The use of the tamoxifen-inducible Cre/*lox*P system is a powerful approach for studying NSPC-specific gene deletion or activation in cerebral ischemia (Battiste et al., 2007; Burns et al., 2007). In this system, transgenic mice are generated that express Cre recombinase fused with a tamoxifen-specific binding domain of a mutated estrogen receptor (Cre-ER^{T2}) (Hayashi and McMahon, 2002). Expression of the recombinase is controlled by the nestin transcriptional promoter (Battiste et al., 2007; Lagace et al., 2007). Cre recombinase is an enzyme from the P1 bacteriophage that acts in mammalian cells to catalyze site-specific recombination between two of its 34-base pair recognition elements, the *lox*P sites (Rossant and Nagy, 1995). This allows for precise excision of an intervening sequence to functionally and conditionally activate or remove a gene of interest (Nagy, 2000). The mutated estrogen receptor ligand binding domain, ER^{T2}, does not bind 17β-estradiol at physiological concentrations, but is activated by the tamoxifen metabolite 4-hydroxy (OH)-tamoxifen (TM). In the absence of tamoxifen, the Cre-ER^{T2} fusion protein is sequestered in the cytoplasm by Hsp90 binding to the estrogen receptor domain, thereby preventing the movement of Cre recombinase into the nucleus and Cre-mediated excision of *lox*P DNA sequences. Binding of 4-OH-TM leads to a disruption of

the interaction with Hsp90, permitting access of Cre-ER^{T2} to the nucleus and initiation of recombination (Figure 1.5).

NESTIN-CRE-TAMOXIFEN TRANSGENIC MICE
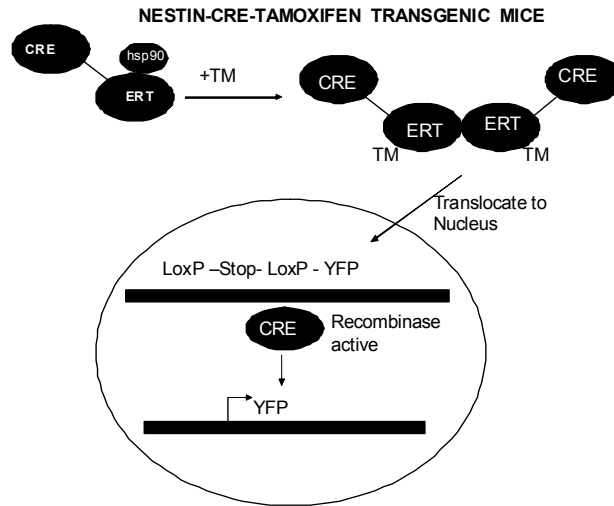
Figure 1.5: Diagram depicting tamoxifen-mediated entry of Cre recombinase into the nucleus, followed by DNA recombination and subsequent YFP expression.

Nestin-CreER^{T2} mice have been generated in which transgene expression is driven by the nestin promoter to restrict Cre-ER^{T2} expression to nestin-positive stem cell populations, providing both spatial and temporal control of recombinase activity, such that expression of Cre recombinase is restricted to nestin-positive cells and is activated only in the presence of tamoxifen. *Nestin*-CreER^{T2} mice were generated using 5.8kB of the nestin promoter and exons 1-3, including the 2nd intronic enhancer, which confers neural-specific expression, and not endothelial or pericyte expression (Lagace et al., 2007). These mice have been crossed with the Rosa Cre-reporter mice, R26R-YFP, to generate bitransgenic *nestin*-Cre-ER^{T2}/R26R-YFP mice (Lagace et al., 2007). The R26R-YFP allele contains a transcriptional 'stop' sequence flanked by 2 *lox*P sites (floxed) that

intervenes between a constitutive transcriptional promoter and the YFP reporter sequence, thereby preventing YFP reporter expression except in cells that harbor activated cre-recombinase. Exposure of *nestin*-CreER^{T2}/R26R-YFP mice to tamoxifen activates Cre recombinase in nestin-positive cells, resulting in excision of the transcriptional 'stop' sequence and transcriptional activation of YFP reporter gene expression in nestin-positive NSPCs and all subsequent progeny. As described in Chapter 4 of this dissertation, we crossed this strain with mice that have floxed *Hif1a* alleles, to generate *nestin*-Cre-ER^{T2}/R26R-YFP/*Hif1a*$^{fl/fl}$ triple transgenic mice in which tamoxifen concomitantly activates YFP reporter expression and bi-allelic *Hif1a* gene deletion in NSPCs of embryonic and postnatal brain.

1.6 Hypothesis and Specific Aims

Our laboratory is interested in the ability of NSPCs to survive sudden-onset hypoxia as well as their contribution to repair processes following stroke (e.g. revascularization, neuroprotection, and regeneration). The ongoing, long term goal of this research is to elucidate molecular mechanisms that regulate NSPC survival and function under ischemic conditions. For these studies, we isolated NSPCs from both embryonic and postnatal brain, expanded them in culture and studied their responses to ischemic models *ex vivo*. **The overarching hypothesis of this dissertation is that hypoxia-inducible factor-1 alpha (HIF-1α) represents an intrinsic regulator of NSPC-mediated neuroprotection, metabolism and survival during ischemic stress.** We addressed this hypothesis by completing the following Specific Aims.

Specific Aim 1: To characterize the neuroprotective effects of NSPCs against hypoxic injury. For these studies we investigated the ability of NSPCs to promote neuronal survival under conditions of oxygen-glucose deprivation (OGD) in culture. We found that NSPCs prevented cell death of cortical neurons in response to OGD, via HIF-1α-regulated release of vascular endothelial growth factor (VEGF). *Chapter 2: Harms KM, Li L, Cunningham LA. 2010. Murine neural stem/progenitor cells protect neurons against ischemia by HIF-1α-regulated VEGF signaling. PLoS ONE. 5:e9767.*

Specific Aim 2: To elucidate the metabolic phenotype of NSPCs, and determine whether HIF-1α regulates NSPC metabolism under normal and/or hypoxic conditions. We utilized NSPCs from embryonic and adult mouse to determine the relative dependence on glycolytic *vs.* oxidative metabolism for survival. These studies demonstrated that NSPCs are primarily glycolytic and display minimal dependence on mitochondrial oxidative phosphorylation. *Hif1a* gene deletion impaired the ability of NSPCs to survive hypoxia, but did not increase the sensitivity of NSPCs to mitochondrial toxins under normoxic conditions or reduce dependence on glycolytic metabolism. *Chapter 3: Candelario KM, Shuttleworth CW, Cunningham LA. Neural stem/progenitor cells display a glycolytic metabolic phenotype under normoxia. In preparation for J. Neurochemistry.* This work is also described in **Chapter 4.**

Specific Aim 3: To establish an *in vivo* model of targeted *Hif1a* gene deletion using *nestin*-CreER^{T2}/R26R-YFP/*Hif1a*$^{fl/fl}$ mice. We have established a triple transgenic mouse colony, designated *nestin*-CreER^{T2}/R26R-YFP/*Hif1a*$^{fl/fl}$, in which tamoxifen administration results in concomitant activation of YFP expression and *Hif1a* gene

19

deletion. For these studies, we also established methods to characterize YFP expression and *Hif1a* gene deletion in isolated NSPCs. This work is described in ***Chapter 4. This work also contributed to a recent paper Li L, Harms KM, Ventura PB, Lagace DC, Eisch AJ, Cunningham LA. 2010. Focal cerebral ischemia induces a multilineage cytogenic response from adult subventricular zone that is predominantly gliogenic. Glia 58:1610-1619.***

2. Murine Neural Stem/Progenitor Cells Protect Neurons against Ischemia by HIF-1α-Regulated VEGF Signaling

Kate M. Harms, Lu Li, and Lee Anna Cunningham

Department of Neurosciences

University of New Mexico Health Sciences Center

Albuquerque, New Mexico 87131

2.1 Abstract

Focal cerebral ischemia following middle cerebral artery occlusion (MCAO) stimulates a robust cytogenic response from the adult subventricular zone (SVZ) that includes massive proliferation of neural stem/progenitor cells (NSPCs) and cellular migration into the injury area. To begin to explore beneficial roles of NSPCs in this response, we investigated the ability of embryonic and postnatal NSPCs to promote neuronal survival under conditions of *in vivo* and *in vitro* ischemia. Intracerebral transplantation of NSPCs attenuated neuronal apoptosis in response to focal ischemia induced by transient MCAO, and prevented neuronal cell death of cortical neurons in response to oxygen-glucose deprivation (OGD) in culture. NSPC-mediated neuroprotection was blocked by the pharmacological inhibitors of vascular endothelial growth factor (VEGF), SU1498 and Flt-1Fc. Embryonic and postnatal NSPCs were both intrinsically resistant to brief OGD exposure, and constitutively expressed both hypoxia-inducible factor 1α (HIF-1α) transcription factor and its downstream target, VEGF. Genomic deletion of *Hif1a* by Cre-mediated excision of exon 2 in NSPC cultures resulted in >50% reduction of VEGF production and ablation of NSPC-mediated neuroprotection. These findings indicate that NSPCs promote neuronal survival under ischemic conditions via HIF-1α-VEGF signaling pathways and support a role for NSPCs in promotion of neuronal survival following stroke.

2.2 Introduction

Two predominant neurogenic regions persist within the adult mammalian brain, located within the subgranular zone (SGZ) of the hippocampal dentate gyrus and the subventricular zone (SVZ) surrounding the lateral ventricles (Eriksson et al., 1998; Gage, 2000; Doetsch, 2003a; Alvarez-Buylla and Lim, 2004). Neural stem/progenitor cells (NSPCs) that reside within these brain regions are mitotically active, self-renewing cells with the potential to differentiate into neurons, oligodendrocytes, or astrocytes (McKay, 1997; Gage, 2000; Temple, 2001; Ivanova et al., 2002).

Following focal cerebral ischemia, neural stem/progenitor cells (NSPCs) in the SVZ proliferate and migrate to the lesioned site in both rodents and humans (Jin et al., 2001b; Zhang et al., 2001; Arvidsson et al., 2002; Parent et al., 2002; Iwai et al., 2003; Jin et al., 2006; Yamashita et al., 2006). Migration of NSPCs and their progeny may be critical for post-ischemic repair, since ablation of progenitor proliferation leads to increased infarct volume (Maysami et al., 2008) and the time course of this migratory response occurs concomitant with partial spontaneous recovery of motor deficits (Kondziolka et al., 2000; Zhang et al., 2005). Although hundreds of thousands of cells emigrate from the SVZ into the injured striatal parenchyma, the number of neuroblasts that survive long-term represents <0.2% of striatal neurons lost to ischemic injury (Kokaia et al., 2006). That such a low number of new neurons contribute significantly to the reconstruction of striatal circuitry seems unlikely. Nevertheless, evidence suggests that SVZ derivatives migrating into the injured striatal parenchyma contribute importantly to the process of endogenous wound healing following ischemic insult, through processes apart or in addition to neuronal replacement (Burns et al., 2009). Additional mechanisms include

stabilization of nascent vasculature following stroke-induced angiogenesis and/or prevention of progressive neuronal cell loss via release of angiogenic and neurotrophic factors.

Vascular endothelial growth factor (VEGF) is the most well-studied angiogenic factor, but also has been shown to exert direct neurotrophic signaling and to promote adult neurogenesis (Connolly et al., 1989; Jin et al., 2002; Ferrara, 2004). The most potent inducer of VEGF gene expression is hypoxia (Shweiki et al., 1992). VEGF is transcriptionally regulated by hypoxia-inducible factor-1α (HIF-1α), which translocates to the nucleus following hypoxia-induced stabilization, dimerizes with HIF-1β (ARNT), and activates the hypoxia response element (HRE) in the promoter region of the VEGF gene (for review see (Semenza, 2003)). VEGF is also regulated by HIF-independent mechanisms including other transcription factors and co-activators (Arany et al., 2008) (for reviews see (Mizukami et al., 2007; Birk et al., 2008)), micro-RNAs (Hua et al., 2006), and inflammatory mediators (McColl et al., 2004). In neurons, VEGF mediates its neurotrophic effects via the receptor tyrosine kinase, VEGFR-2 (Flk-1/KDR) (Jin et al., 2002). Following stroke, exogenous administration of VEGF has been shown to reduce infarct size and improve neurological performance (Sun et al., 2003). These effects are thought to be due to both a direct neurotrophic action of VEGF on neurons and stimulation of angiogenesis for re-establishment of blood flow following ischemic damage. Transgenic mice with VEGF-overexpression also display increased neurogenesis, decreased infarct volume, and improved motor function (Wang et al., 2007).

Neural stem cells have previously been shown to provide neuroprotection when transplanted into the adult brain in rodent models of stroke (Hayashi et al., 2006; Chu et al., 2008; Jin et al., 2010b), raising the possibility that the endogenous SVZ response to stroke may also provide neuroprotection of penumbral neurons at risk of delayed cell death. We have previously demonstrated that embryonic neural stem cells secrete diffusible VEGF, which underlies their ability to protect endothelial cells against severe ischemia and promote angiogenesis in ischemic striatum (Roitbak et al., 2008). In the present study, we investigated whether embryonic or postnatal NSPCs also provide neuroprotection against cerebral ischemia utilizing both *in vitro* and *in vivo* approaches. Here, we demonstrate that both embryonic and postnatal NSPCs are robustly resistant to oxygen-glucose deprivation (OGD), and provide neuroprotection under ischemic conditions, an effect that is mediated by HIF-1α-regulated release of diffusible VEGF by primary NSPCs. These studies have important implications for both the therapeutic use of exogenous NSPCs in stroke and also suggest a potential neuroprotective role for endogenous NSPCs in adult brain repair.

2.3 Materials and Methods

2.3.1 Primary cortical neuronal and neural stem/progenitor cultures

Ethics Statement: This study was approved by the University of New Mexico Animal Care and Use Committee and conformed to the NIH Guidelines for use of animals in research. Timed pregnant female mice were sacrificed by isoflurane overdose and the embryos removed by cesarean section. Primary neuronal cultures were established from cerebral cortices of C57BL/6J embryos (The Jackson Laboratory, Bar Harbor, ME, USA) at gestation day 15, using enzymatic dissociation with trypsin as previously described

(Wetzel et al., 2008). For immunocytochemistry, 3.9 x 10^5 dissociated cells were plated on poly-L-lysine-coated coverslips (0.1 mg/ml; Sigma, St Louis, MO, USA) in 24-well plates. For biochemical procedures, 1.95 x 10^6 cells were plated on precoated poly-L-lysine six-well plates (BD Biosciences, San Diego, CA, USA). The cultures were maintained under serum-free conditions in neurobasal medium (Invitrogen Corp., Carlsbad, CA, USA), supplemented with B-27 supplement (2%; Invitrogen Corp.), glutamine (0.5 mM; Sigma), glutamate (25 μM; Sigma), penicillin (100 U/ml) and streptomycin (100 μg/ml; Invitrogen Corp.). At 4 days *in vitro* (DIV), half of the medium was removed and replaced with fresh medium without glutamate, as indicated by the manufacturer. At 7 DIV, neuronal cultures were used for experimentation. Embryonic neural stem/progenitor cells (eNSPC) were established from whole telencephalon of EGFP-C57BL/6J embryos at gestation day 14 (E14), as described previously (Ray et al., 1993). Postnatal NSPCs (pNSPC) were established from postnatal day 28 male EGFP-C57BL/6J mice. NSPCs were plated on pre-coated poly-L-lysine six-well plates (BD Biosciences). Growth factors were added every other day and cells were passaged at least twice prior to use. NSPCs used for coculture were plated on 0.4 μM pore size transwells (BD Biosciences) coated with poly-L-lysine (0.1 mg/mL; Sigma). The cultures were maintained under serum-free conditions in neurobasal medium (Invitrogen Corp.), supplemented with B-27 supplement (2%; Invitrogen Corp.), glutamine (2.0 mM; Sigma), penicillin (100 U/ml; Invitrogen Corp.), streptomycin (100 μg/ml; Invitrogen Corp.), EGF (10 ng/mL; Invitrogen Corp.), and bFGF (10 ng/mL; Invitrogen Corp.). All cultures were maintained in a humidified incubator at 37°C with 5% CO_2. The cultures were incubated with the following compounds: SU1498 (70 nM-50 μM; Calbiochem, San

26

Diego, CA, USA), IgG-Fc (5 ng/mL-1 μg/mL; Jackson ImmunoResearch Laboratories, West Grove, PA, USA), and Flt-1-Fc (5 ng/mL-1 μg/mL; R&D Systems, Minneapolis, MN, USA).

2.3.2 Oxygen-glucose deprivation

Oxygen-glucose deprivation (OGD) was performed as previously described (Plesnila et al., 2001; Wetzel et al., 2008). Primary cortical neuronal cultures and/or NSPCs were placed in an anaerobic chamber (Coy Laboratories, Grass Lake, MI, USA) containing a gas mixture of 5% CO_2, 5% H_2 and 85% N_2 (<0.2% O_2). Normal culture media was replaced with deoxygenated, glucose-free Earle's balanced salt solution, and the cultures were maintained under glucose-free anaerobic conditions at 37°C for 2 h. OGD was terminated by returning the cultures to normoxic conditions and neurobasal medium supplemented with 2% B-27 supplement, 0.5 mM glutamine, 100 U/ml penicillin and 100 μg/ml streptomycin. As a control, sister cultures were placed in Earle's balanced salt solution containing 25 mM glucose (Sigma) for 2 h at 37°C under normoxic (21% O_2) conditions and then returned under normoxic conditions to neurobasal medium supplemented with 2% B-27 supplement, 0.5 mM glutamine, 100 U/ml penicillin and 100 μg/ml streptomycin.

2.3.3 Mild transient middle cerebral artery occlusion (MCAO)

Adult male C57BL/6J mice 20-25 g (The Jackson Laboratory) were housed under a 12 h light: 12 h dark cycle with food and water available *ad libitum*. Mice (20-25 g; n=20) were anesthetized with 4% isoflurane for induction and maintained on 1.0% isoflurane.

The body temperature was maintained at 37°C with a heating pad. Mice were subjected to 30 minutes of transient MCAO as previously described(Kokovay et al., 2006). Briefly, the right common carotid artery was exposed through a midline incision. The internal carotid artery was isolated from external carotid artery which was ligated with 6-0 silk suture. A 2-cm length of 6-0 rounded tip nylon suture was advanced from the common carotid artery (CCA), through the internal carotid artery up to the level of the anterior cerebral artery. The suture was inserted 10 to 11 mm from the bifurcation of CCA to occlude the middle cerebral artery (MCA). After 30 min of MCAO, the suture was slowly withdrawn to allow for reperfusion. Reperfusion time was 3 days post-MCAO. The mice were anesthetized with sodium pentobarbital (150 mg/kg, Fort Dodge Animal Health, Fort Dodge, IA, USA) administered intraperitoneally, and were transcardially perfused first with preperfusing solution (0.01 mg/ml heparin and 1 mg/ml procaine) and subsequently with 4% paraformaldehyde in 0.1 M phosphate buffered saline (PBS). The brains were removed, post-fixed overnight in 4% paraformaldehyde, and cryoprotected with 30% sucrose (w/v) in 0.1 M PBS for 48 hours at 4°C. For immunohistochemical procedures (described below), the brains were sectioned at 30 μm using a sliding microtome (AO Scientific Instruments, Buffalo, NY, USA).

2.3.4 Embryonic NSPC transplantation

NSPCs isolated from E14 EGFP-expressing transgenic C57BL/6J mouse embryos were expanded in culture as described above and transplanted into 8 week-old C57BL/6J mouse striatum. Mice were anaesthetized with 2% isoflurane inhalation. Stereotaxic injections were performed using Hamilton microsyringe with a 26-gauge blunt needle. Each animal received an injection of 2.5 μl (at the rate of 1 μl /min, and concentration

28

5×10^4 cells/μl) of EGFP-NSPCs into the striatum (from bregma: A +1.0mm, L +2.0 mm, V -2.6mm). To identify fragmentation of DNA characteristic of apoptosis, TUNEL labeling was performed on paraformaldehyde fixed tissue from 30 minutes MCAO using Neurotacs™ II kit (Trevigen, Inc, Gaithersburg, MD, USA), according to the manufacturer's protocol. Tissue treated with TACs-nuclease™ or without terminal deoxynucleotidyl transferase served as positive and negative controls, respectively. NIH ImageJ software was used to quantify TUNEL+ cells from fluorescent images using Sholl analysis, with concentric rings placed at increasing distances (635 μm apart) around the perimeter of the graft.

2.3.5 Immunohistochemistry

Cultured cells were fixed on coverslips with 4% paraformaldehyde and incubated in monoclonal mouse anti-Nestin (1:500; Chemicon, Temecula, CA, USA), polyclonal rabbit anti-MAP-2 (1:500; Chemicon), and/or polyclonal rabbit anti-GFAP (1:500; Accurate, Westbury, NY, USA). Histological sections (30 μm) were incubated in monoclonal mouse anti-NeuN (1:1000, Chemicon) or polyclonal rabbit anti-MPO (1:500, Santa Cruz Biotechnology, Santa Cruz, CA, USA). Immunofluorescence was visualized using FITC- or Cy3-conjugated secondary antibodies (1:250; Jackson ImmunoResearch Laboratories). DAPI nuclear stain was used to identify cell bodies of cultured cells (Invitrogen Corp.). Immunofluorescence was analyzed using high-resolution confocal microscopy (Zeiss LSM510, Thornwood, NY, USA) or conventional fluorescence microscopy.

2.3.6 Immunoassays

Soluble VEGF or BDNF were assayed from conditioned media using the Quantikine Mouse Immunoassay for the appropriate protein (R&D Systems). HIF-1α was measured in cell lysates using Surveyor[TM] IC Human/Mouse Total HIF-1α Immunoassay (R&D Systems). Transcriptional activity of HIF-1α was measured in nuclear extract using the TransAM HIF-1 kit (Active Motif, Carlsbad, CA, USA), substituting the primary antibody for one that recognizes mouse (Novus Biologicals, Littleton, CO, USA). Nuclear extracts used in this assay were isolated using the NE-PER Nuclear and Cytoplasmic Extraction Reagent Kit (Pierce, Rockford, IL, USA). Absorbance for all assays was read using a microplate reader (Dynex Technologies, Chantilly, VA, USA): Quantikine assays were read at 450 nm with background subtraction of 570 nm; TransAM assay was read at 450 nm with a background subtraction of 630 nm.

2.3.7 MTT cell viability assay

Cell viability was assessed using methylthiazolyldiphenyl-tetrazolium bromide (MTT) dissolved in PBS (0.5 mg/mL; Sigma). Cultures were incubated with MTT at 37°C for 4 hr. Formazan crystals were solubilized using 1:1 ethanol:DMSO solution. Absorbance was measured at 570 nm with a background subtraction of 630 nm.

2.3.8 *Hif1a* gene deletion from NSPCs

NSPCs were isolated from embryonic day 14 transgenic mice containing loxP-flanked exon 2 of the *Hif1a* gene (*Hif1a*^fl/fl^) (Ryan et al., 2000) that were crossed to the C57BL/6J background (The Jackson Laboratory). NSPCs were passaged twice prior to 48 hr treatment with an adenovirus expressing Cre-recombinase (Ad-CMV-Cre; Vector

Biolabs, Philadelphia, PA, USA) at 50 MOI (multiplicity of infection). This method recombines the DNA between the two loxP sites to excise the intervening sequence. Twenty-four hours after infection, NSPCs were passaged twice more before used in experiments. To confirm deletion of exon 2 of the *Hif1a* gene, DNA was isolated and efficiency of cre-recombination was detected with PCR using forward primer 5'- TGT TAA ATA AAA GCT TGG AC -3' and reverse primer 5'- GCA GTT AAG AGC ACT AGT TG -3' (Milosevic et al., 2007). Successful DNA recombination yields *Hif1a* gene-deleted NSPCs (HIF-1$\alpha^{\Delta/\Delta}$), as indicated by the loss of the 1200 bp band amplification product and appearance of a 250 bp band. Experiments using HIF-1$\alpha^{\Delta/\Delta}$ eNSPCs were compared to wild-type C57BL/6J eNSPCs treated similarly with Ad-CMV-Cre.

2.3.9 Statistical Analyses

Data are expressed as means $\pm$ S.E.M. Significant differences between means were determined by student's t-test or analysis of variance (ANOVA) with Tukey multiple comparisons *post hoc* analysis using Prism software (Graphpad Software, San Diego, CA, USA). P values < 0.05 are considered statistically significant.

2.4 Results

2.4.1 NSPCs provide neuroprotection against focal ischemia *in vivo.*

To determine whether mouse NSPCs are neuroprotective in our animal model of focal ischemia, we isolated embryonic NSPCs from transgenic mice that express enhanced green fluorescent protein (EGFP) under the β-actin promoter. We have previously demonstrated that these NSPCs fulfill the criteria of multi-potentiality and self-renewal

31

(Roitbak et al., 2008). EGFP-NSPCs were expanded in culture and subsequently transplanted into the right dorsal striatum of adult recipient mice. Control mice received vehicle injections of phosphate buffered saline only. Seventy-two hours following transplantation, recipients were subjected to an ipsilateral transient middle cerebral artery occlusion (MCAO) for 30 minutes, followed by three days of reperfusion. As shown in Figure 2.1 A, MCAO resulted in a robust apoptotic response at three days as assessed by TUNEL labeling of injured striatum in vehicle treated mice. EGFP-NSPC recipients displayed >50% fewer TUNEL+ nuclei compared to vehicle controls (Figure 2.1 B), particularly in the area immediately surrounding the graft and extending out to at least 4.5 mm from the graft border (Figure 2.1 E,F). Conversely, healthy appearing NeuN$^+$ neuronal nuclei were numerous near the graft, whereas control mice displayed widespread loss of NeuN$^+$ cells (Figure 2.1 C,D). These data demonstrate robust NSPC-mediated neuroprotection against focal ischemia in the MCAO model. We previously reported that NSPC-transplant promotes vascularization and proliferation of blood vessels within the ischemic striatum (Roitbak et al., 2008), suggesting an effect of NSPCs on the vasculature. Activated neutrophils, as identified by myeloperoxidase (MPO) staining, were not observed in either vehicle- or NSPC-injected striatum, suggesting that NSPC transplantation does not alter the inflammatory response following stroke (Figure 2.7). To test whether NSPCs have a direct effect on neurons during ischemia, we shifted to an *in vitro* cell culture system using a well-characterized OGD model (Plesnila et al., 2001).

2.4.2 NSPCs provide neuroprotection against OGD and are intrinsically resistant to *in vitro* ischemia.

We utilized a transwell coculture paradigm to begin to delineate the mechanisms underlying NSPC-mediated neuroprotection. NSPCs and cortical neurons were cultured separately as monocultures or were cocultured in separate compartments of porous transwells (0.4 μm pore size), which allowed for sharing of conditioned media but did not allow cell-cell contact between NSPCs and neurons seeded in the upper *vs.* lower compartments, respectively. As shown in Figure 2.2, cortical cultures contained MAP-2^{+} neurons, with minimal contamination by GFAP^{+} astrocytes, and NSPC cultures were uniformly immunopositive for the stem cell marker, nestin. Neuronal and NSPC cultures were subjected to control or OGD conditions for 2 hours and assessed for cell viability 24 hr later using an MTT assay. As shown in Figure 2.2 B, cortical cultures underwent approximately 40% cell loss within 24 hr following OGD, as previously described (Wetzel et al., 2008), but only ~12% cell loss when cocultured with NSPCs. Importantly, NSPC monocultures were robustly resistant to 2 hour OGD and displayed no significant cell loss at 24 hours (Figure 2.2 C). These data indicate that NSPCs provide robust neuroprotection of cortical neurons in culture via diffusible substance(s), and are themselves resistant to OGD conditions.

2.4.3 Diffusible VEGF is responsible for NSPC-mediated neuroprotection against OGD.

HIF-1α is a key mediator of the adaptive cellular response to hypoxia and acts through transcriptional and non-transcriptional pathways to regulate the activities of genes involved in cell survival and angiogenesis, including VEGF. As shown in Figure 2.3 A, NSPC monocultures constitutively expressed HIF-1α and displayed a nearly 3-fold

increase in HIF-1α expression measured 24 hr following a 2 hr exposure to OGD. In contrast, HIF-1α was not measurable in neuronal monocultures under nonhypoxic conditions or at 24 hr following a 2 hr OGD exposure (not shown). As shown in Figure 2.3 B, both neuronal and NSPC monocultures constitutively expressed the HIF-1α target gene, VEGF, and released VEGF into the culture media. VEGF release was not statistically different in cortical monocultures following OGD, but was increased 2.5-fold in NSPC monocultures as measured 24 hr following 2 hr exposure to OGD. Culture media from NSPCs was also used to measure the presence of brain-derived neurotrophic factor (BDNF), however BDNF was undetected in both control and OGD-exposed NSPC media (data not shown).

To determine whether diffusible VEGF is responsible for NSPC-mediated neuroprotection, neurons in monoculture or in transwell coculture with NSPCs were exposed to OGD in the presence or absence of the VEGFR2 kinase inhibitor, SU1498 (10 μM; Figure 2.4 A) or the VEGF decoy receptor, Flt-1-Fc (1.0 μg/ml; Figure 2.4 B) added at the onset of OGD and present for 24 hr thereafter. As demonstrated in Figure 2.4 A, SU1498 had no effect on neuronal viability under non-ischemic conditions, but completely inhibited the ability of NSPCs to provide neuroprotection against OGD in coculture. Prevention of VEGF-VEGFR interaction at the cell surface with Flt-1-Fc also impaired the neuroprotection provided by cocultured NSPCs (Figure 2.4 B). Dose-response analysis for both SU1498 and Flt-1-Fc showed that neither compound was cytotoxic to neurons in monoculture at the concentration used in this study (Figure 2.8). Exposure of neuronal cultures to NSPC-conditioned media resulted in significant neuroprotection against OGD, an effect that was also blocked by SU1498 and Flt-1-Fc

inhibition of VEGF signaling (Figure 2.4 C). Flt-1-Fc was not cytotoxic to NSPCs, and had no effect on the ability of NSPCs to withstand OGD conditions (Figure 2.9). These data indicate that NSPC-mediated neuroprotection is mediated by diffusible VEGF and dependent on neuronal VEGFR signaling.

2.4.4 Gene deletion of *Hif1a* impairs NSPC-mediated neuroprotection.

To determine the extent to which endogenous NSPC HIF-1α governs VEGF expression and NSPC-mediated neuroprotection, eNSPCs were isolated from transgenic mice that harbor loxP sites flanking exon 2 of the *Hif1a* gene at both alleles (*Hif1a*$^{fl/fl}$) (Ryan et al., 2000). *Hif1a*$^{wt/wt}$ and *Hif1a*$^{fl/fl}$ NSPC cultures were incubated for 24 hr with adenovirus harboring a bacterial Cre-recombinase gene sequence to confer Cre expression (Ad-CMV-Cre). As shown in Figure 2.5 A, transduction of NSPC cultures with Ad-CMV-Cre resulted in excision of *Hif1a* exon 2 in *Hif1a*$^{fl/fl}$ NSPCs (*Hif1a*$^{\Delta/\Delta}$), but not in *Hif1a*$^{wt/wt}$ NSPCs, as indicated by PCR analysis of genomic DNA isolated 24 hr following removal of Ad-CMV-Cre. HIF-1α transcriptional activity was completely abolished as assessed by the inability of nuclear extract proteins to bind the hypoxia response element (HRE) in *Hif1a*$^{\Delta/\Delta}$ cells, but not in *Hif1a*$^{wt/wt}$ cells (Figure 2.5 B). *Hif1a* gene deletion in NSPCs also resulted in a 50% reduction of VEGF release by *Hif1a*$^{\Delta/\Delta}$ NSPCs compared to *Hif1a*$^{wt/wt}$ NSPCs in response to anoxia (Figure 2.5 C). *Hif1a* gene deletion had no effect on NSPC survival at 24 hr following 2 hr OGD (96.8 % $\pm$ 8.5 % *vs.* 101.6 % $\pm$ 6.7 %, *Hif1a*$^{wt/wt}$ *vs.* *Hif1a*$^{\Delta/\Delta}$, respectively, ns, n=4; Figure 2.10), but abrogated the neuroprotective effects of NSPC conditioned media (Figure 2.5 D). Thus,

HIF-1α appears to be necessary for NSPC-mediated neuroprotection since media from *Hif1a*$^{\Delta/\Delta}$ cultures failed to protect neurons from OGD-induced death.

2.4.5 <u>Postnatal NSPCs are neuroprotective, resistant to ischemia and constitutively express stabilized HIF-1α and VEGF.</u>

To determine whether postnatal NSPCs also confer neuroprotection and are resistance to *in vitro* ischemia, we isolated NSPCs from postnatal day 28 mouse SVZ and expanded the pNSPCs in culture using the same paradigm as for eNSPCs. As shown in Figure 2.6 (A and B), pNSPCs constitutively expressed stabilized HIF-1α and VEGF at levels similar to eNSPCs under non-ischemic conditions, with robust induction of both proteins in response to 24 hr anoxia. pNSPCs also displayed resistance to 2 hr OGD exposure (Figure 2.6 C), and media conditioned by pNSPCs provided neuroprotection against 2 hr OGD (Figure 2.6 D).

2.5 Discussion

In this study, we investigated the neuroprotective effects of embryonic and postnatal NSPCs under conditions of ischemia, and the role of HIF-1α-regulated VEGF signaling in this process. We found that exogenous NSPCs protect neurons against focal ischemic injury induced by MCAO *in vivo*, and protect embryonic cortical neurons against OGD exposure in culture. In contrast to primary cortical neurons, NSPCs display intrinsic resistance to brief 2 hr OGD exposure in culture, and constitutively express stabilized HIF-1α and its downstream target, VEGF. Pharmacological blockade of VEGF signaling in culture impairs neuroprotection, and *Hif1a* gene deletion in NSPCs results in both impaired VEGF production and impaired neuroprotection against OGD. These

36

observations provide evidence that NSPCs promote neuronal survival under conditions of ischemia via HIF-1α-regulated VEGF signaling and suggest that NSPCs may play a neuroprotective role following stroke.

VEGF is recognized as both a vasculotrophic factor and a neurotrophic factor. VEGF expression in the brain is downregulated in early postnatal life after formation of the cerebral vasculature is complete, but becomes upregulated in adult brain in response to stroke or mechanical injury (Kovacs et al., 1996; Krum and Rosenstein, 1998; Marti and Risau, 1999). Administration of exogenous VEGF following stroke results in reduced neuronal cell death, increased angiogenesis and increased vascular permeability (Zhang et al., 2000; Sun et al., 2003; Greenberg and Jin, 2005) (reviewed in(Carmeliet and Storkebaum, 2002; Greenberg and Jin, 2005; Hansen et al., 2008)). VEGF also exerts a direct neuroprotective effect against *in vitro* ischemia, mediated by neuronal VEGFR2 signaling and downstream activation of the phosphatidylinositol 3-kinase (PI3 kinase)/Akt pathway in cultured neurons (Jin et al., 2000; Jin et al., 2001a; Ogunshola et al., 2002; Rosenstein et al., 2003; Kilic et al., 2006; Taoufik et al., 2008). Our studies suggest that VEGF release by NSPCs underlies *in vitro* neuroprotection against ischemia, via direct activation of neuronal VEGFR2 receptors, since neuroprotection was abrogated by the presence of the VEGFR2 kinase inhibitor, SU1498, and by the presence of the VEGFR decoy receptor, Flt-1-Fc. In conjunction with our previous report (Roitbak et al., 2008), VEGF could have a dual effect in the graft: improved revascularization and direct neuroprotection.

VEGF production by both embryonic and adult NSPCs in culture has previously been reported (Madhavan et al., 2008; Roitbak et al., 2008; Teng et al., 2008; Wang et al.,

2008). NSPC expression of VEGF is known to be upregulated in response to hypoxic and metabolic stress (Madhavan et al., 2008; Roitbak et al., 2008). Our present study demonstrates that cortical cultures also release diffusible VEGF under normoxic conditions but do not display increased VEGF production at 24 hr following 2 hr OGD, whereas VEGF release by NSPCs is increased 2-3 fold within 24 hr post-OGD. Although inhibition of VEGFR2 signaling blocks NSPC-mediated neuroprotection, inhibition of VEGFR2 signaling has no impact on the survival of neurons under normoxic conditions, and has no effect on the ability of NSPCs to survive ischemic insult. These observations suggest that increased VEGF production by NSPCs underlies neuronal protection against *in vitro* ischemia, but does not mediate NSPC resistance to ischemic conditions and is not required for survival of cortical neurons under normoxic conditions.

One of the most potent regulators of VEGF expression is HIF-1α. HIF-1α is primarily regulated at the post-translational level, with protein stability dependent upon pO_2. In most mammalian cell types, HIF-1α protein is hydroxylated under normoxic conditions, binds the von Hippel-Lindau (VHL) protein, and is rapidly degraded by the 26S proteosome. Under conditions of hypoxia, HIF-1α is not hydroxylated and rapidly accumulates to enter the nucleus and dimerize with HIF-1β (ARNT), forming the HIF-1 transcriptional complex that regulates target genes through cis-acting hypoxia response elements (HREs). In most cell types *Hif1a* mRNA is constitutively transcribed and translated, but the protein only has a half-life of less than 5 minutes under non-hypoxic conditions (for review, see (Semenza, 2003; Weidemann and Johnson, 2008)). Our observation that HIF-1α is constitutively stabilized by cultured NSPCs, even at 21% O_2,

suggests that NSPCs may also utilize a non-oxygen dependent mechanism for maintaining HIF-1α stability and that HIF-1α plays a fundamental role in NSPC homeostasis under both normoxic and hypoxic conditions. Previous studies have demonstrated O_2-independent stabilization of HIF-1α by heat shock protein 90 (HSP-90) through binding the PAS domain of HIF-1α (Isaacs et al., 2002). HSP-90 has also been shown to be involved in the regulation of HIF-1α stability in embryonic mesencephalic NSPCs (Xiong et al., 2009).

While the role of constitutive HIF-1α stabilization in NSPCs is not completely understood, HIF-1α is recognized as a multifunctional protein that regulates the expression and activity of multiple genes involved in angiogenesis, glucose metabolism, proliferation and self-renewal, apoptosis, and migration through both transcriptional and non-transcriptional signaling pathways (Bergeron et al., 1999; Bernaudin et al., 1999; Gustafsson et al., 2005; Chen et al., 2009). Others have shown that upregulation of HIF-1α in neural progenitor cells enhances their ability to survive *in vitro* and following transplantation (Theus et al., 2008), as well as provide neuroprotection against ischemia (Chu et al., 2008). In addition to VEGF, HIF-1α is a potent inducer of erythropoietin (EPO), which promotes neurogenesis, NSPC proliferation and neuroprotection following ischemia (Bernaudin et al., 1999; Shingo et al., 2001; Tsai et al., 2006; Chen et al., 2007b). However, neural-specific EPOR knockdown does not increase infarct volume following focal cerebral ischemia and therefore endogenous levels of EPO may not provide neuroprotection following stroke (Tsai et al., 2006). Conversely, antisense blockade of VEGF *in vivo* results in an enlargement of infarct volume caused by transient MCAO (Yang et al., 2002). In the present study, we found that *Hif1a* gene deletion

results in >50% reduction of VEGF production and a concomitant impairment of neuroprotective activity in NSPC-conditioned medium. However, these data also indicate that VEGF production is at least partially regulated by HIF-1α-independent mechanisms in NSPCs, since *Hif1a* gene deletion did not completely block VEGF production.

We previously demonstrated that embryonic NSPCs protect endothelial cells against ischemia-induced damage and stimulate increased endothelial cell proliferation via HIF-1α-regulated VEGF signaling mechanisms (Roitbak et al., 2008). Here, we extend those studies to demonstrate that NSPCs also provide neuroprotection through similar signaling mechanisms. While neural stem cells were initially recognized as potential therapeutic agents for stroke and neurodegenerative disease based on their potential to replace lost neurons and integrate into host circuitry, our studies support the possibility that the therapeutic potential of neural stem cells may lie predominantly in their ability to promote endogenous brain repair processes. Following stroke, NSPCs and their progeny migrate to the lesioned area and inhibition of this migration leads to an increase in infarct size (Maysami et al., 2008). Our study reveals that NSPCs may directly protect against ischemic injury through the release of diffusible VEGF. Further studies will require NSPC-targeted gene deletion of *Vegf* and *Hif1a* to delineate the role of endogenous NSPCs in neuroprotection *in vivo*, as well as their effects on other cell types within the neurovascular niche. While *in vitro* modeling is crucial to understanding the molecular mechanisms of the interactions between neurons and NSPCs, *in vivo* studies will account for the ischemic microenvironment.

While our studies suggest that NSPCs themselves are neuroprotective and important for vascular remodeling following stroke, care must be taken with development of therapeutical strategies. Direct NSPC transplantation into the post-ischemic environment may lead to graft overgrowth and tumor formation due to their pluripotency and ability to self-renew (Seminatore et al., 2010). While VEGF infusion may look promising, injection of recombinant human VEGF has been shown to promote blood vessel permeability as well as blood-brain barrier leakage (Zhang et al., 2000). Thus, elucidating the mechanisms by which NSPCs protect the ischemic penumbra following stroke will provide novel therapeutic strategies for facilitating the contribution of endogenous NSPCs for brain repair.

2.6 Figure Legends

Figure 2.1: NSPCs protect against 30 minute MCAO. (A-D) Coronal histological sections through the ischemic striatum 3 days following MCAO, stained for TUNEL (A,B) or NeuN (C,D). Mice received intrastriatal injections of exogenous PBS (A,C) or EGFP$^+$NSPCs (B,D,E) 72 hr prior to MCAO. Inset in (B) shows 40X magnified view of the injection site. **(E)** Monochrome conversion of image shown in B to demonstrate concentric ring structures used for Sholl analysis. **(F)** Quantification of TUNEL+ cells using Sholl analysis performed on fluorescent images. *p<0.05, n=5 mice per group. Scale bar: A,B = 20 μm; C,D = 10 μm.

Figure 2.2: NSPCs provide neuroprotection against OGD and are resistant to *in vitro* ischemia. (A) Diagram of transwell coculture. Micrograph depicts cortical neurons in lower compartment immunofluorescently labeled for MAP-2 (red) and GFAP (green).

NSPCs in upper compartment are immunofluorescent for nestin (red). Nuclei are labeled with DAPI (blue). **(B)** Neuronal survival at 24 hrs following 2 hr exposure to OGD in the absence (left) or presence (right) of NSPCs. **(C)** Survival of NSPCs grown as monocultures in upper compartment. Data were acquired using the MTT colorimetric viability assay as described in methods section. *$p < 0.01$, Student's t-test, n=4 cultures/group.

Figure 2.3: HIF-1α and VEGF expression in eNSPC cultures under control *vs.* OGD conditions. **(A)** HIF-1α protein levels in cell lysates from eNSPCs at 24 hrs following a 2 hr exposure to OGD or control conditions. **(B)** VEGF within neuronal or NSPC conditioned media following 2 hr exposure to control or OGD conditions. Media was conditioned for 24 hrs following exposure to OGD or control conditions. *$p < 0.05$, Student's t-test, n=4 cultures/group.

Figure 2.4: Pharmacological inhibition of VEGF signaling impairs the neuroprotective effects of eNSPCs. **(A,B)** Neuronal viability 24 hrs following exposure to 2 hr OGD vs. control conditions in the presence or absence of NSPCs and the VEGFR kinase inhibitor, SU1498 (A) or the VEGF receptor decoy receptor, Flt-1-Fc (B). **(C)** Neuronal viability in the presence or absence of NSPC-conditioned media and SU1498 or Flt-1Fc. *$p < 0.05$, n=4 cultures/group.

Figure 2.5: Gene deletion of *Hif1a* impairs neuroprotective ability of eNSPC. **(A)** PCR amplification products from genomic DNA isolated from wild-type and *Hif1a*$^{fl/fl}$ NSPCs exposed to 50 MOI Ad-CMV-Cre for 48 hrs. Excision of exon 2 from *Hif1a* gene is indicated by the shorter band at 250 bp, present after Ad-CMV-Cre exposure of *Hif1a*$^{fl/fl}$ but not wild-type NSPCs. **(B)** Transcriptional activity of HIF-1α in wild-type vs. *Hif1a*$^{\Delta/\Delta}$ NSPCs assayed by HRE binding assay. **(C)** VEGF in 24 hr conditioned media from wild-type vs. *Hif1a*$^{\Delta/\Delta}$ NSPCs. **(D)** Viability of cortical cultures 24 hr following 2 hr OGD in the presence or absence of wild-type *vs.* *Hif1a*$^{\Delta/\Delta}$ NSPCs CM. *p<0.05, n= 4 cultures/group.

Figure 2.6: Postnatal NSPCs are neuroprotective and resistant to ischemia. **(A)** HIF-1α protein levels in cell lysates and **(B)** VEGF concentration in conditioned medium from pNSPCs at 24 hr following 2 hr exposure to control or OGD conditions. **(C)** Viability of pNSPCs at 24 hr post-OGD. **(D)** Viability of cortical neuronal cultures 24 hr following 2 hr OGD in the presence of neuronal *vs.* pNSPC conditioned medium. *p<0.05, n=4 cultures/group.

Figure 2.7: Myeloperoxidase (MPO) staining for activated neutrophils. (A-D) Myeloperoxidase (MPO) staining of coronal histological sections through the ischemic striatum 3 days following MCAO. Mice received intrastriatal injections of exogenous EGFP⁺NSPCs **(A-C)** or PBS **(D)** 72 hr prior to MCAO. Scale bar: 10 μm.

Figure 2.8: Dose-response of neurons to SU1498 and Flt-1-Fc. Neurons were exposed to increasing concentrations of the VEGFR2 inhibitor SU1498 **(A)** or the decoy VEGFR1 Flt-1-Fc **(B)**. SU1498 was cytotoxic at concentrations of 50 and 100 µM, but not at 10 µM which was the dose used in our experiments **(A)**. A toxic dose of Flt-1-Fc was not determined **(B)**.

Figure 2.9: NSPC response to inhibition of autocrine VEGF. Embryonic NSPCs were exposed to the VEGFR1 decoy Flt-1-Fc (1 µg/mL). Flt-1-Fc did not impair the viability of eNSPCs, and did not impair their ability to survive OGD.

Figure 2.10: NSPC viability in response to 2 hr OGD. Deletion of exon 2 of the *Hif1a* gene did not impair eNSPC ability to survive 2 hr OGD, as compared to wild-type eNSPCs.
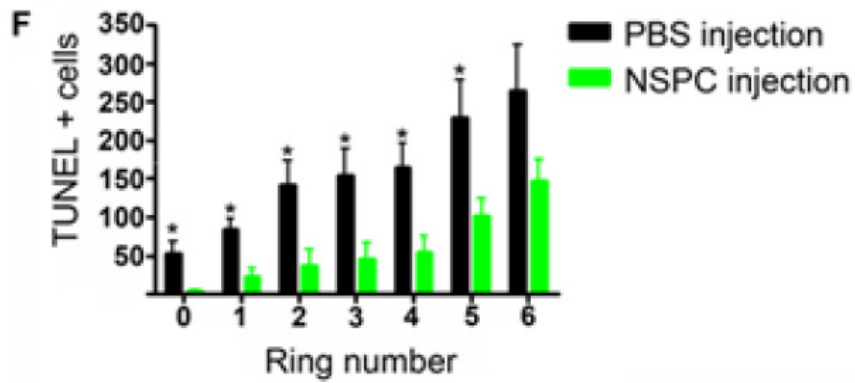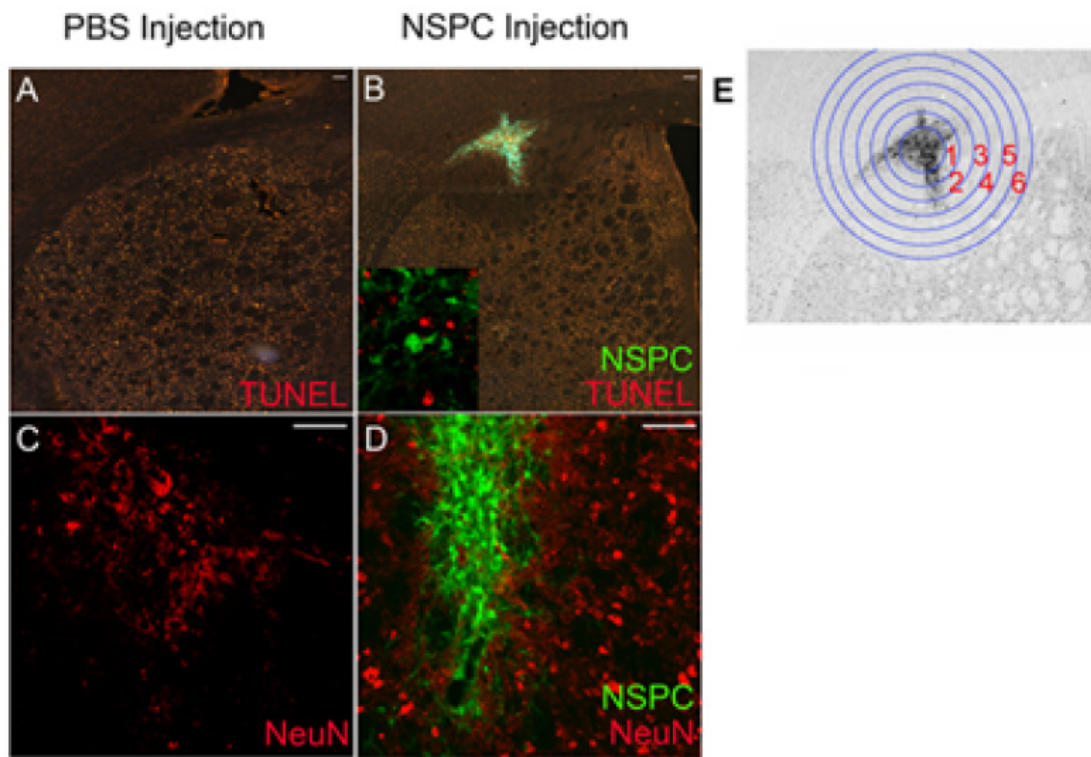
Figure 2.1: NSPCs protect against 30 minute MCAO.
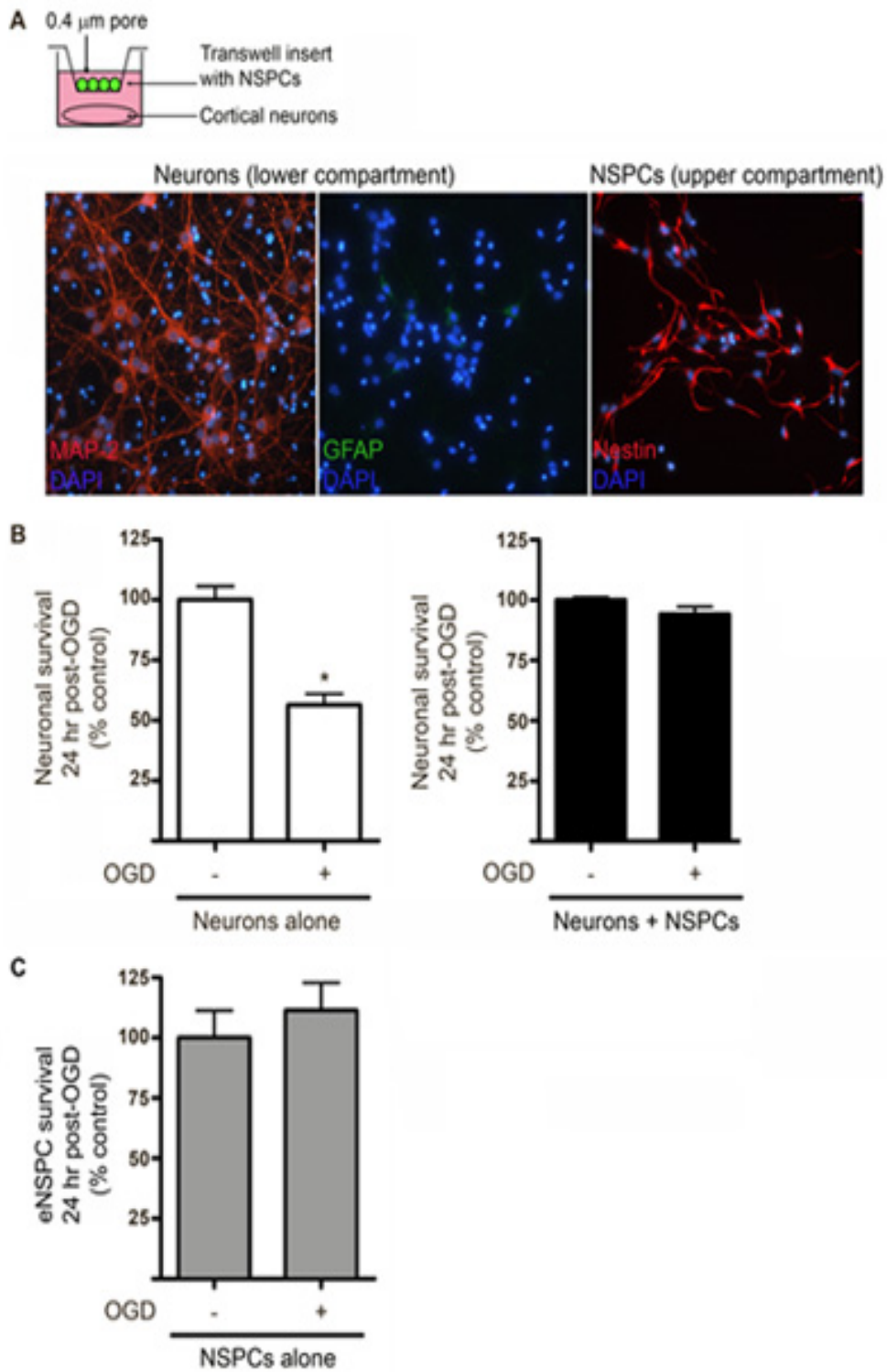
Figure 2.2: NSPCs provide neuroprotection against OGD and are resistant to *in vitro* ischemia.
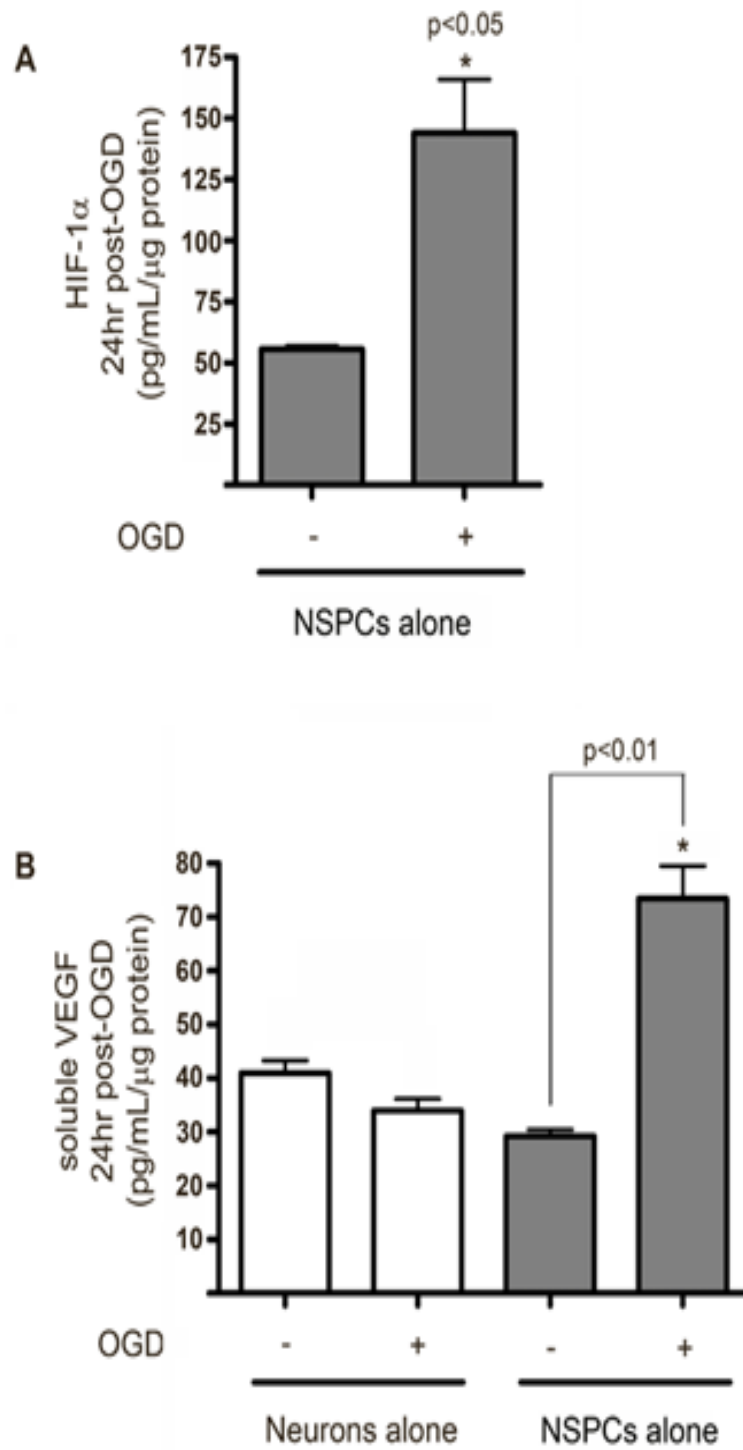
Figure 2.3: HIF-1α and VEGF expression in eNSPC cultures under control vs. OGD conditions.
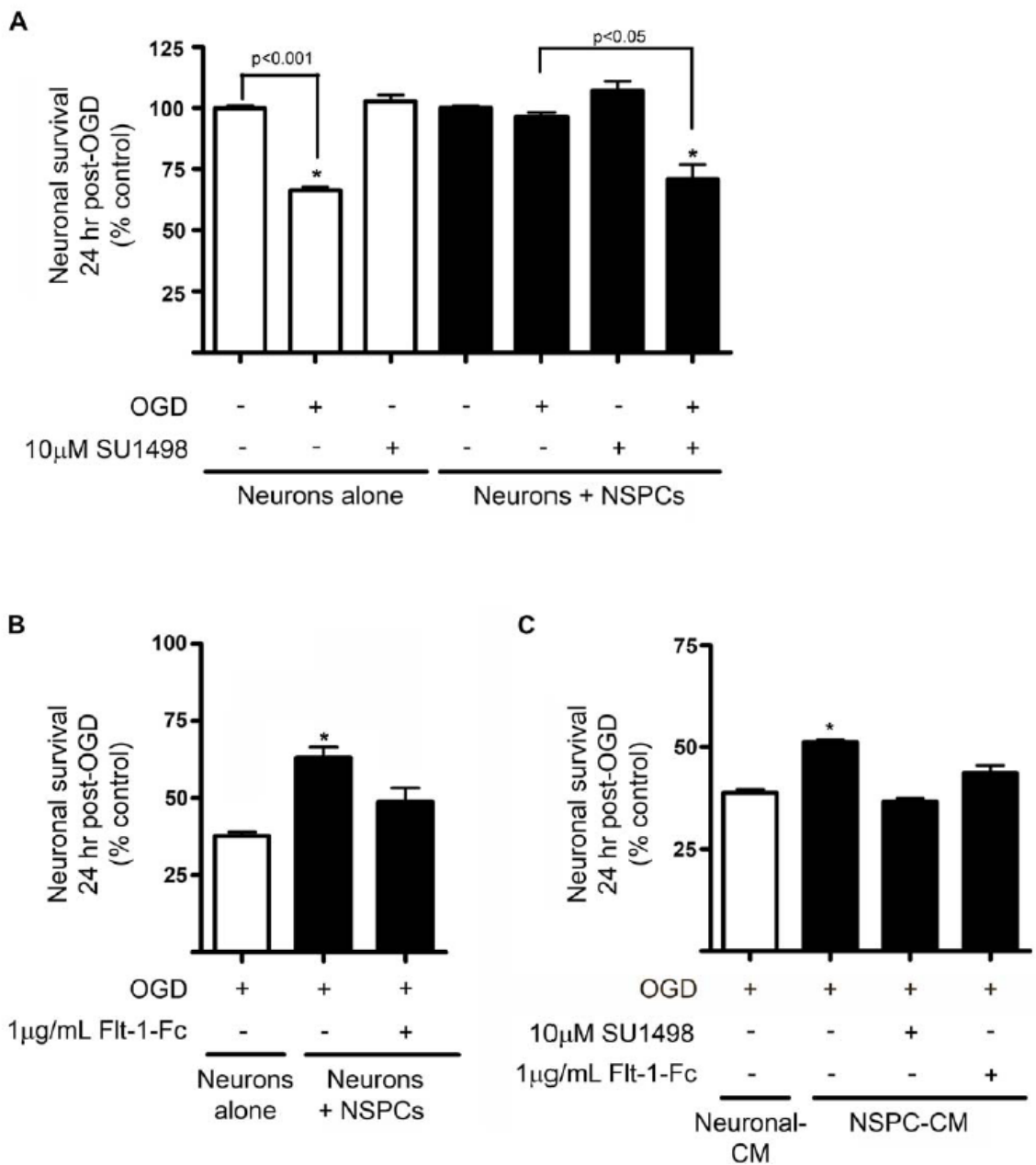
Figure 2.4: Pharmacological inhibition of VEGF signaling impairs the neuroprotective effects of eNSPCs.
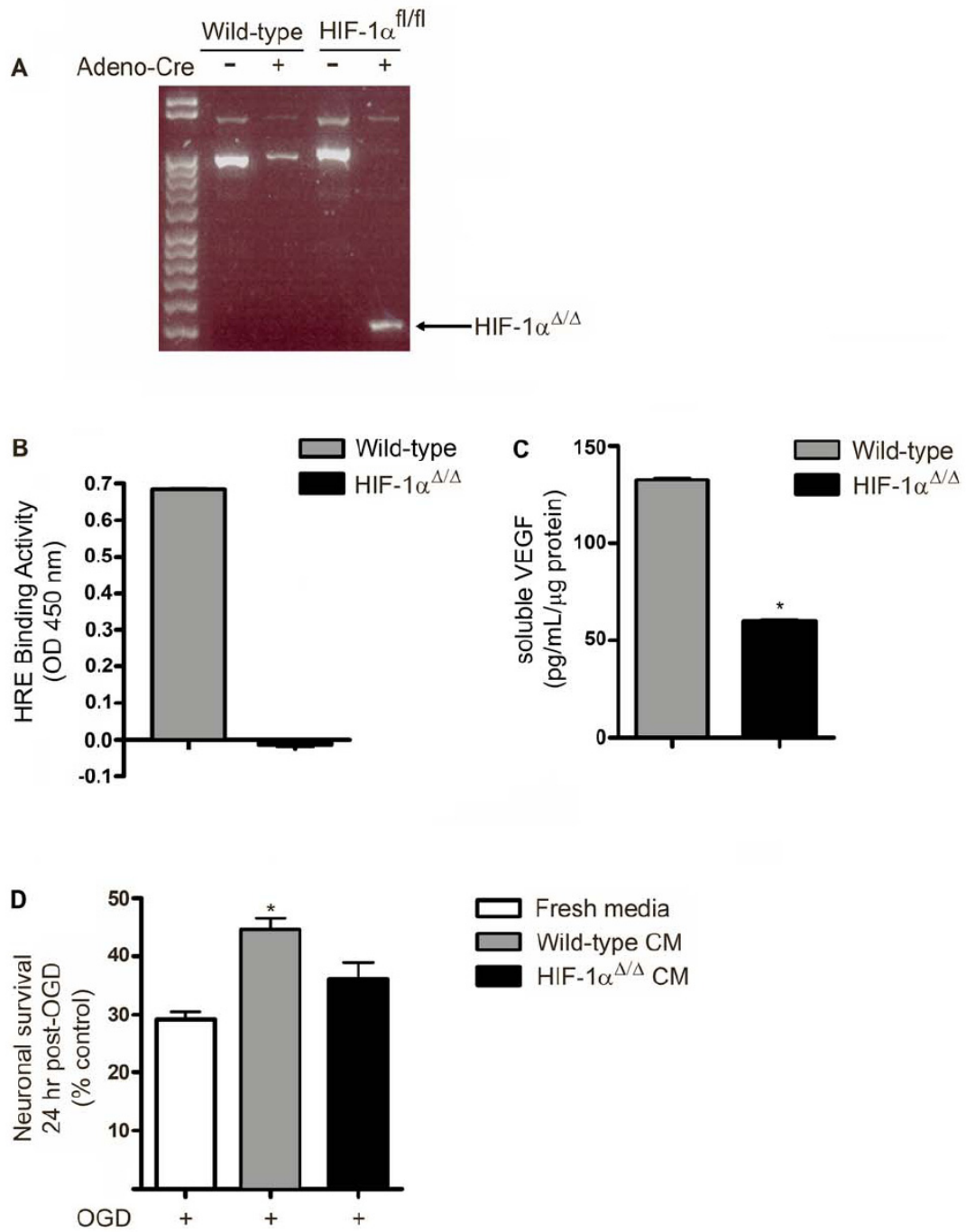
Figure 2.5: Gene deletion of HIF-1α impairs neuroprotective ability of eNSPC.
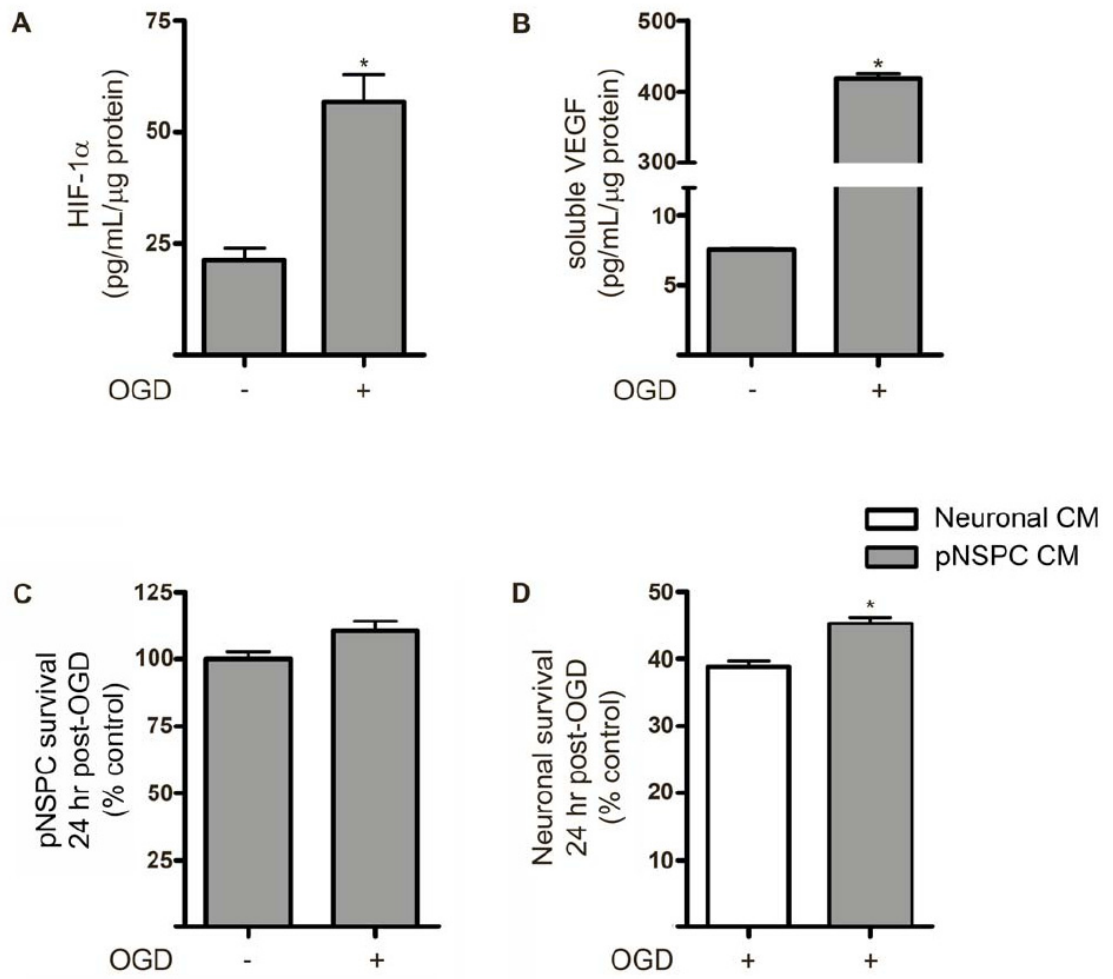
Figure 2.6: Postnatal NSPCs are neuroprotective and resistant to ischemia.
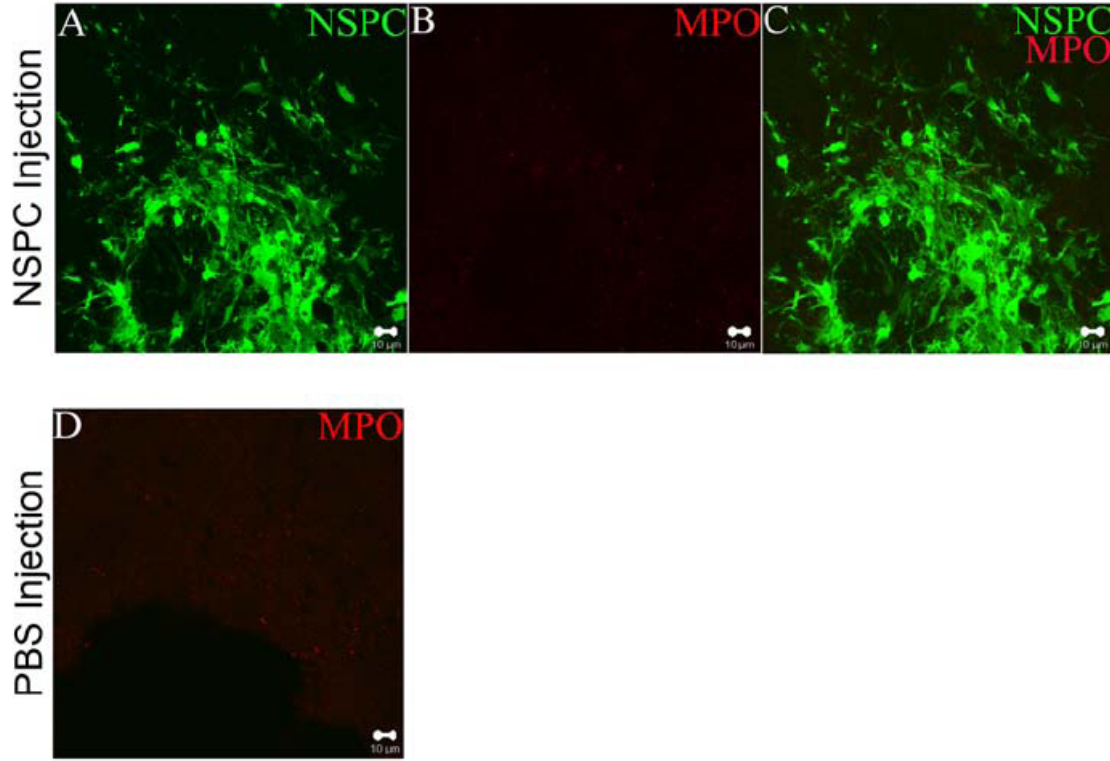
Figure 2.7: Myeloperoxidase (MPO) staining for activated neutrophils.
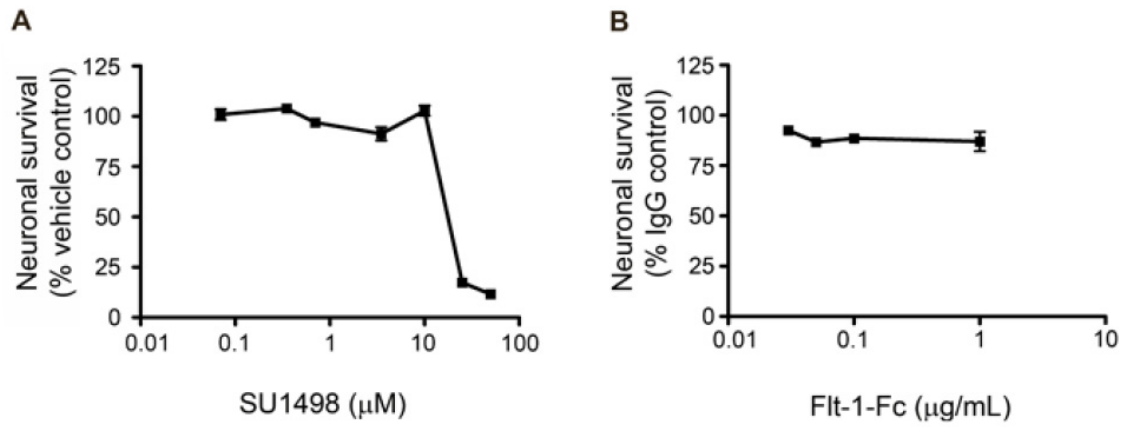
Figure 2.8: Dose-response of neurons to SU1498 and Flt-1-Fc.
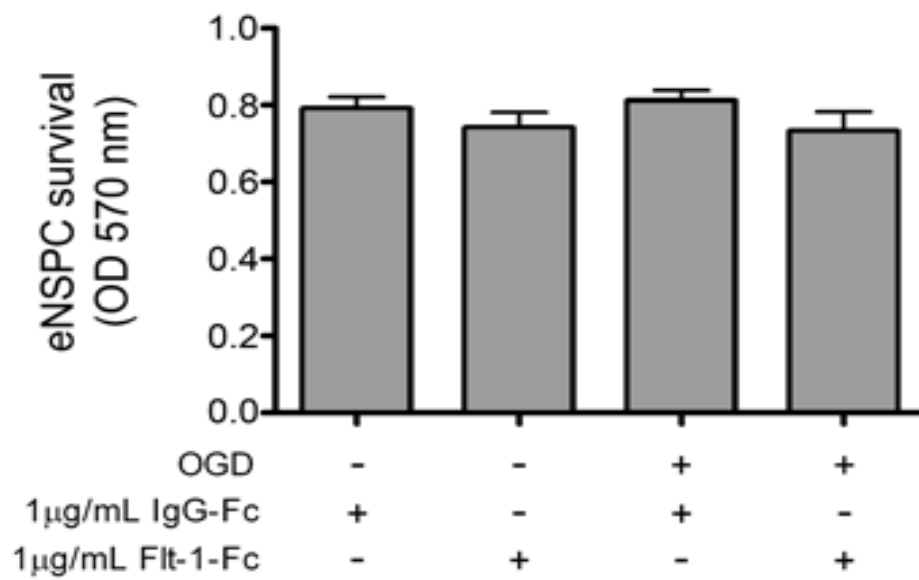
Figure 2.9: NSPC response to inhibition of autocrine VEGF.
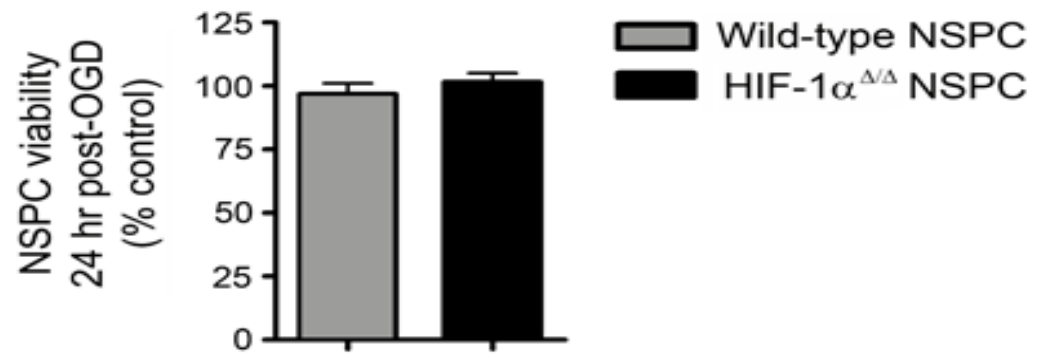
Figure 2.10: NSPC viability in response to 2 hr OGD.

3. Neural Stem/Progenitor Cells Display a Glycolytic Metabolic Phenotype Under Normoxia

Kate M. Candelario, C. William Shuttleworth, and Lee Anna Cunningham

Department of Neurosciences

University of New Mexico Health Sciences Center

Albuquerque, New Mexico 87131

3.1 Abstract

Neural stem/progenitor cells (NSPCs) of the subventricular zone (SVZ) lie in a niche in close contact with the vasculature. *In vitro*, NSPCs thrive under low oxygen tensions. Whether progenitors in the SVZ live in a hypoxic niche *in vivo* remains to be determined, but it is becoming increasingly apparent that oxygen tension influences embryonic and adult neural stem/progenitor cell properties. Very little is known concerning the bioenergetics of NSPCs, and determining their metabolic phenotype may assist in understanding basic stem cell properties as well as NSPC response to metabolic insults. To explore the metabolic phenotype of NSPCs in culture, we investigated the ability of embryonic and postnatal NSPCs to survive prolonged hypoxia and metabolic inhibition. NSPCs were compared to mature cortical neurons known to depend on oxidative metabolism. We show that NSPCs survive 24 h anoxia but are readily injured by glucose depletion. In addition, NSPCs were unable to utilize substrates for mitochondrial metabolism, but relied on both glycolysis and the pentose phosphate pathway in the cytosol. Conditioned media from cultured NSPCs contained elevated lactate production as well as elevated intracellular LDH activity compared to neuronal cultures. NSPCs displayed decreased oxygen consumption rate and increased extracellular acidification rate compared to neurons. Taken together, these data indicate that NSPCs utilize glycolysis under normoxic conditions and display a different metabolic phenotype compared to differentiated neurons.

3.2 Introduction

Neural stem cells are multipotent cells with self-renewing capabilities. During embryonic development radial glial cells within the ventricular zone serve as primitive neural stem cells that give rise to both neuronal and glial lineages (for review, see (Kriegstein and Alvarez-Buylla, 2009)). Neural stem cells derived from embryonic radial glia persist throughout adulthood within restricted regions that include the forebrain subventricular zone (SVZ) and hippocampal dentate subgranular zone (SGZ), where they continue to give rise to new neurons and glia of the adult olfactory bulb and dentate gyrus, respectively (Eriksson et al., 1998; Gage, 2000; Doetsch, 2003a, b; Alvarez-Buylla and Lim, 2004). Although the role of adult neurogenesis in normal brain function remains controversial, the potential therapeutic use of neural stem cells to replace damaged neurons and glia within the adult central nervous system is an area of intense research and clinical significance. Therapeutic approaches include transplantation of neural stem cells that have been expanded in an undifferentiated state *ex vivo*, and manipulation of endogenous neural stem cells that are resident within the adult brain. The therapeutic significance of understanding neural stem cell biology is also underscored by a potential link with CNS cancer stem cells, which share many properties with normal adult neural stem cells (Germano et al., 2010; Mohyeldin et al., 2010). Finally, neural stem cells of the adult brain display a remarkable capacity to withstand many types of metabolic and traumatic brain injuries as well as mount an endogenous regenerative response (Lichtenwalner and Parent, 2006), making them attractive targets for promoting structural and functional brain repair.

It is becoming increasingly apparent that oxygen levels have a profound effect on the stem cell niche and strongly influence the proliferation, self-renewal, and phenotypic fate choice of neural stem cells during normal development and disease (Csete, 2005; Simon and Keith, 2008; Panchision, 2009). Low oxygen tension promotes self-renewal of neural stem cells in culture and the preferential development of certain cell types upon differentiation (Morrison et al., 2000; Studer et al., 2000; Chen et al., 2007a; Pistollato et al., 2007; Burgers et al., 2008; Horie et al., 2008; Santilli et al., 2010). Disruption of oxygen availability by perinatal hypoxia/ischemia (Yang and Levison, 2006, 2007) or following stroke in adulthood (Arvidsson et al., 2002; Thored et al., 2006; Li et al., 2010) stimulates increased proliferation of cells within the SVZ and re-directed migration of SVZ-derivatives into the hypoxic brain region. In culture, neural stem/progenitor cells (NSPCs) are relatively resistant to brief periods of oxygen-glucose deprivation (OGD) when compared to primary cortical neurons (Roitbak et al., 2008; Harms et al., 2010), which are highly dependent upon oxidative metabolism for survival (Pellerin et al., 2002). Although studies have demonstrated that neural stem cells thrive under low oxygen conditions in cell culture (Morrison et al., 2000; Studer et al., 2000; Santilli et al., 2010), very little is known concerning the bioenergetics of NSPCs or how metabolic homeostasis is regulated in these cells. Such processes are, however, fundamental for maintenance of the neural stem/progenitor cell pool and neural stem/progenitor cell survival following a metabolic insult such as cerebral ischemia and stroke.

Much evidence indicates that adult stem cells from various tissues, embryonic stem cells derived from the inner cell mass of the blastocyst, and cancer stem cells all share common aspects of metabolic phenotype defined by high glycolytic flux, low oxygen

consumption, and minimal dependence on mitochondrial oxidative phosphorylation for ATP synthesis and survival (Chung et al., 2007; Lonergan et al., 2007; Kang et al., 2009; Panchision, 2009; Prigione et al., 2010). This form of metabolism is thought to underlie self-renewal and maintenance of the undifferentiated phenotype (Smith et al., 2000; Diehn et al., 2009). In the present study, we investigated the metabolic phenotype of embryonic and adult neural stem/progenitor cells (NSPCs) by testing their relative dependence on glycolysis *vs*. mitochondrial oxidative phosphorylation for survival.

3.3 Materials and Methods

3.3.1 Primary cell culture

This study was approved by the University of New Mexico Animal Care and Use Committee and conformed to the NIH Guidelines for use of animals in research. Timed pregnant female mice were sacrificed by isoflurane overdose and the embryos removed by cesarean section.

3.3.1.1 NSPC cultures

Neural stem/progenitor cells (NSPCs) were isolated from embryonic day 14.5 (E14.5) or from postnatal day 28 (PD28) C57BL/6J mice (The Jackson Laboratory, Bar Harbor, ME, USA). Embryonic NSPCs (eNSPC) were established from whole telencephalon as previously described (Ray et al., 1993; Harms et al., 2010). Postnatal NSPCs (pNSPC) were established from the microdissected SVZ of PD28 male C57BL/6J mice using described protocols (Babu et al., 2007; Smrt et al., 2007; Li et al., 2008) in conjunction with the MACS Neural Tissue Dissociation Kit (Miltenyi Biotec, Auburn, CA, USA). Following dissociation, NSPCs were plated in six-well tissue culture plates pre-coated

with poly-L-lysine (BD Biosciences) or on poly-L-lysine-coated glass coverslips within 24-well culture plates at a density of 3.125 x 10^4 cells/cm^2. The cultures were maintained under serum-free conditions in Neurobasal medium (Invitrogen) supplemented with B-27 supplement (2%; Invitrogen), glutamine (2.0 mM; Sigma), penicillin (100 U/ml; Invitrogen), streptomycin (100 μg/ml; Invitrogen), epidermal growth factor (EGF; 10 ng/mL; Invitrogen), and basic fibroblast growth factor (bFGF; 10 ng/mL; Invitrogen) (Ray et al., 1993; Wachs et al., 2003). Growth factors (EGF and bFGF) were added every other day and cells were passaged at least twice prior to use. These cultures have been previously shown to be uniformly nestin-positive and to undergo spontaneous differentiation into neurons and glia after growth factor withdrawl (Roitbak et al., 2008; Harms et al., 2010).

3.3.1.2   Cortical neuron cultures

Primary neuronal cultures were established from cerebral cortices of C57BL/6J embryos at gestation day 15.5 (E15.5), using enzymatic dissociation with trypsin as previously described (Wetzel et al., 2008; Harms et al., 2010). For cell viability assays, 3.9 x 10^5 dissociated cortical cells were plated on poly-L-lysine-coated coverslips (0.1 mg/ml; Sigma, St Louis, MO, USA) in 24-well plates (2.0 x 10^5 cells/cm^2). For biochemical procedures, 1.95 x 10^6 cells were plated on precoated poly-L-lysine six-well plates (2.0 x 10^5 cells/cm^2; BD Biosciences, San Diego, CA, USA). The cultures were maintained under serum-free conditions in Neurobasal medium (Invitrogen Corp., Carlsbad, CA, USA), supplemented with B-27 supplement (2%; Invitrogen Corp.), glutamine (0.5 mM; Sigma), glutamate (25 μM; Sigma), penicillin (100 U/ml), and streptomycin (100 μg/ml; Invitrogen Corp.). At 4 days *in vitro* (DIV), half of the medium was removed and

replaced with fresh medium without glutamate. At 7 DIV, neuronal cultures were used for experimentation. All cultures were maintained in a humidified incubator at 37°C with 5% CO_2.

3.3.2 Glucose or Oxygen Deprivation

3.3.2.1 Glucose deprivation

NSPC or neuronal cultures were deprived of glucose for 24 h by replacing culture media (25 mM glucose) with glucose- and pyruvate-free Neurobasal media (Invitrogen), supplemented with B-27 supplement (2%; Invitrogen Corp.), glutamine (0.5 mM; Sigma), glutamate (25 μM; Sigma), penicillin (100 U/ml) and streptomycin (100 μg/ml; Invitrogen Corp.), with or without added pyruvate (1.0-20 mM; Sigma) as indicated. For colorimetric assays (see below), phenol red-free Neurobasal media was used (Invitrogen).

3.3.2.2 Oxygen deprivation

For oxygen deprivation, primary NSPCs or cortical neuronal cultures were placed in an anaerobic chamber (Coy Laboratories, Grass Lake, MI, USA) containing a gas mixture of 5% CO_2, 5% H_2, and 85% N_2 (<0.2% O_2) for 24 h. Normal culture media was replaced with deoxygenated culture media (Invitrogen). Media was supplemented as described above for the appropriate cell type. Sister cultures placed at 37°C under normoxic (21% O_2) conditions served as non-hypoxic negative controls. Cell viability was normalized to non-hypoxic controls in all experiments.

3.3.3 Pharmacological Treatments

NSPC or neuronal cultures were exposed for 24 h to the following compounds, added directly to the culture media: sodium cyanide (CN; 0.01-2.0 mM; Sigma), rotenone (0.1-

100 μM; Sigma), oligomycin (Sigma; 0.5-10 μM), carbonyl cyanide 4-(trifluoromethoxy)phenylhydrazone (FCCP; 0.5-10 μM; Sigma), 2-deoxy-D-glucose (2-DG; 10 mM; Sigma), galactose (25 mM; Sigma), dichloroacetate (DCA; 500 μM; Sigma), and 6-aminonicotinamide (6-AN; 1-1000 μM; Sigma). Figure 3.1 depicts the metabolic pathways targeted by each of these drugs.

3.3.4 MTT cell viability assay

Cell viability was assessed using methylthiazolyldiphenyl-tetrazolium bromide (MTT) dissolved in PBS (0.5 mg/mL; Sigma) as described (Harms et al., 2010). Cultures were incubated with MTT at 37°C for 4 hr. In anaerobic cultures, the MTT solution was equilibrated to anoxia prior to addition to the culture wells. Formazan crystals were solubilized using 1:1 ethanol:DMSO solution. Absorbance was measured at 570 nm with a background subtraction of 630 nm.

3.3.5 Lactate dehydrogenase (LDH) and lactate colorimetric assays

For all colorimetric assays, NSPC or neuronal cultures were incubated in phenol red-free culture media for 24 h prior to assay measurements. Intracellular lactate dehydrogenase (LDH) activity was measured using the CytoTox96® Non-Radioactive Cytotoxicity Assay (Promega Corporation, Madison, WI, USA), according to the manufacturer protocol, and absorbance measured at 490 nm. Lactate concentration was measured in culture media using the colorimetric assay protocol from the Lactate Assay Kit (BioVision, Mountain View, CA, USA), and absorbance was measured at 570 nm. LDH and lactate measurements were normalized to protein using the MicroBCA kit (Pierce, Rockford, IL, USA).

3.3.6 Respiration and medium acidification rates

To monitor oxygen consumption and glycolysis in real time, we utilized a Seahorse Bioscience XF24 multiwell extracellular flux analyzer (Seahorse Bioscience, North Billerica, MA). The Seahorse XF24 instrumentation is a highly sensitive 24-well format for measuring oxygen consumption and medium acidification (rate of glycolysis). The XF24 utilizes a specialized 24-well culture plate, to allow for lowering an array of sensors to enclose a 7 µl fluid volume above a layer of attached cells in each well. Oxygen consumption rate (OCR) and medium extracellular acidification rate (ECAR) are monitored by fluorescence probes immobilized in matrices attached to the sensor and are measured in near real time over several hours at 37°C.

To compare oxygen consumption and glycolytic rates of neurons *vs*. NSPCs, embryonic cortical neurons or embryonic NSPCs were plated onto 24-well XF cell culture plates (Seahorse Bioscience) coated with poly-L-lysine (0.1 mg/mL; Sigma). Neurons were plated at a density of 1.95 x 10^5 cells/cm^2 and utilized after 7 days *in vitro* (DIV), with one-half media change at 4 DIV. eNSPCs were plated at a density of 6.0 x 10^5 cells/cm^2 and used at 3 DIV when they reached confluency. The XF sensor cartridge was loaded into the Seahorse analyzer following the manufacturer's instructions. All experiments were performed at 37°C with starting volume of 675 µL/well of DMEM containing 5 mM glucose (Sigma), 1mM pyruvate (Invitrogen), and 1 mM glutamine (Sigma). Mitochondrial inhibitors and vehicles were administered to all wells in a volume of 75 µL each/well via automated injector ports. Final concentrations of mitochondrial inhibitors were as follows: oligomycin (1 µM), FCCP (5 µM), and rotenone (1 µM). Each oxygen consumption and acidification rate data point represents one measurement

averaged over 2-3 wells. One measurement cycle is comprised of a mixing time of 3 minutes, followed by a wait time of 2 minutes, and a data acquisition period of 4 minutes. Data points established for the OCR/ECAR graph (Figure 3.6 C) are the mean of four measurement cycles per treatment group. At the end of the experiment, protein levels for each cell type were determined by the MicroBCA kit (Pierce). All oxygen consumption rates and acidification rates were normalized per μg protein/well.

3.4 Results

3.4.1 NSPCs require glucose for survival and are resistant to 24 hours of anoxia

We previously demonstrated that both embryonic and postnatal NSPCs survive 2-3 h oxygen-glucose deprivation (OGD) (Roitbak et al., 2008; Harms et al., 2010), whereas embryonic cortical neurons undergo significant cell death (Wetzel et al., 2008; Harms et al., 2010). To determine the relative dependence of NSPCs on oxygen *vs.* glucose availability for survival, we compared the viability of NSPCs following 24 h exposure to oxygen (<0.2% O_2) or glucose deprivation using an MTT cell viability assay. As shown in Figure 3.2 A, NSPCs survived 24 h anoxia in the presence of 25 mM glucose, but were unable to withstand 24 h glucose deprivation even under normoxic conditions. Glucose deprivation resulted in >75% cell loss under normoxia and >90% loss under anoxia. That NSPCs survive anoxia, but not glucose deprivation, suggests that NSPCs can rely more on glycolysis than on oxidative phosphorylation for survival.

3.4.2 NSPCs are resistant to pharmacologic inhibition of mitochondrial electron transport

Glucose serves as a primary metabolic substrate for the generation of ATP. Glycolysis is the anaerobic arm of glucose metabolism, and occurs within the cytosol to generate 2

molecules ATP per molecule of glucose. Oxidation of the glycolytic end product pyruvate occurs within the mitochondria via electron transfer and oxidative phosphorylation to generate up to 36 molecules of ATP per molecule of glucose (Vander Heiden et al., 2009).

To determine whether NSPCs require mitochondrial oxidative phosphorylation for survival, we exposed both embryonic NSPCs (eNSPC) and postnatal NSPCs (pNSPC) to pharmacological inhibitors of mitochondrial electron transport for 24 h under normoxic conditions. Primary cortical neurons, known to be highly reliant on oxidative phosphorylation for survival, served as a positive control for mitochondrial toxicity.

3.4.2.1   Complex I, IV, and V inhibition

As shown in Figure 3.2 B, neuronal cultures experienced approximately 75% cell loss following 24 h exposure to the complex IV inhibitor, cyanide (1.0 mM), whereas NSPCs displayed no appreciable loss in cell viability (Figure 3.2 B). Exposures up to 2.0 mM cyanide also resulted in no significant loss of NSPC viability, although neuronal cell death reached a maximal level at the lowest dose of 0.5 mM cyanide (Appendix Figure A1 A). To rule out the possibility that NSPC resistance to cyanide may be due to a short half-life of cyanide in culture media, we replaced the culture media containing fresh cyanide (1 mM) at 8 and 20 hours. Addition of cyanide three times to culture media decreased the number of viable eNSPCs by approximately 40% and neuronal survival by 90% (Figure 3.2 C). Both eNSPCs and pNSPCs also displayed relative resistance to the Complex V ATP synthase inhibitor, oligomycin (Figure 3.2 D; 1.0 μM), and to the complex I inhibitor, rotenone (Figure 3.2 E; 1 μM). Dose response curves for oligomycin

and rotenone are presented in the Appendix (Figure A1 B and C). Interestingly, pNSPCs displayed the greatest resistance to mitochondrial inhibition.

3.4.2.2 <u>Mitochondrial electron transport chain-oxidative phosphorylation uncoupling</u>

We next tested the sensitivity of neurons and eNSPCs to the uncoupler, FCCP (carbonyl cyanide 4-(trifluoromethoxy)phenylhydrazone). Ionophores such as FCCP uncouple mitochondrial electron transfer from oxidative phosphorylation (ATP synthesis) by creating electrical short circuit across the mitochondrial membrane. This stimulates oxygen consumption in an attempt to re-establish the proton gradient, slows mitochondrial ATP synthesis, which is reliant on a proton-motive force, and depletion of mitochondrial ATP and consumption of cytoplasmic ATP as complex V activity begins to run in reverse. As anticipated, FCCP treatment for 24 h resulted in a dose-dependent decrease in viability of both neurons and eNSPCs (Figure 3.3 A). However, concomitant exposure to oligomycin (0.5 μM) partially rescued eNSPCs, but not neurons, from FCCP toxicity. As shown in Figure 3.3 B, eNSPC cultures exposed to FCCP (5 μM) in the presence of oligomycin (0.5 μM) displayed a 14% increase in survival compared to treatment with FCCP alone ($p<0.05$). Oligomycin blockade of reversed ATP synthase activity prevents depletion of cytosolic ATP during FCCP treatment. The differential ability of oligomycin to rescue NSPCs, but not neurons, from FCCP toxicity suggests that NSPCs are more heavily reliant on cytosolic ATP production for survival.

3.4.3 NSPCs are reliant on glycolysis for energy metabolism and survival

3.4.3.1 Glycolytic inhibition with pyruvate replacement

To further explore the extent to which NSPCs are reliant on the anaerobic glycolytic arm of glucose metabolism for energy production and survival, NSPCs were grown under conditions of glycolytic inhibition in the presence or absence of the mitochondrial TCA substrate, pyruvate. Glycolytic inhibition was achieved by glucose deprivation combined with the glycolytic inhibitor 2-deoxy-D-glucose (2-DG; 10 mM). 2-DG is a competitive substrate for hexokinase phosphorylation; however, unlike glucose, phosphorylated 2-DG cannot be further metabolized, leading to its accumulation and blockade of the glycolytic arm of glucose metabolism (Pelicano et al., 2006). The glycolytic end product, pyruvate, is a primary mitochondrial oxidation substrate for ATP synthesis through oxidative phosphorylation, and can substitute for glucose in cells dependent upon mitochondrial oxidative phosphorylation for survival. Therefore we tested whether NSPCs could be rescued from glycolytic inhibition by pyruvate replacement (0.1-20 mM) for 24 h under normoxic conditions. As shown in Figure 3.4 A, primary cortical neurons were rescued from glycolytic inhibition by the TCA substrate pyruvate in a dose-dependent manner, whereas NSPCs underwent loss of viability following glycolytic inhibition independent of the presence of pyruvate (up to 20 mM) (Figure 3.4 A).

3.4.3.2 Inhibition of the pentose phosphate pathway

2-DG treatment not only blocks glycolysis, but also inhibits the pentose phosphate pathway (hexose monophosphate shunt) which requires glucose-6-phosphate to drive nicotinamide adenine dinucleotide phosphate (NADPH) production as well as generate important metabolic intermediates for macromolecule synthesis (Pelicano et al., 2006).

Proliferating cells require this pathway to generate biomass in preparation for production of a daughter cell (Vander Heiden et al., 2009). Although production of ATP through glycolysis is inefficient compared to complete metabolism of glucose through the TCA cycle and the electron transport chain, previous studies have demonstrated that highly proliferative cells have a relatively low ATP requirement but a tremendous glucose requirement to provide substrate for the pentose phosphate pathway (Vander Heiden et al., 2009). Shunting of glucose-6-phosphate from glycolysis toward the pentose pathway is achieved by glucose-6-phosphate dehydrogenase (G6PD), which converts glucose-6-phosphate to 6-phosphogluconolacetone. To determine whether NSPCs are reliant on the pentose phosphate pathway, G6PD was inhibited with 6-aminonicotinamide (6-AN; 100 μM; Figure 3.4 B), in the presence of glucose under normoxic conditions. As anticipated, NSPC survival was significantly impaired in the presence of 6-AN treatment compared to neurons, indicating NSPCs rely on the pentose phosphate pathway for survival and/or continued proliferation. A dose-response curve for 6-AN is presented in the Appendix (Figure A1 D).

3.4.3.3 <u>Galactose replacement</u>

To simultaneously maintain substrate for the pentose phosphate pathway and inhibit glycolysis, we substituted galactose for glucose in the culture medium. Galactose can be converted to glucose-6-phosphate via the Leloir pathway, but this reaction occurs too slowly for ATP synthesis to be maintained and forces use of glutamine as an energy source for mitochondrial metabolism (Weinberg and Chandel, 2009). Glutamine is converted to glutamate, which in turn is converted to α-ketoglutarate, a TCA cycle intermediate. Thus, substituting galactose for glucose tends to drive mitochondrial

respiration while keeping the pentose phosphate shunt relatively intact (Weinberg and Chandel, 2009). For these experiments, eNSPCs were exposed to 25 mM galactose and 1 mM pyruvate in the absence of glucose for 24 h at normoxia. As shown in Figure 3.4 C, eNSPC viability was decreased by >60% when galactose was provided as an alternative substrate. These results indicate that NSPCs are dependent upon glycolysis for survival and can not utilize pyruvate or glutamine as alternate substrates.

3.4.3.4 Inhibition of pyruvate dehydrogenase kinase (PDK)

In most oxidative cell types, pyruvate is converted to acetyl coenzyme A (acetyl-CoA) via the mitochondrial enzyme, pyruvate dehydrogenase, which is in turn regulated by the pyruvate dehydrogenase inhibitor, pyruvate dehydrogenase kinase (PDK). In glycolytic cell types, PDK phosphorylates and thereby inhibits pyruvate dehydrogenase to shunt pyruvate away from mitochondrial TCA metabolism (Semenza, 2010b).   To determine whether increased PDK activity may be responsible for shunting pyruvate from mitochondrial toward cytosolic metabolism, we treated NSPCs with the pyruvate dehydrogenase kinase inhibitor dicholoroacetate (DCA; 500 μM) (Bonnet et al., 2007). However, exposure to DCA did not render NSPCs sensitive to cyanide toxicity (500 μM; Figure 3.4 D), indicating that blocking PDK activity does not result in a metabolic shift toward mitochondrial respiration in these cells. Taken together, these data suggest that NSPCs rely on glycolysis and that pharmacological manipulation cannot force a metabolic shift toward mitochondrial respiration.

3.4.4 Lactate production and LDH activity are upregulated in NSPC cultures

Cells that rely heavily on glycolysis *vs.* mitochondrial oxidative phosphorylation for energy production shunt pyruvate toward lactate production and thereby display high enzymatic activity of lactate dehydrogenase (LDH). Conversion of pyruvate to lacate via LDH also results in increased production of NAD^+, which feeds back into the glycolytic pathway at the level of glyceraldehyde-3-phosphate to ensure a high rate of glycolytic flux. To determine whether NSPCs display increased lactate production under normoxic conditions, we measured lactate within 24 h eNSPC-conditioned media and measured LDH activity within these cells. As shown in Figure 3.5 A and B, both lactate production and LDH activity were 1.5- and 2-fold higher in NSPCs compared primary cortical neurons, respectively. These data are consistent with a high rate of glycolytic flux in NSPCs under normoxic conditions**.**

3.4.5 eNSPCs diplay diminished mitochondrial respiratory capacity and reduced Pasteur effect compared to neurons following mitochondrial inhibition

3.4.5.1 Oxygen consumption rate (OCR) and extracellular acidification rate (ECAR)

To further explore the metabolic phenotype of eNSPCs, we performed a mitochondrial stress test to compare the mitochondrial profile of eNSPCs to that of neurons. Using the XF-24 metabolic flux analyzer (Seahorse Bioscience), we measured the oxygen consumption rate (OCR) and extracellular acidification rate (ECAR) at baseline and in the presence of mitochondrial inhibitors. Baseline OCR was similar in both cultures, and addition of oligomycin (1.0 μM) did not reduce OCR, indicating a higher dose of oligomycin is required to distinguish the percent of oxygen consumption devoted to ATP production versus the amount devoted to maintenance of the proton gradient (Figure 3.6

70

A). To estimate the maximal respiratory capacity of the mitochondria, FCCP (5 μM) was added and resulted in a dramatic increase in OCR in both cell types (Figure 3.6 A). The maximal respiratory capacity of neurons was greater than eNSPCs (188.9% ± 9.6% *vs.* 154.8% ± 9.8% of baseline, respectively, $p<0.05$). The addition of the complex I inhibitor rotenone (1 μM) resulted in a further reduction of OCR values for both neurons and eNSPCs (13.48% ± 1.62% *vs.* 15.21% ± 2.56% of baseline, respectively, data not significant). Addition of rotenone, however, did not significantly alter ECAR in eNSPC cultures over baseline (109.7% ± 9.7%) yet decreased the ECAR of neurons to 38.01% ± 1.51% of baseline, indicating an ability of eNSPCs to utilize glycolysis regardless of mitochondrial function (Figure 3.6 B).

3.4.5.2   OCR/ECAR ratios

The ratio of OCR to ECAR provides insight as to whether a cell type is primarily glycolytic or oxidative. Plotting OCR as a function of ECAR, and setting up an arbitrary grid between the basal levels for each cell type, one can visualize that eNSPCs appear more glycolytic than neurons (Figure 3.6 C). In general, OCR/ECAR readings for eNSPCs are more toward the lower right quadrant, indicating that they are more glycolytic and less aerobic than neurons. Addition of FCCP reveals that eNSPCs have a maximal respiratory capacity with a lower OCR and a higher ECAR than neurons, and addition of rotenone shows that eNSPCs maintain increased ECAR compared to neurons. Taken together, the mitochondrial stress test reveals that eNSPCs are more glycolytic than neurons.

3.4.5.3   <u>Structural integrity of mitochondria</u>

Diminished respiratory capacity could be due to reduced number or reduced function of mitochondria in NSPCs. To determine whether NSPCs harbor mitochondria, cells were stained using MitoTracker® Red (Invitrogen) which accumulates in active mitochondria based on the membrane potential. As shown in the Appendix (Figure A2 A), NSPCs appeared to contain mitochondria. Furthermore, transmission electron microscopy (TEM) revealed elongated mitochondria within NSPCs with reasonably developed cristae structure (Figure A2 B). Thus reduced respiratory capacity does not appear to be due to the absence of mitochondria, or to underdeveloped cristae structure. Reduced respiratory capacity in NSPCs *vs.* neurons should also be reflected by differences in mitochondrial density, which were not quantified in this study.

3.5 Discussion

Understanding the metabolic phenotype of neural stem cells is important not only for fundamental cell biology, but also for understanding how these cells respond to metabolic insults. Despite this, very little was known of the metabolic requirements of neural stem cells. Previous studies have indicated that many stem cell types, including neural stem cells, thrive under low oxygen conditions, yet the metabolic underpinnings of these effects had remained largely unexplored. Here, we have investigated the metabolic phenotype of both embryonic and adult neural stem/progenitor cells in culture and demonstrate that these cells rely on glycolysis for survival, even under conditions of normoxia, and are relatively insensitive to mitochondrial metabolic toxins. Furthermore, we demonstrate that NSPCs cannot be rescued from glycolytic inhibition by providing alternative energy substrates such as glutamine or pyruvate, but do require the pentose

phosphate pathway. These studies provide insight into metabolic regulation in NSPCs and may provide important clues for understanding NSPC survival under pathologic metabolic insult.

We found that eNSPCs and pNSPCs are resistant to mitochondrial inhibitors of oxidative phosphorylation. Interestingly, pNSPCs were more resistant than eNSPCs. This seems surprising since eNSPCs would be expected to be adapted to the relative hypoxic environment of the embryo, which develops in an environment containing 3% O_2 before the circulatory system is established (Mitchell and Yochim, 1968; Rodesch et al., 1992; Fischer and Bavister, 1993; Simon and Keith, 2008). Our studies, therefore, indicate that eNSPCs and pNSPCs are not identical in sensitivity to mitochondrial toxins. Although relatively resistant, both embryonic and postnatal NSPCs eventually succumb to mitochondrial toxins at high concentrations. Since these experiments were performed in the presence of oxygen, it is possible that toxicity at high concentrations could be due to free radical formation. Flux through the electron transport chain leads to the formation of reactive oxygen species (ROS) which can cause cell death through damage to proteins, lipids, and nucleic acids (Saretzki et al., 2004; Lee and Wei, 2005). Further experiments testing these toxins under conditions of anoxia could help to resolve this issue.

Interestingly, free radical formation can not only act as a toxic agent to kill highly proliferative cells (Seyfried and Shelton, 2010), but is also involved in cell signaling and differentiation (Tsatmali et al., 2006). Cultured NSPCs proliferate rapidly due to stimulation with epidermal growth factor (EGF), which selects for the transient amplifying progenitor cell population of the SVZ that divides rapidly *in vivo* (Doetsch et al., 1997; Riquelme et al., 2008). We found that NSPCs could not be forced to rely on

mitochondrial respiration. Although electron transport and oxidative phosphorylation is the most efficient pathway for the generation of ATP, it is also a producer of ROS. Reactive oxygen species are not only toxic to proliferating cells, but ROS production (e.g. superoxide and hydrogen peroxide) can also signal differentiation of certain stem cell types including both cardiac stem cells (Puceat, 2005) and NSPCs (Tsatmali et al., 2006). As neuronal differentiation proceeds, higher levels of ROS are produced compared to the undifferentiated phenotype (Tsatmali et al., 2005). Cellular differentiation appears to be coupled with a shift in cellular metabolism from glycolysis to oxidative phosphorylation (Piccoli et al., 2005; Chung et al., 2007; Chen et al., 2008), which is likely to underly the shift in ROS production and ROS signaling as well. Thus mitochondrial function may be inextricably linked to maintaining stem cell phenotype through limiting ROS signaling and subsequent differentiation.

The degree of stemness appears to be correlated with bioenergentic function, with stem cell populations displaying glycolysis and differentiated cells utilizing oxidative phosphorylation (Piccoli et al., 2005; Chung et al., 2007; Chen et al., 2008). Our studies suggest that as NSPCs differentiate into post-mitotic neurons, there is a switch towards oxidative phosphorylation to drive synthesis of ATP, possibly due to a maturation of the mitochondria. However, EM analysis shows that NSPCs have normal appearing mitochondria and do not appear immature. Therefore, the lack of mitochondrial respiration is not due to a lack of mature mitochondria with normal cristae structure. In contrast, primitive stem cell types such as embryonic stem cells derived from the blastocyst, as well as adult stem cells such as cardiac stem cells, display low oxygen consumption coupled with mitochondria harboring poorly developed cristae structure

(Sathananthan et al., 2002; Perez-Terzic et al., 2003; Sturmey and Leese, 2003; Chung et al., 2007).

The high glucose requirement of NSPCs may explain their anatomical proximity to blood vessels *in vivo,* which would ensure an abundance of glucose. While one molecule of glucose is sufficient to generate more than enough ATP required by a proliferating cell, several molecules of glucose are required to generate the NADPH necessary for sufficient nucleotide and fatty acid synthesis (Vander Heiden et al., 2009). Cell division by the progenitor population requires biomass to create a daughter cell. Therefore the majority of glucose consumed by the cell is used to produce a daughter cell such that its conversion to glucose-6-phosphate is shunted toward nucleotide synthesis via the pentose phosphate pathway. It is via the pentose phosphate pathway that NADPH is produced (Vander Heiden et al., 2009). NSPC need for glucose may be related to their high rate of proliferation, balanced by a relatively minimal ATP requirement.

Shunting of the glycolytic product pyruvate away from the mitochondria results in increased lactate production. The conversion of pyruvate to lactate by the enzyme lactate dehydrogenase also yields NAD^+, an electron acceptor that can be fed back into the cytosolic glycolytic pathway at the level of glyceraldehyde-3-phosphate and reduced by glyceraldehyde-3-phosphate dehydrogenase. Interestingly, lactate production has also been shown to facilitate cell migration via modification of the extracellular matrix (e.g. increased acidification of the extracellular matrix by lactate production in cancer cells has been shown to facilitate metastasis) (Schlappack et al., 1991; Gatenby and Gillies, 2004). Lactate can also serve as a neuronal energy source (Bouzier-Sore et al., 2003), which raises the possibility of NSPC-neuron metabolic coupling similar to that of astrocytes.

Dependence upon glycolysis under aerobic conditions has been termed the Warburg effect, and is a predominant feature of many cancer cell types (Gatenby and Gillies, 2004). The mechanisms that drive glycolysis in the presence of oxygen are not entirely clear. Growth factor signaling, tyrosine kinase activity, and PI3K/Akt activity have been shown to upregulate the glycolytic phenotype through modulation of glycolytic enzymes, as well as stimulation of glucose uptake and utilization (Vander Heiden et al., 2009). Several studies have also suggested that constitutive expression of stabilized hypoxia-inducible factor-1α (HIF-1α) drives the glycolytic phenotype in many types of cancer cells. HIF-1α is a transcription factor that regulates the transcription of glycolytic enzymes in cancer cells, including the glucose transporters GLUT1 and GLUT3, lactate dehydrogenase, and all of the enzymes involved in glycolysis (Semenza, 2010b). We have previously demonstrated that NSPCs express constitutive HIF-1α stabilization in culture, through mechanisms that are not completely understood (Roitbak et al., 2008; Harms et al., 2010). Other studies have shown that HIF-1α is important in maintaining the undifferentiated phenotype of other stem cell types (Simon and Keith, 2008), but whether HIF-1α is driving the glycolytic phenotype under aerobic conditions in NSPCs has not yet been demonstrated (see Chapter 4).

Our work described here, together with other studies, demonstrate that low oxygen environments promote the survival and proliferation of NSPCs grown in culture (Morrison et al., 2000; Studer et al., 2000; Burgers et al., 2008; Santilli et al., 2010). In the adult mouse, brain tissues range from 0.5-8% O_2 and are said to be at "physiological hypoxia" compared to the surrounding atmosphere containing 21% O_2 (Zhu et al., 2005). However, NSPCs reside within a highly vascularized niche (Tavazoie et al., 2008) and it

is thus difficult to assume that these cells are oxygen-deficient. Never-the-less, the primitive metabolic phenotype of NSPCs may indeed underlie their ability to withstand a precipitous decline in oxygen tension under conditions of pathological hypoxia, e.g., following cerebral infarction.

3.6 Figure Legends

Figure 3.1: Diagram of metabolic inhibition. Glucose metabolism occurs in the cytosol via glycolysis and the pentose phosphate pathway. Pyruvate can be shunted into the mitochondria, where cellular metabolism occurs via the TCA cycle within the mitochondrial matrix and electron transport across the inner mitochondrial membrane. Media supplements used in this study are depicted in the color red. Glycolytic inhibitors include 2-deoxy-D-glucose (2-DG) and galactose. The pentose phosphate shunt is inhibited by 6-aminonicotinamide (6-AN). Dichloroacetate (DCA) inhibits pyruvate dehydrogenase kinase (PDK) to allow increased activity of pyruvate dehydrogenase (PDH). Electron transport chain inhibitors include rotenone, cyanide, and oligomycin. FCCP is a protonophore that uncouples the oxidation of NADH from the phosphorylation of ADP within the electron transport chain.

Figure 3.2: NSPCs survive anoxia and do not require electron transport. (A) MTT colorimetric viability assay of embryonic NSPCs exposed to 24 h oxygen and/or glucose deprivation. **(B-D)** MTT colorimetric viability assay of neurons, eNSPCs, and pNSPCs with 24 h exposure to mitochondrial inhibitors at normoxia: **(B-C)** cyanide, **(D)** oligomycin, **(E)** rotenone. Experiments depicted in B, D, and E were treated with the

inhibitor one time. For figure 3.2 C, cells were treated with cyanide 3 times. n=4 per treatment group. *p<0.05. **p<0.01. ***p<0.001. ****p<0.0001.

Figure 3.3: NSPCs utilize cytosolic production of ATP. (A) MTT colorimetric viability assay of neurons and eNSPCs in response to 24 h incubation with increasing concentrations of the ionophore FCCP (0.5-10 μM) at normoxia. **(B)** MTT colorimetric viability assay of neurons and eNSPCs in the presence or absence of oligomycin (0.5 μM) and/or FCCP (5 μM). n=4 per treatment group. *p<0.05.

Figure 3.4: NSPCs do not utilize mitochondrial respiration and rely on the pentose phosphate shunt. (A-B) MTT colorimetric viability assay of neurons and eNSPCs at normoxia following 24 h treatment in the presence of: **(A)** 2-DG (10 mM) plus pyruvate (0.1-20 mM), **(B)** 6-aminonicotinamide (6-AN; 100 μM), or **(C)** galactose (25 mM). **(D)** MTT colorimetric viability assay of eNSPCs incubated for 24 h at normoxia with cyanide (500 μM) and/or DCA (500 μM). n=4 per treatment group. **p<0.001. ***p<0.0001.

Figure 3.5: LDH activity and lactate production are elevated in NSPC cultures. (C) Intracellular LDH activity in neurons and eNSPCs. **(D)** Lactate concentration in the media of neuron and eNSPC cultures. n=4 per treatment group. *p<0.05. ***p<0.0001.

Figure 3.6: NSPCs display decreased maximal respiratory capacity and increased extracellular acidification compared to neurons. Measurement of **(A)** oxygen consumption rate (OCR), **(B)** extracellular acidification rate (ECAR), and **(C)** OCR to ECAR ratio of neurons *vs.* eNSPCs at baseline and in the presence of oligomycin (oligo; 1.0 μM), FCCP (5 μM), and rotenone (1 μM). n=2-3 per treatment group.

Figure A1: Dose-response curves of neurons and eNSPCs in the presence of cellular respiration inhibitors: (A) cyanide (0.1-2 mM), **(B)** oligomycin (1-10 μM), **(C)** rotenone (0.1-100 μM), and **(D)** 6-aminonicotinamide (6-AN; 1-1000 μM).

Figure A2: Visualization of mitochondria using **(A)** MitoTracker Red staining or **(B)** transmission electron microscopy. For immunocytochemistry in (A), NSPCs were identified using an antibody against nestin (green).
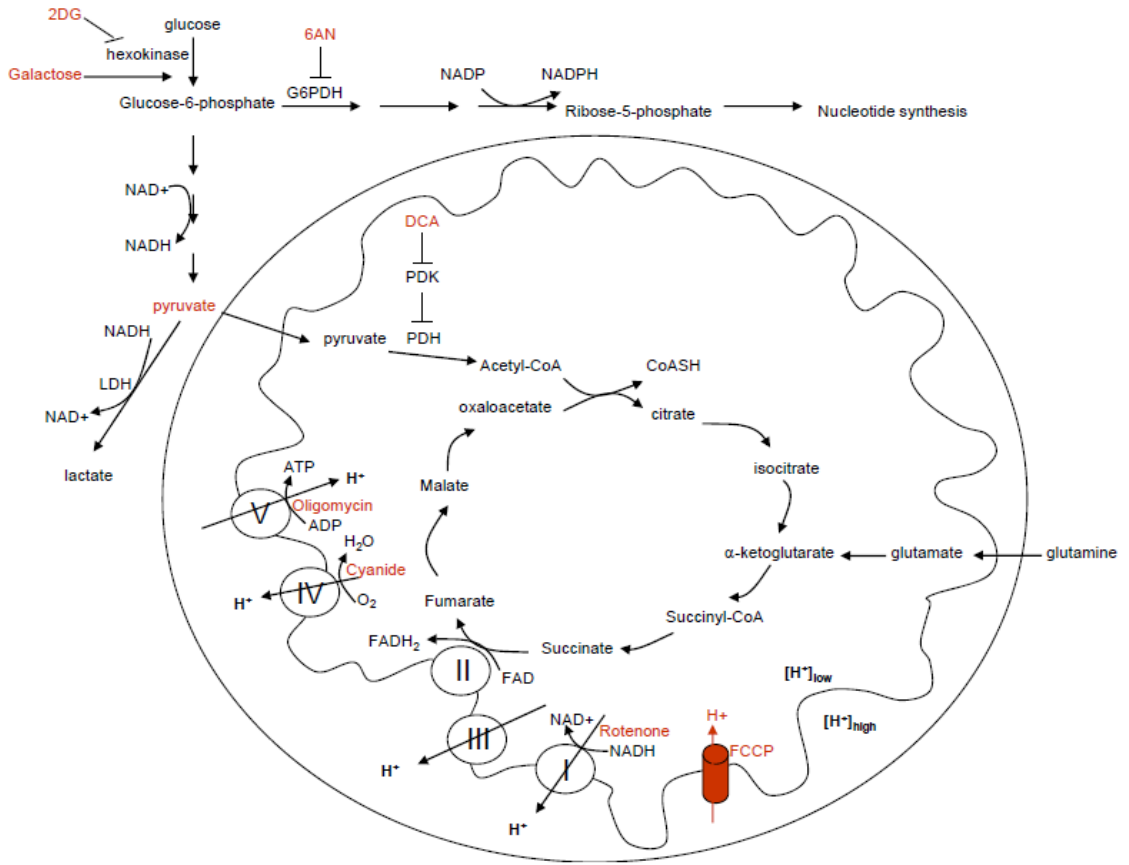
Figure 3.1: Diagram of metabolic inhibition.
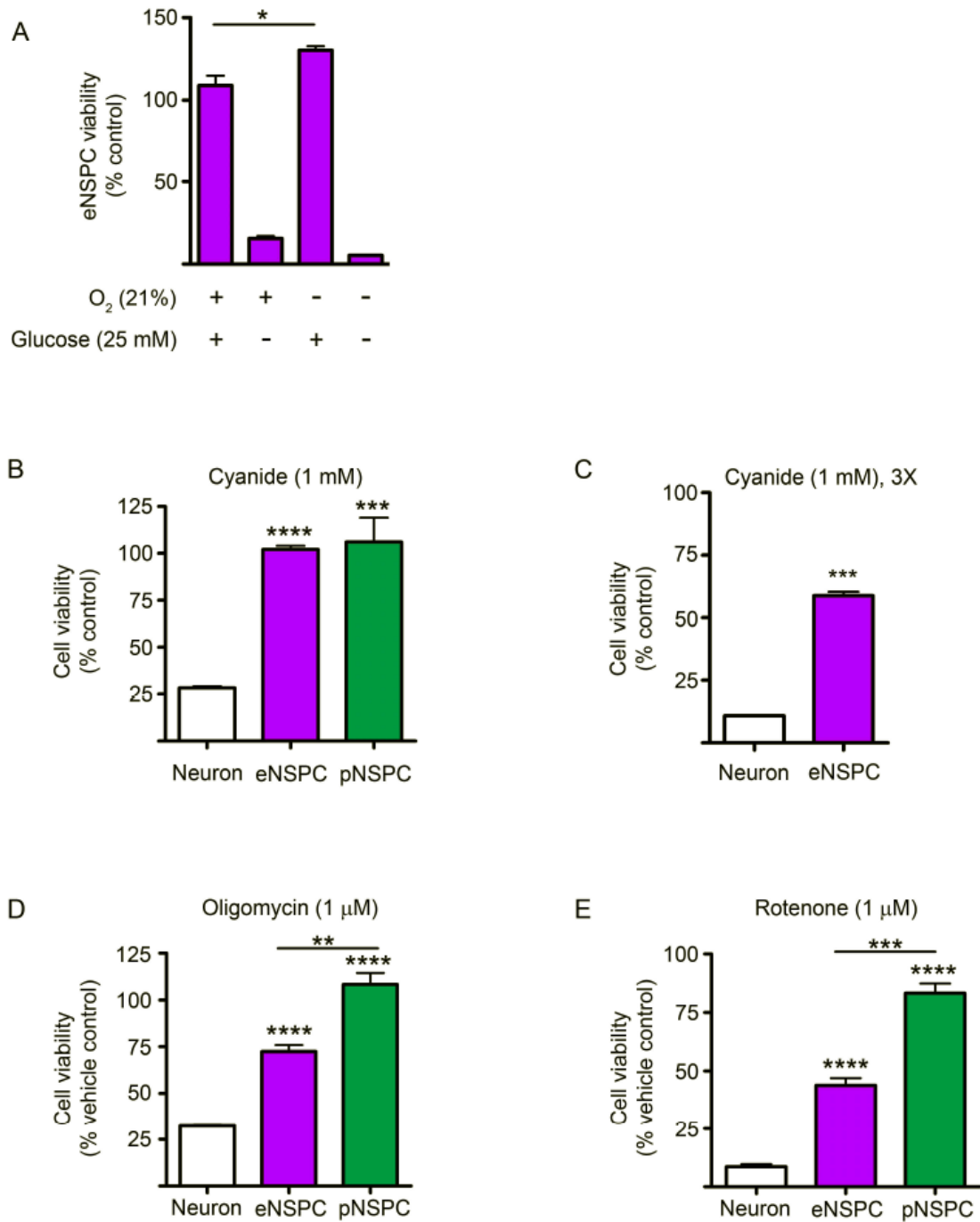
Figure 3.2: NSPCs survive anoxia and do not require electron transport
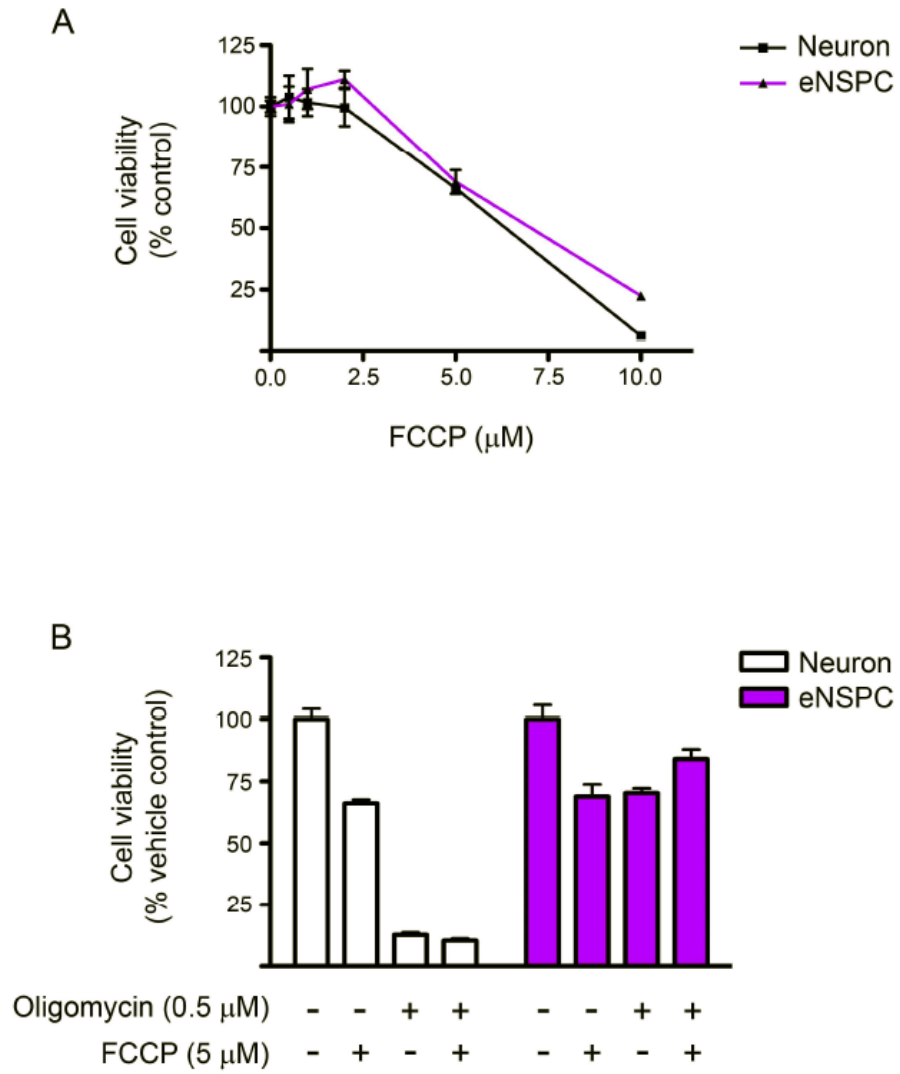
Figure 3.3: NSPCs utilize cytosolic production of ATP
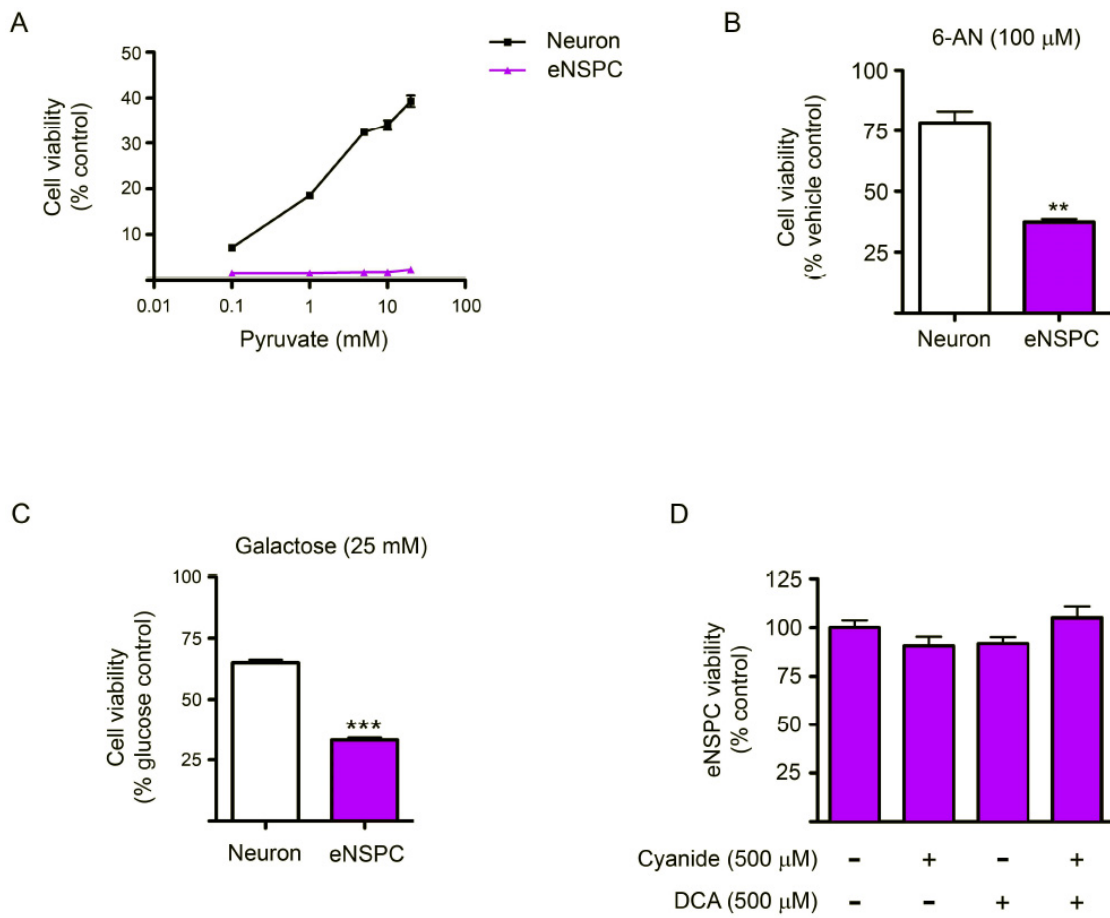
Figure 3.4: NSPCs do not utilize mitochondrial respiration and rely on the pentose phosphate shunt
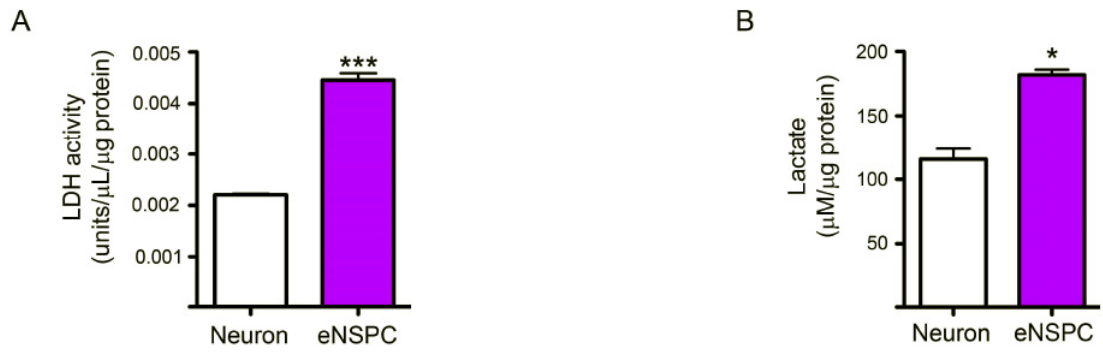
Figure 3.5: LDH activity and lactate production are elevated in NSPC cultures
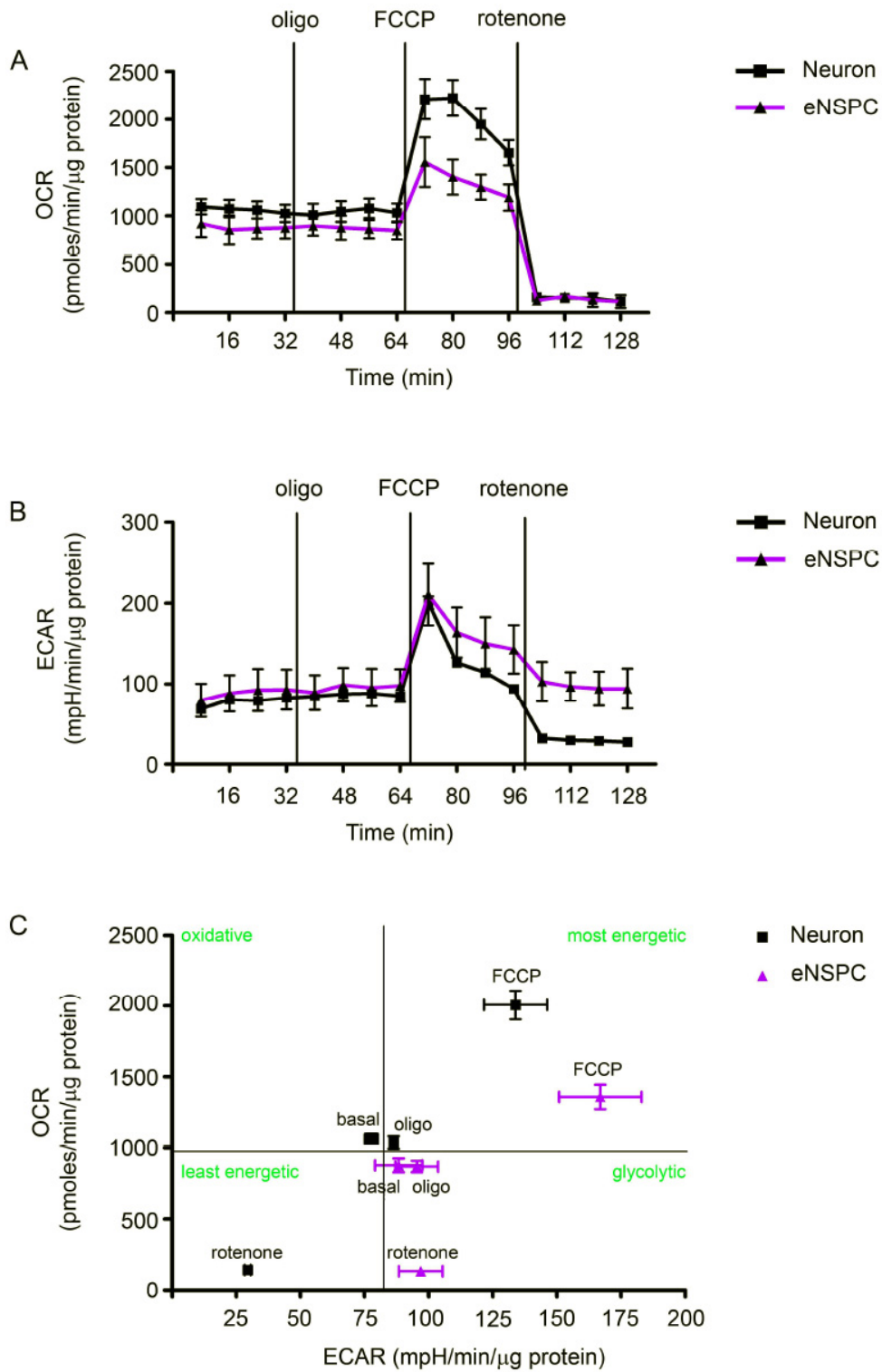
Figure 3.6: NSPCs display decreased maximal respiratory capacity and increased extracellular acidification compared to neurons

4. Use of *nestin*-CreER[T2]/R26R-YFP/*Hif1a*^{fl/fl} mice to study HIF-1α regulation of NSPC metabolic phenotype

Kate M. Candelario*[1], Lu Li*[1], Kelsey Thomas[1], Diane Lagace[2], Amelia Eisch[3], and Lee Anna Cunningham[1]

*These authors contributed equally to this work

[1]Department of Neurosciences, University of New Mexico Health Sciences Center, Albuquerque, New Mexico 87131

[2]Department of Cellular and Molecular Medicine, University of Ottawa, Ottawa, Ontario Canada K1H 8M5

[3]Department of Psychiatry, University of Texas Southwestern Medical Center, Dallas, Texas 75390

4.1 Abstract

We have shown previously that hypoxia-inducible factor-1α (HIF-1α) protein is stabilized in neural stem/progenitor cells (NSPCs) *in vitro* at normoxia and upregulated with exposure to hypoxia. We have also determined that NSPCs utilize glycolysis under normoxic conditions and are not affected by mitochondrial inhibition. To investigate the role of HIF-1α in NSPC viability and metabolism, we generated a conditional and inducible transgenic mouse model to specifically ablate expression of *Hif1a* from nestin-positive NSPCs. Administration of tamoxifen to *nestin*-CreER^{T2}/R26R-YFP/*Hif1a*$^{fl/fl}$ mice results in complete deletion of the *Hif1a* gene from NSPCs. Experimentation on embryonic and postnatal NSPCs cultured from these mice reveal that HIF-1α is required for the ability of NSPCs to withstand 24 h anoxia, but does not regulate the glycolytic metabolic phenotype. These studies implicate a role for HIF-1α in NSPCs as well as provide a useful tool for examining this role *in vivo*.

4.2 Introduction

Embryonic and adult neural stem/progenitor cells (NSPCs) express low levels of constitutively stabilized hypoxia-inducible factor-1α (HIF-1α) *in vitro* (Harms et al., 2010) and within the adult subventricular zone (SVZ) and subgranular zone (SGZ) *in vivo* (Roitbak et al., 2010). Furthermore, we have demonstrated that both embryonic and postnatal NSPCs are primarily reliant on glycolysis and display minimal dependence on mitochondrial oxidative phosphorylation for ATP synthesis and survival (Chapter 3). These metabolic characteristics may be extremely important to ensure survival of NSPCs under conditions of metabolic injury, such as severe hypoxia that can occur following stroke or other pathological conditions. In this chapter, we describe the generation and characterization of a unique triple transgenic mouse, *nestin*-CreER^T2/R26R-YFP/*Hif1a*^fl/fl, to test the hypothesis that HIF-1α represents a cell-intrinsic regulator of NSPC metabolism, important for NSPC cytogenesis under normal and stroke conditions.

High glycolytic flux and low mitochondrial oxygen consumption under non-hypoxic conditions is known as the Warburg effect and is driven by constitutive HIF-1α stabilization in several cancer cell types. To determine whether aerobic glycolysis in NSPCs is also dependent on constitutive HIF-1α expression, it is necessary to utilize methods that allow for NSPC-specific gene deletion of *Hif1a*. Previous studies utilizing lentivector shRNAi resulted in a partial knockdown of HIF-1α by approximately 70% that was not sustained over multiple passages (Roitbak et al., 2008) (and unpublished observations). Therefore, we have utilized a Cre/LoxP approach to achieve complete *Hif1a* gene deletion from NSPCs in culture and to generate mice for conditional and inducible ablation of HIF-1α protein expression selectively from NSPCs *in vivo*.

For these studies, we have crossed *nestin*-CreER[T2]/R26R-YFP mice (generated by A. Eisch, UTSW) (Lagace et al., 2007) to mice that harbor bi-allelic floxed exon 2 of the *Hif1a* gene sequence (generated by Randall Johnson, UCSD) (Ryan et al., 2000). This approach is depicted in Figure 4.1. The *Hif1a*^{fl/fl} mutant mice have been well-characterized and utilized to generate many conditional and/or inducible transgenic mice to study cell-type specific knockout of the *Hif1a* gene. Specific examples of Cre drivers that have been used include phosphoenolpyruvate carboxykinase (PEPCK) (Higgins et al., 2007), synapsin I (Rempe et al., 2006), nestin (Milosevic et al., 2007), and calcium/calmodulin-dependent kinase II promoter (Sheldon et al., 2009). Also, the *Hif1a*^{fl/fl} mouse has been used to study the role of neuronal/glial HIF-1α on ischemic tolerance in adult brain (Vangeison et al., 2008). Similarly, the *nestin*-CreER[T2]/R26R-YFP mice have been crossed with *lox*P transgenics to study cell-intrinsic signaling molecules that regulate neurogenesis *in vivo*. For example, Gao and colleagues demonstrated the role of NeuroD1 for survival and maturation of newborn granule cells (Gao et al., 2009); and Lagace and colleagues utilized this line to show cyclin dependent kinase 5 (Cdk5) as a critical neural stem cell intrinsic regulator of adult hippocampal neurogenesis (Lagace et al., 2008).

In the present study, we established a *nestin*-CreER[T2]/R26R-YFP/*Hif1a*^{fl/fl} triple transgenic mouse, and charactered Cre-mediated recombination *in vitro* and *in vivo*. Our findings indicate that *Hif1a* gene deletion impairs the ability of NSPCs to survive hypoxia, but surprisingly loss of *Hif1a* expression does not result in a shift in metabolic phenotype under aerobic conditions.

4.3 Materials and Methods

4.3.1 Generation of *nestin*-CreER^{T2}/R26R-YFP/*Hif1a*$^{fl/fl}$ triple transgenic mice

This study was approved by the University of New Mexico Animal Care and Use Committee and conformed to the NIH Guidelines for use of animals in research. *Nestin*-CreER^{T2}/R26R-YFP mice were obtained from the laboratory of Amelia Eisch at the University of Texas Southwestern Medical Center (Lagace et al., 2007). *Hif1a* floxed mice were obtained from The Jackson Laboratory (Bar Harbor, ME, USA), which were originally generated and described by Randall Johnson's group at the University of California, San Diego (Ryan et al., 2000). Both the nestin-CreER^{T2}/R26R-YFP mouse and the *Hif1a* floxed mouse (*Hif1a*$^{fl/fl}$) had been crossed to the C57BL/6J background.

To generate a tamoxifen-inducible *nestin*-CreER^{T2}/R26R-YFP/*Hif1a*$^{fl/fl}$ mouse, the *nestin*-CreER^{T2}/R26R-YFP mouse was crossed to the *Hif1a* floxed mouse (*Hif1a*$^{fl/fl}$). The first cross of these two lines generated an F1 population that was heterozygous at all three alleles (Cre$^{+/-}$ YFP$^{+/-}$ HIF$^{wt/fl}$). Crosses made from the F1 population yielded progeny predicted by Mendelian genetics, such that each allele segregated in a 1:2:1 fashion. Further crosses were performed by selecting for *nestin*-CreER^{T2} positive, R26R-YFP homozygous, and *Hif1a*$^{fl/fl}$ mice. To confirm the genotype of each mouse, DNA from the tissue was isolated and amplified with polymerase chain reaction (PCR) using the following primers: Cre forward 5'– ATT TGC CTG CAT TAC CGG TC -3', Cre reverse 5'- ATC AAC GTT TTC TTT TCG G -3' (Indra et al., 1999); YFP primer 1: 5'- AAA GTC GCT CTG AGT TGT TAT -3', YFP primer 2: 5'- GCG AAG AGT TTG TCC TCA ACC -3', YFP primer 3: 5'- GGA GCG GGA GAA ATG GAT ATG -3'

(Soriano, 1999); HIF forward HF26: 5'- TGATGTGGGTGCTGGTGTC -3' and HIF

reverse HF27: 5'- TTGTGTTGGGGCAGTACTG -3' (Schipani et al., 2001).

4.3.2 Cre-mediated recombination

NSPCs were isolated from embryonic day 14 telencephalon or post-natal day 28 SVZ

from wild-type, $Hif1a^{fl/fl}$, $nestin$-CreER^{T2}/R26R-YFP bitransgenic, or $nestin$-

CreER^{T2}/R26R-YFP/$Hif1a^{fl/fl}$ triple transgenic mice by methods described previously

(Harms et al., 2010) (Chapters 2 and 3). The efficiency of Cre-mediated recombination

was tested using a) direct exposure to the tamoxifen metabolite 4-hydroxy-tamoxifen (4-

OH-TM) in culture, b) exposure to Ad-CMV-Cre in culture, and c) $in vivo$ administration

of tamoxifen prior to NSPC isolation.

4.3.2.1   4-hydroxy-tamoxifen in culture

The efficacy of 4-hydroxy-tamoxifen (4-OH-TM) to induce Cre-mediated recombination

was initially tested in NSPCs isolated from $nestin$-CreER^{T2}/R26R-YFP bitransgenic

mice. NSPCs were isolated from embryonic $nestin$-CreER^{T2}/R26R-YFP mice as

previously described and exposed to increasing concentrations of 4-OH-TM (0.1-100

µM; Sigma) for 24 h. 4-OH-TM binds to the mutated estrogen receptor (ER^{T2}). Cre-

mediated recombination was visualized by YFP expression in $nestin$-CreER^{T2}/R26R-YFP

(see immunocytochemical procedures below).

4.3.2.2   Ad-CMV-Cre in culture

As an alternative approach to 4-OH-TM exposure, we tested the recombination efficacy

following incubation of NSPCs with adenovirus that confers Cre recombinase expression

under the CMV constitutive transcriptional promoter. Embryonic NSPCs were isolated from wild-type, $Hif1a^{fl/fl}$, or $nestin$-CreER^{T2}/R26R-YFP mice and passaged twice. Following the second passage NSPCs were plated on poly-L-lysine coated 6-well plates (BD Biosciences) at a density of 2.6×10^4 cells/cm^2 and allowed to adhere to the plate overnight. Based on previous observations, NSPCs multiply by a factor of 2 over 24 h. Twenty-four hours after plating, we assumed a cell density of 5.2×10^4 cells/cm^2 and infected cells with $0.0005 \times 10^{10} - 0.01 \times 10^{10}$ plaque formation units (PFU) of Ad-CMV-Cre (Vector Biolabs, Philadelphia, PA, USA), yielding a concentration of 10-200 MOI (multiplicity of infection). NSPCs were incubated in Ad-CMV-Cre for 48 h, then washed and incubated in fresh media for an additional 24 h. NSPCs were then passaged twice more before used in experiments.

4.3.2.3 *In vivo* tamoxifen administration

To induce Cre-mediated recombination in embryonic NSPCs, tamoxifen induction of Cre recombinase was achieved by interperitoneal (i.p.) injection of timed pregnant females at gestational day 10.5 (E10.5) with tamoxifen (75 mg/kg; Sigma, St. Louis, MO) dissolved in 10% ethanol/90% sunflower oil. Two injections of tamoxifen 6 hours apart were administered, as described (Battiste et al., 2007). On gestational day 14.5 (E14.5), the pregnant female mice were sacrificed by isoflurane overdose and the embryos were removed by cesarean section. To induce Cre-recombination in post-natal NSPCs, post-natal day 28 male mice were injected with tamoxifen (180 mg/kg per day) i.p. for 5 consecutive days (Lagace et al., 2007), and sacrificed 5 days after the last injection with isoflurane overdose. NSPC cultures were set-up as described (Harms et al., 2010) (Chapters 2 and 3). To isolate the YFP-positive population, unlabeled NSPCs were

sorted using flow cytometry (ex/em 488 nm/530 nm; Beckman Coulter Legacy MoFlo, Brea, CA, USA). For cell sorting, the use of an antibody was not required. YFP-positive NSPCs were expanded in culture prior to use in experiments.

4.3.3 PCR analysis of *Hif1a* gene deletion from isolated NSPCs

To confirm deletion of exon 2 of the *Hif1a* gene either following Ad-CMV-Cre treatment or cell sorting, DNA was isolated and efficiency of cre-recombination was detected with PCR using forward primer 5'- TGT TAA ATA AAA GCT TGG AC -3' and reverse primer 5'- GCA GTT AAG AGC ACT AGT TG -3' (Milosevic et al., 2007). Successful DNA recombination yields *Hif1a* gene-deleted NSPCs ($Hif1a^{\Delta/\Delta}$), as indicated by the loss of the 1200 bp band amplification product and appearance of a 250 bp band.

4.3.4 Oxygen deprivation, MTT viability, and treatment with mitochondrial and metabolic inhibitors were all performed as described previously (Chapters 2 and 3)

4.3.5 Immunocytochemistry

Cultured cells were fixed on coverslips with 4% paraformaldehyde and incubated in monoclonal mouse anti-nestin (1:200; Chemicon, Temecula, CA, USA) and rabbit polyclonal anti-green fluorescent protein (GFP; 1:200; Invitrogen). Immunofluorescence was visualized using FITC- or Cy3-conjugated secondary antibodies (1:250; Jackson ImmunoResearch Laboratories). DAPI nuclear stain was used to identify cell bodies of cultured cells (Invitrogen). Immunofluorescence was analyzed using high-resolution confocal microscopy (Zeiss LSM510, Thornwood, NY, USA) or conventional fluorescence microscopy.

Data are expressed as means $\pm$ S.E.M. Significant differences between means were determined by student's t-test, one-way analysis of variance (ANOVA) with Tukey multiple comparisons *post hoc* analysis, or two-way ANOVA using Bonferroni comparisons *post hoc* analysis using Prism software (Graphpad Software, San Diego, CA, USA). P values < 0.05 are considered statistically significant.

4.4 Results

4.4.1 4-hydroxy-tamoxifen treatment of NSPCs results in high toxicity and low recombination efficiency in culture

The *nestin*-CreER^{T2} gene drives expression of Cre recombinase fused to an estrogen receptor containing a mutated ligand-binding domain (ER^{T2}) that preferentially binds the tamoxifen metabolite 4-hydroxy-tamoxifen (4-OH-TM) in nestin-positive cells (Lagace et al., 2007). In our cultures, binding of 4-OH-TM to ER^{T2} induces receptor dimerization and translocation of Cre recombinase to the nucleus, permitting Cre-mediated excision of the STOP codon and subsequent expression of YFP. Hayashi and McMahon demonstrated that addition of 1 μM 4-OH-TM to fibroblast cultures causes Cre-mediated recombination to occur *in vitro* (Hayashi and McMahon, 2002).

To determine the efficacy and potential toxicity of 4-OH-TM, we treated embryonic *nestin*-CreER^{T2}/R26R-YFP NSPCs to increasing concentrations of 4-OH-TM (0.1-100 μM) for 24 h (Figure 4.2 A). Whereas doses of 1-2 μM did not appear to have cytotoxic effects of NSPCs, we found that 10 μM and 100 μM doses significantly decreased the

number of viable cells in culture by 46 and 98 percent, respectively (Figure 4.2 A). That 10 μM 4-OH-TM is toxic to other cell types has been previously reported (Coezy et al., 1982). However, YFP expression was not optimal at non-toxic doses of 4-OH-TM (Figure 4.2 C). These results indicate low efficacy and high toxicity of 4-OH-TM to NSPCs in culture.

4.4.2 Ad-CMV-Cre stimulates highly efficient recombination *in vitro* with low toxicity

We tested the use of adenovirus that utilizes a strong constitutive cytomegalovirus (CMV) promoter to drive Cre recombinase expression (Ad-CMV-Cre) in transduced NSPCs. Initial studies were performed to determine the dose and timecourse for use of Ad-CMV-Cre on NSPCs cultured from bitransgenic embryonic *nestin*-CreER[T2]/R26R-YFP mice. Cultures were incubated with Ad-CMV-Cre up to 48 h at multiplicities of infection (MOI) of 10-200, based on a previous report performed in mouse primary osteoblasts (Fulzele et al., 2007). Cell viability, as measured using MTT reduction, was not reduced by viral infections of 10-100 MOI Ad-CMV-Cre after 48 h incubation. However, at 200 MOI the adenoviral vector was cytotoxic to NSPCs (Figure 4.3 A). Confocal images of fixed cultures stained with an antibody against green fluorescent protein (GFP) revealed maximal YFP reporter gene expression with incubation of Ad-CMV-Cre at a dose of 50 MOI for 48 h (Figure 4.3 B), indicating maximal Cre recombinase-induced recombination at this dose.

Prior to completion of the triple-transgenic *nestin*-CreER[T2]/R26R-YFP/*Hif1a*^{fl/fl} mouse, preliminary studies to delete *Hif1a* from NSPCs in culture were performed on cells obtained from *Hif1a*^{fl/fl} mice using Ad-CMV-Cre. To delete *Hif1a* from NSPCs in

culture, Ad-CMV-Cre was added at a dose of 50 MOI for 48 h to NSPCs cultured from $Hif1a^{fl/fl}$ mice. As reported in Chapter 2 of this dissertation, PCR of genomic DNA isolated from these cells failed to amplify exon 2 sequences in the $Hif1a$ gene, indicating that recombination between the loxP sites was effective (Figure 2.5 A). Transcriptional activity of HIF-1α protein was ablated as determined by an HRE Binding Activity assay (Figure 2.5 B). Based on these data, the estimated efficiency of recombination induced by 50 MOI Ad-CMV-Cre is 100%. The results suggest high recombination efficiency at non-toxic doses of Ad-CMV-Cre.

4.4.3 *In vivo* deletion of *Hif1a* using *nestin*-CreER^{T2}/R26R-YFP/*Hif1a*$^{fl/fl}$

To create a mouse where $Hif1a$ could be specifically deleted from nestin-positive NSPCs *in vivo*, we crossed the *nestin*-CreER^{T2}/R26R-YFP mouse to the $Hif1a^{fl/fl}$ mouse as described under the Methods section. To track the segregation of the alleles for the three genes, nestin-CreER^{T2}, R26R-YFP, and $Hif1a^{fl/fl}$, PCR was performed with genomic DNA from tissue of each animal. For the $Hif1a$ gene, the PCR product from the wild-type gene appeared around 300 bp whereas the product from the floxed allele appeared at around 350 bp, due to inclusion of one loxP site (Figure 4.4 A). The PCR of genomic DNA in Figure 4.4 B illustrates one animal that is homozygous for the R26R-YFP transgene (YFP$^{+/+}$), positive for *nestin*-CreER^{T2} (Cre^{+}), and homozygous for the mutant floxed $Hif1a$ gene (HIF$^{fl/fl}$), demonstrating our ability to create a *nestin*-CreER^{T2}/R26R-YFP/*Hif1a*$^{fl/fl}$ triple-transgenic mouse (Figure 4.4 B).

Recombination of the DNA between two loxP sites is required for the excision of the intervening sequence. To stimulate Cre expression, mice were injected with tamoxifen,

the metabolite of which binds to the mutated estrogen receptor (ER^{T2}), allowing $CreER^{T2}$ to translocate to the nucleus in nestin-positive cells. In these triple-transgenic mice, cre-mediated excision permits YFP expression and simultaneous deletion of exon 2 of the *Hif1a* gene to disrupt the generation of a functional HIF-1α protein. To ensure *Hif1a* deletion, Cre-mediated excision at both loci was determined by expression of YFP. NSPCs were sorted following *in vitro* expansion after two passages using a flow cytometer capable of single cell deposition. Cellular expression of YFP was excited by the laser (ex 488 nm) without the need to label with an antibody, and YFP+ cells were found to be 10-25% of the total cell population (Figure 4.4 C and D). Only the YFP+ cells were collected and expanded for experiments. PCR analysis of genomic DNA isolated from YFP+ NSPCs in culture confirmed that exon 2 of the *Hif1a* gene was successfully deleted from all YFP+ cells (Figure 4.4 E). Data shown in figures 4.4 C-E were generated from postnatal NSPCs; however, similar data were obtained from embryonic NSPCs (data not shown).

4.4.4 Impact of *Hif1a* gene deletion on NSPC metabolic phenotype

4.4.4.1 *Hif1a* deletion impairs NSPC survival under hypoxia

We reported previously that NSPCs survive 24 h anoxia, and that they express basal levels of HIF-1α protein which is upregulated with anoxia (Harms et al., 2010) (Chapter 2). To determine whether HIF-1α expression is required for NSPCs to remain viable during anoxia, *nestin*-CreER^{T2}/R26R-YFP/*Hif1a*$^{wt/wt}$ *vs. nestin*-CreER^{T2}/R26R-YFP/*Hif1a*$^{Δ/Δ}$ NSPCs were exposed to 24 h anoxia. The number of surviving NSPCs was reduced by over 45% with *Hif1a* gene deletion (Figure 4.5 A). These data confirmed our

preliminary findings using Ad-CMV-Cre to delete *Hif1a in vitro* (Figure 4.5 B). These

data suggests that NSPCs require HIF-1α expression to survive 24 h anoxia.

4.4.4.2   *Hif1a*$^{\Delta/\Delta}$ NSPCs remain insensitive to mitochondrial toxins

HIF-1α has been shown in cancer cells to control expression of genes involved in cellular

metabolism (Semenza, 2010b), including upregulation of glucose transporters and

glycolytic enzymes, including lactate dehydrogenase (LDH). HIF-1α also upregulates

the enzyme pyruvate dehydrogenase kinase (PDK), which phosphorylates and deactivates

pyruvate dehydrogenase (PDH), preventing the conversion of pyruvate into acetyl-CoA

for use in the tricarboxylic acid (TCA) cycle (Kim et al., 2006; Papandreou et al., 2006).

Electrons generated by the TCA cycle are used in the electron transport chain to carry out

oxidative phosphorylation, where the reduction of oxygen is coupled to the

phosphorylation of ADP to generate ATP. Cytochrome c oxidase is the complex of the

electron transport chain that uses oxygen as a final electron acceptor, which can be

chemically inhibited by cyanide. We showed previously that while cyanide is cytotoxic

to neurons, a cell that relies on oxidative metabolism, it is not cytotoxic to NSPCs

(Chapter 3). Since deletion of *Hif1a* from NSPCs rendered these cells susceptible to

oxygen deprivation (Figure 4.5), we asked whether *Hif1a*-deleted NSPCs would also be

susceptible to cyanide treatment, as cyanide and oxygen would be expected to act on the

same electron transport complex.

Experiments employing the tamoxifen-inducible system to induce recombination *in vivo*

using NSPCs isolated from *nestin*-CreER^{T2}/R26R-YFP/*Hif1a*$^{\Delta/\Delta}$ *vs. nestin*-

CreER^{T2}/R26R-YFP/*Hif1a*$^{wt/wt}$ revealed that *Hif1a* deletion does not render NSPCs

susceptible to cyanide treatment (1 mM; Figure 4.6 A), a similar finding as data

generated from Ad-CMV-Cre-induced deletion of *Hif1a* (Figure 4.6 G). Furthermore,

Hif1a deletion in NSPCs did not change their sensitivity to the ATP synthase inhibitor

oligomycin (1 μM; Figure 4.6 B) nor to the complex I inhibitor rotenone (1 μM; Figure

4.6 C). Dose-response curves for cyanide, oligomycin, and rotenone appear in the

Appendix (Figure B1). These data suggest that HIF-1α does not regulate NSPC use of

mitochondrial respiration.

4.4.4.3   *Hif1a*$^{\Delta/\Delta}$ NSPCs remain glycolytic

To determine whether HIF-1α regulates the glycolytic phenotype of NSPCs described

previously (Chapter 3), glycolysis was blocked using the hexokinase inhibitor 2-deoxy-

D-glucose (2-DG; 10 mM) and pyruvate (10 mM) was added as an alternative substrate

to glucose. Interestingly, tamoxifen-induced *Hif1a* deletion did not increase NSPC

ability to utilize pyruvate (Figure 4.6 D), a finding similar to data generated from *Hif1a*$^{fl/fl}$

NSPCs treated with Ad-CMV-Cre (Figure 4.6 H). In addition, NSPC utilization of

pyruvate and glutamine in the presence of the glycolytic inhibitor galactose was not

upregulated with *Hif1a* deletion (Figure 4.6 E). Whereas NSPCs display a glycolytic

metabolic phenotype (Chapter 3), these data indicate that HIF-1α does not regulate this

phenotype.

Treatment of *nestin*-CreER^{T2}/R26R-YFP/*Hif1a*$^{\Delta/\Delta}$ NSPCs with the pentose phosphate

shunt inhibitor 6-aminonicotinamide (6-AN; 500 μM) resulted a small but significant

increase in the number of viable cells compared to *nestin*-CreER^{T2}/R26R-

YFP/*Hif1a*^{wt/wt} NSPCs (Figure 4.6 F). These data suggest that HIF-1α may play a role in NSPC reliance on the pentose phosphate shunt.

4.5 Discussion

The *nestin*-CreER[T2]/R26R-YFP/*Hif1a*^{fl/fl} mouse allows for conditional induction of Cre recombinase in nestin-positive cells *in vivo*, induced with tamoxfen injection at a chosen point in time in development or adulthood. This model circumvents the problems that arise from addition of inducers of Cre recombinase into culture media. Whereas others have found that addition of 4-OH-TM to culture media induces cre-recombination in fibroblasts cultured from CreER[T2] mice (Hayashi and McMahon, 2002), we found that non-toxic concentrations of 4-OH-TM did not provide sufficient recombination in our cultures. The reason for this discrepancy may be due to reporter expression differences (β-galactosidase activity *vs.* YFP expression).

Ad-CMV-Cre-mediated recombination led to greater expression of YFP compared to 4-OH-TM-induced Cre expression. The increased efficiency of recombination with Ad-CMV-Cre is likely due to the higher levels of Cre recombinase expression that is driven by the cytomegalovirus promoter, and the independence from tamoxifen-mediated nuclear translocation. Although treatment of NSPCs with Ad-CMV-Cre did not appear to impact NSPC viability, we observed an inability of NSPCs to survive differentiation following growth factor withdrawal in cultures treated with adenovirus (data not shown). Thus, Ad-CMV-Cre treatment provides a useful tool for studying the *in vitro* effects of *Hif1a* deletion on NSPC metabolism, but may not be appropriate for studies focused on lineage fate *in vitro* or *in vivo*.

Use of tamoxifen to stimulate recombination *in vivo* prior to isolation of NSPCs allows for tamoxifen clearance prior to harvesting of the recombined NSPC cell population. This ensures that any interaction tamoxifen would have with endogenous estrogen receptors are avoided during experimentation. In addition, Cre-mediated recombination in the *nestin*-CreER^{T2}/R26R-YFP/*Hif1a*$^{fl/fl}$ mouse turns on the genetic reporter gene (YFP), which provides an indelible label marking recombined cells and all progeny.

Intraperitoneal (i.p) administration of tamoxifen to *nestin*-CreER^{T2}/R26R-YFP/*Hif1a*$^{wt/wt}$ and *nestin*-CreER^{T2}/R26R-YFP/*Hif1a*$^{fl/fl}$ mice yielded a recombined population of YFP-positive cells that reflected only 10-25% of the total NSPCs population expanded in culture from both embryonic and post-natal mice. We anticipated a higher recombination efficiency since our NSPC cultures are uniformly nestin-positive (Chapter 2, Figure 2.2). This correlates with our observation *in vivo* that only 20% of doublecortin-positive migrating neuroblasts expressed YFP six weeks following transient middle cerebral artery occlusion (MCAO) in *nestin*-CreER^{T2}/R26R-YFP mice (Li et al., 2010) (Appendix). The *in vitro* capability to sort out the YFP-positive NSPCs ensures a relatively pure population of recombined cells for *ex vivo* study. Following cell sorting, YFP-positive NSPCs proliferate in culture, survive multiple passages, maintain YFP expression, and, in the case of *nestin*-CreER^{T2}/R26R-YFP/*Hif1a*$^{\Delta/\Delta}$ cells, maintain deletion of exon 2 of the *Hif1a* gene. Therefore, suboptimal labeling efficiency using tamoxifen injections does not hinder our ability to use these cells for experiments in cell culture.

We have also begun to characterize the *in vivo* behavior of *Hif1a*-deleted NSPCs following tamoxifen administration to adult *nestin*-CreER^{T2}/R26R-YFP/*Hif1a*$^{fl/fl}$ mice.

Preliminary data suggest that *Hif1a* gene deletion results in NSPC depletion from SVZ and SGZ and a reduced cytogenic response to stroke (Appendix C).

Prior to the creation of this model, it was not possible to delete *Hif1a* from nestin-positive NSPCs *in vivo*. Systemic deletion of *Hif1a* results in embryonic lethality by embryonic day 11 due to underdevelopment of the vasculature and cardiac malformation (Iyer et al., 1998; Ryan et al., 1998; Kotch et al., 1999). Deletion of *Hif1a* from nestin-positive cells driven by Cre recombinase activity throughout embryonic development leads to hydrocephalus, neuronal loss, decreased proliferation, and impaired spatial memory (Tomita et al., 2003, Milosevic, 2007 #116). Administration of tamoxifen to activate Cre recombinase in adult mice allows the animal to develop normally prior to Cre-mediated excision of *Hif1a*, Thus, the results of our studies are not confounded by impairments in brain development.

In addition to deletion of *Hif1a*, tamoxifen-induced Cre-recombination turns on the expression of YFP in nestin-positive cells. This provides us with a tool to map the fate of recombined NSPCs (see the appended manuscript (Li et al., 2010)). This method has advantages over the use of bromodeoxyuridine (BrdU), a thymidine analog that incorporates into dividing cells during S phase, which is diluted as the cell divides and can also label damaged cells undergoing DNA repair (Gould and Gross, 2002; Rakic, 2002; Taupin, 2007). In the genetic model, the "unstopped" YFP gene is transmitted genetically and YFP is maintained in all progeny originally induced to express Cre recombinase.

The ability of HIF-1α to protect NSPCs from anoxia-induced cell death was not surprising given its ability to regulate genes involved in the survival of hypoxic cancer cells (Semenza, 2003). In most cell types, HIF-1α protein is degraded when oxygen is present. However, under hypoxia, HIF-1α protein is stabilized and able to enter the nucleus to act as a transcription factor (Semenza, 2003). In cancer cells, HIF-1α transcriptional regulation of glycolytic enzymes shifts cellular metabolism away from the mitochondria, even when oxygen is abundant, to exclusively glycolytic (Seagroves et al., 2001), where cells produce all required ATP via glycolysis (Warburg effect). Given our observation that NSPCs also utilize glycolysis without mitochondrial metabolism, and that HIF-1α protein is stabilized in normoxic NSPCs, we hypothesized that HIF-1α regulates the metabolic phenotype of NSPCs. However, our data suggest unexpectedly that HIF-1α does not regulate this phenotype as NSPCs remain glycolytic in the absence of HIF-1α. How HIF-1α regulates the ability of NSPCs to survive anoxia remains to be determined.

Of interest is that HIF-1α deletion decreases NSPC susceptibility to the pentose phosphate pathway inhibitor 6-AN. The pentose phosphate pathway is required for nicotinamide adenine dinucleotide phosphate (NADPH) production as well as nucleotide synthesis. HIF-1α has been shown previously to enhance the rate of pentose phosphate pathway activity (Soucek et al., 2003). Production of NADPH has been shown to combat the production of reactive oxygen species, for NADPH serves as a cofactor for antioxidant enzymes and acts to maintain high levels of reduced glutathione, an antioxidant. In conjunction with our findings that NSPCs rely more heavily on the

pentose phosphate pathway than neurons (Chapter 3), constitutive expression of HIF-1α may act to regulate the reliance of NSPCs on this pathway.

Adult NSPCs reside within complex microenvironmental niches specialized to support NSPC self-renewal and to regulate the production of newborn neurons and glia within the adult brain. The ability to parse microenvironmental NSPC-extrinsic factors (e.g. vasculature, secreted factors, extracellular matrix, cell-cell interactions, neurotransmitters) *vs*. NSPC-intrinsic molecular mediators (e.g. cyclins, intracellular signaling cascades) of adult neurogenesis has been greatly facilitated by the use of inducible genetic approaches in which gene expression can be manipulated specifically in NSPCs within the context of the adult brain. The inducible model can be used to study the importance of NSPC-specific HIF-1α both *in vitro and in vivo*, and its role in proliferation, migration, and differentiation without affecting the development of the animal. This model will serve as a tool to better understand the role of HIF-1α in NSPCs under non-pathological conditions as well as recovery following stroke.

4.6 Figure Legends

Figure 4.1: Diagram of genetic manipulations to create nestin-specific *Hif1a* knock-out mice. Recombination in *nestin*-CreER^{T2}/R26R-YFP/*Hif1a*$^{fl/fl}$ triple transgenic mice is induced with tamoxifen to drive expression of YFP and delete exon 2 of the *Hif1a* gene.

Figure 4.2: Cre-mediated recombination using 4-OH-TM. **(A)** MTT colorimetric viability assays measuring the viability of embryonic NSPCs from *nestin*-CreER^{T2}/R26R-YFP mice treated with 4-OH-TM for 24 h compared to untreated controls. **(B,C)** NSPCs

grown from embryonic nestin-CreER^{T2}/R26R-YFP mice were untreated (B) or treated with 2 μM 4-OH-TM (C). Fixed cells were labeled with antibodies to detect yellow fluorescent protein (GFP; green) and nestin (red). Images taken at 40X. ***p<0.001. n=3 per treatment group.

Figure 4.3: Cre-mediated recombination using Ad-CMV-Cre. (A) MTT colorimetric viability assay measuring the viability of embryonic NSPCs from *nestin*-CreER^{T2}/R26R-YFP mice in the presence of increasing concentrations of Ad-CMV-Cre (10-200 MOI) for 48 h compared to untreated controls. **(B)** Immunocytochemistry for nestin (red) and YFP (green) of fixed *nestin*-CreER^{T2}/R26R-YFP embryonic NSPCs following 48 h incubation in 50 MOI Ad-CMV-Cre. Scale bar = 20 μm. *p<0.05. n=3 per treatment group.

Figure 4.4: Tamoxifen-inducible Cre-mediated recombination. (A) PCR products generated using primers to detect *Hif1a* alleles, both wild-type (HIF$^{wt/wt}$) and floxed (HIF$^{fl/fl}$). Genomic DNA was isolated from tissue. **(B)** PCR products generated using primers to detect the presence of R26R-YFP (YFP$^{+/+}$), *nestin*-CreER^{T2} (Cre^{+}), and *Hif1a*$^{fl/fl}$ (HIF$^{fl/fl}$) alleles. The gel shown depicts one mouse that is homozygous at all three genes. Genomic DNA was isolated from tissue. **(C)** Cell sorting using flow cytometry of *nestin*-CreER^{T2}/R26R-YFP/*Hif1a*$^{wt/wt}$ post-natal NSPCs using a 488 nm laser. The YFP+ (R2 and R3) population is approximately 25% of the total number of cells. **(D)** Cell sorting using flow cytometry of *nestin*-CreER^{T2}/R26R-YFP/*Hif1a*$^{Δ/Δ}$ post-natal NSPCs using a 488 nm laser. The YFP+ (R2 and R3) population is approximately 10% of the total number of cells. **(E)** PCR products produced from the amplification of

genomic DNA isolated from post-natal NSPCs grown in culture from both cells that were unsorted and those that were sorted using flow cytometry for expression of YFP. Deletion of exon 2 from *Hif1a* is indicated by the loss of the 1200 bp band amplification product and appearance of a 250 bp band (HIF$^{\Delta/\Delta}$).

Figure 4.5: NSPC viability in the presence of 24 h anoxia. (A,B) MTT colorimetric viability assay of embryonic NSPCs exposed to 24 h anoxia. **(A)** Cre recombinase was induced with injection of tamoxifen into *nestin*-CreER^{T2}/R26R-YFP/*Hif1a*$^{wt/wt}$ (Cre/YFP/HIF$^{wt/wt}$) and *nestin*-CreER^{T2}/R26R-YFP/*Hif1a*$^{\Delta/\Delta}$ (Cre/YFP/HIF$^{\Delta/\Delta}$) mice. Experiments were performed on YFP+ NSPCs. **(B)** Cre recombinase was induced in *Hif1a*$^{fl/fl}$ NSPCs with the addition of Ad-CMV-Cre (HIF$^{\Delta/\Delta}$). Wild-type cultures also received Ad-CMV-Cre (HIF$^{wt/wt}$). **p<0.01. n=4 per treatment group.

Figure 4.6: Effect of *Hif1a* gene deletion on NSPC metabolic phenotype. MTT colorimetric viability assays of embryonic NSPC cultures. **(A-F)** NSPCs cultured from embryonic *nestin*-CreER^{T2}/R26R-YFP/*Hif1a*$^{wt/wt}$ (Cre/YFP/HIF$^{wt/wt}$) and *nestin*-CreER^{T2}/R26R-YFP/*Hif1a*$^{\Delta/\Delta}$ (Cre/YFP/HIF$^{\Delta/\Delta}$) mice where Cre-mediated recombination was induced *in vivo* using tamoxifen. Cultures were treated with the following inhibitors for 24 hr: (A) cyanide (1 mM), (B) oligomycin (1 μM), (C) rotenone (1 μM), (D) 2-deoxy-D-glucose (2-DG; 10 mM) plus pyruvate (10 mM), (E) galactose (25 mM) plus pyruvate (1 mM), and (F) 6-aminonicotinamide (6-AN; 500 μM). **(G-H)** NSPCs cultured from wild-type (HIF$^{wt/wt}$) and *Hif1a*$^{\Delta/\Delta}$ (HIF$^{\Delta/\Delta}$) embryonic NSPCs where cre-recombination was induced by Ad-CMV-Cre. NSPCs were treated with the following

inhibitors for 24 h: (G) cyanide (1 mM) and (H) 2-deoxy-D-glucose (2-DG; 10 mM) plus pyruvate (0.1-100 mM). **p<0.01. n=3-4 per treatment group.

Figure B1: Dose-response to mitochondrial inhibitors. **(A-C)** *Nestin*-CreER^{T2}/R26R-YFP/*Hif1a*$^{wt/wt}$ (Cre/YFP/HIF$^{wt/wt}$) and *nestin*-CreER^{T2}/R26R-YFP/*Hif1a*$^{\Delta/\Delta}$ (Cre/YFP/HIF$^{\Delta/\Delta}$) cultures were exposed to the following inhibitors for 24 h at normoxia: **(A)** cyanide (0.1-1 mM), **(B)** oligomycin (0.1-10 μM), and **(C)** rotenone (0.1-100 μM). **(D)** Dose-response of wild-type and *Hif1a*$^{\Delta/\Delta}$ embryonic NSPCs treated with Ad-CMV-Cre to cyanide (0.1-2 mM) for 24 h at normoxia.

Figure 4.1: Diagram of genetic manipulations to create nestin-specific *Hif1a* knock-out mice

Figure 4.2: Cre-mediated recombination using 4-OH-TM

A)

NSPC survival (% control)

Ad-CMV-Cre (MOI)

B)

YFP
Nestin
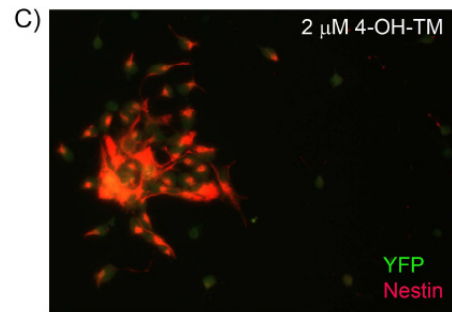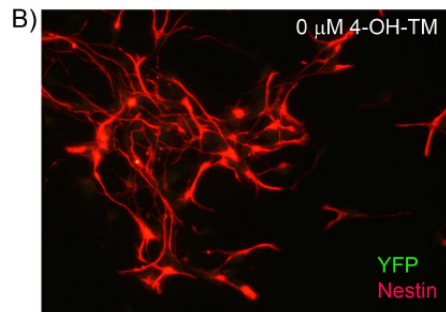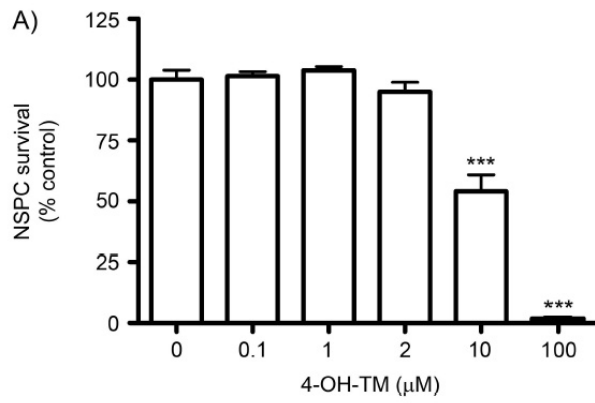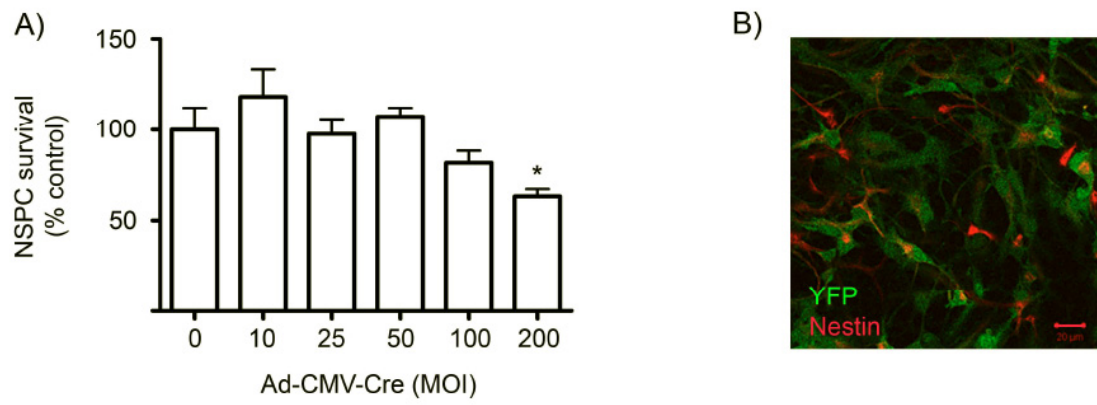
Figure 4.3: Cre-mediated recombination using Ad-CMV-Cre

Figure 4.4: Tamoxifen-inducible Cre-mediated recombination

A) *In vivo* TAM injection

B) *In vitro* Ad-CMV-Cre
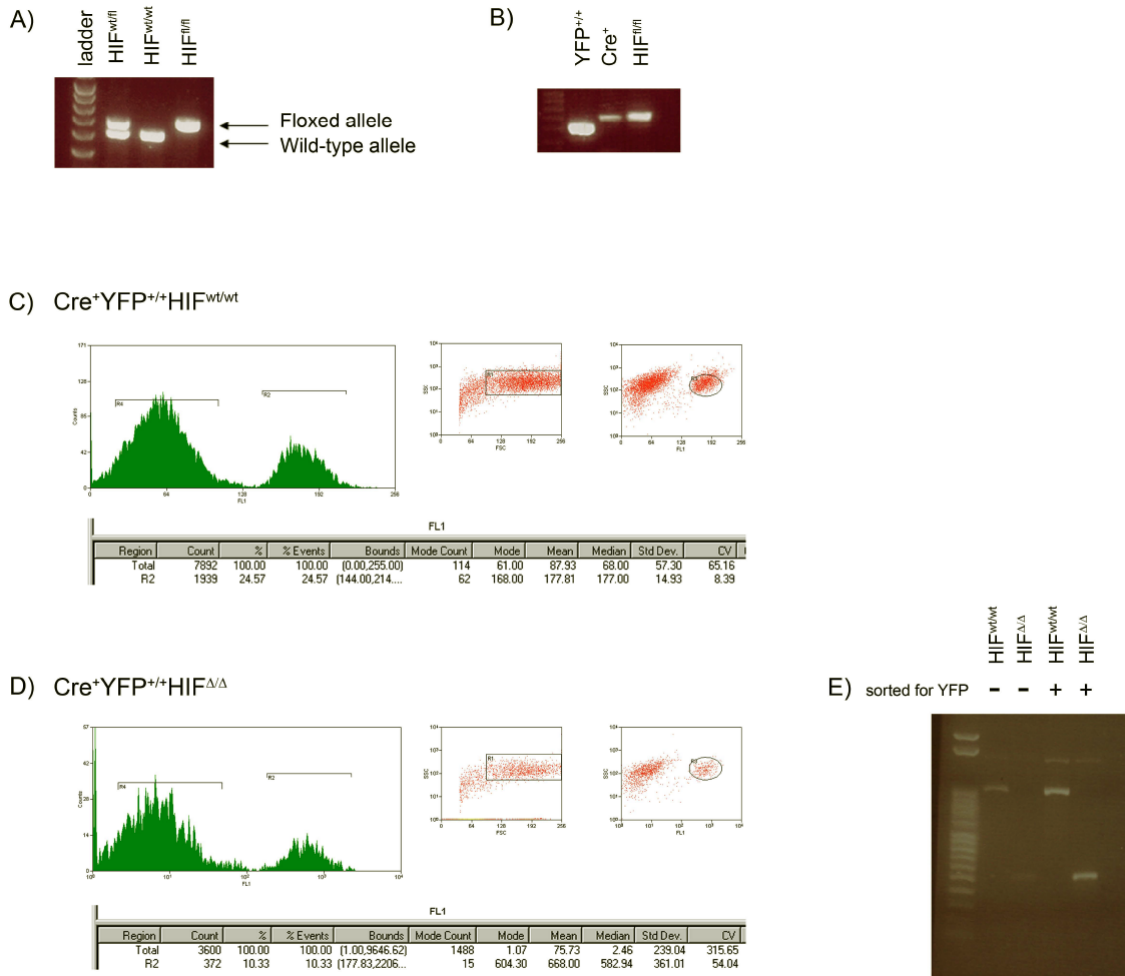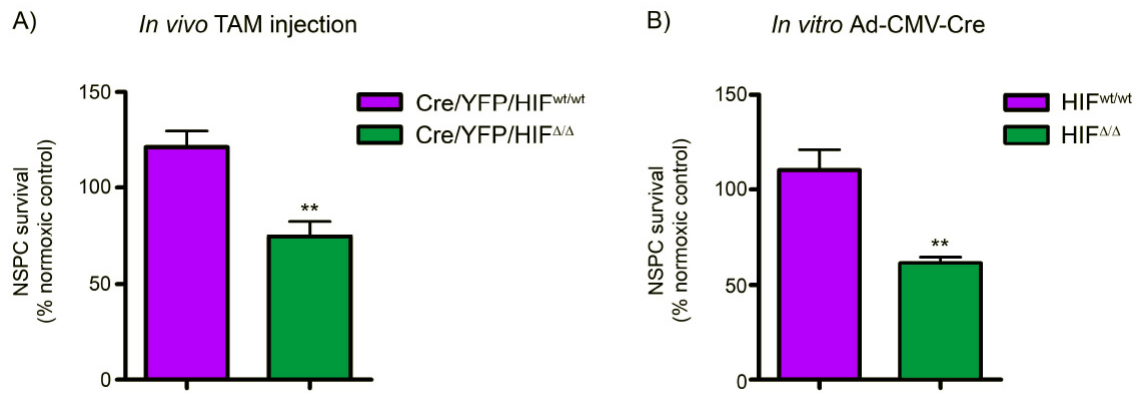
Figure 4.5: NSPC viability in the presence of 24 h anoxia

Figure 4.6: Effect of *Hif1a* gene deletion on NSPC metabolic phenotype

113
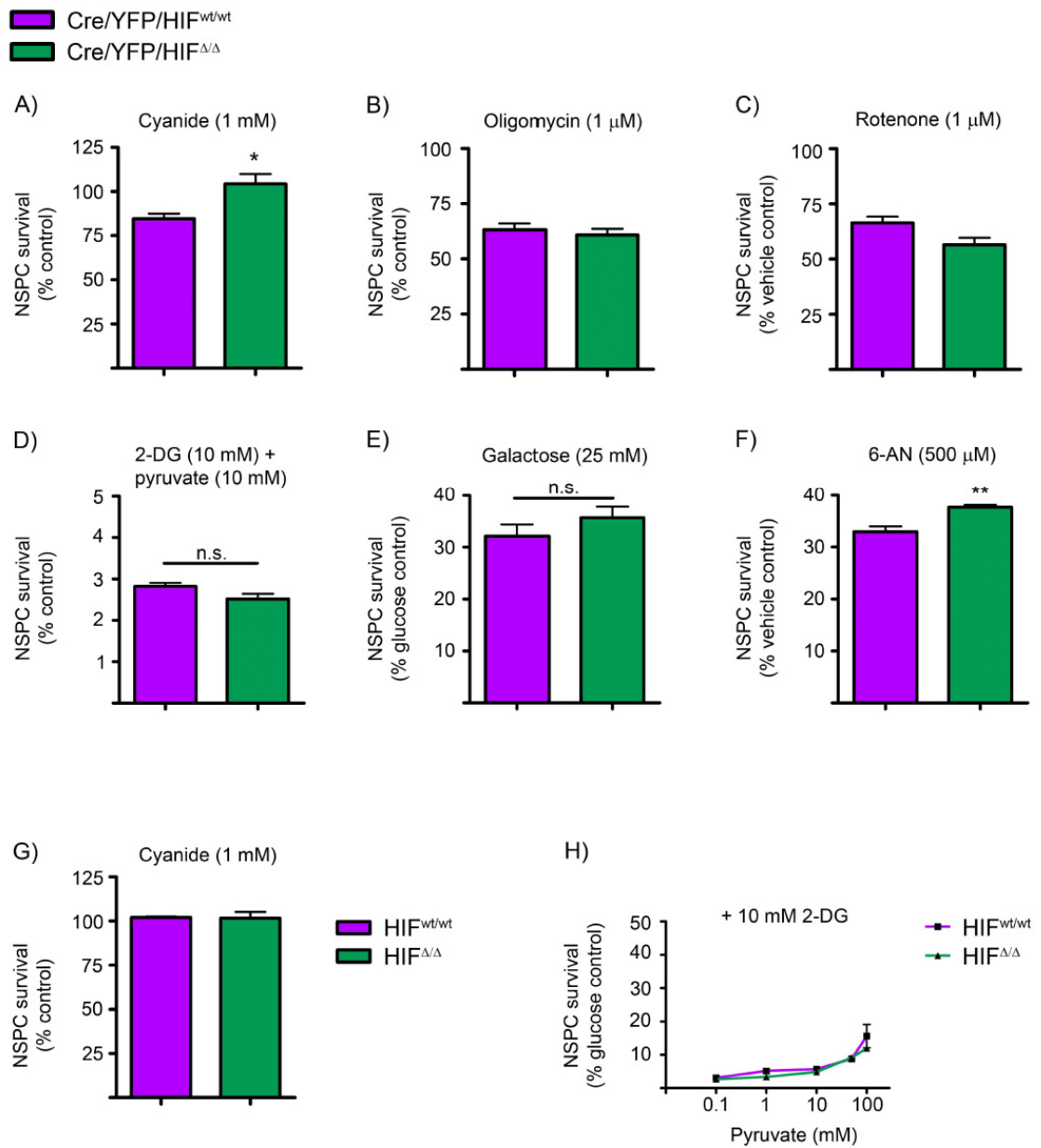
5. Discussion

5.1 Summary

These studies have provided increased understanding of the role of HIF-1α in the regulation of NSPC function under both non-pathological and *ex vivo* ischemic conditions (Figure 5.1). We have demonstrated that NSPCs constitutively stabilize HIF-1α protein, which underlies their resistance to brief periods of OGD and prolonged periods of hypoxia. In addition, we have demonstrated that HIF-1α-regulated VEGF signaling protects neurons against ischemic death, supporting a beneficial role for NSPCs following stroke. We have also characterized the metabolic phenotype of NSPCs as primarily glycolytic with relatively low dependence on oxidative phosphorylation for survival. We have demonstrated, nevertheless, that HIF-1α is not essential to maintain glycolytic dependence. Finally, we have established and characterized a novel *nestin*-CreER^{T2}/R26R-YFP/*Hif1a*$^{fl/fl}$ triple transgenic mouse for conditional and inducible *Hif1a* gene deletion in nestin-positive NSPCs *in vivo* that can be used to study NSPC properties both *in vivo* and *ex vivo*. Initial characterization of these mice indicate that *Hif1a* gene deletion in adult NSPCs *in vivo* results in the depletion of the NSPC pool within the SVZ and SGZ and attenuation of the SVZ cytogenic response to stroke. These studies support a role for HIF-1α as an intrinsic regulator of NSPC survival and function in response to cerebral ischemia and provide increased understanding of NSPC bioenergetics and metabolism.
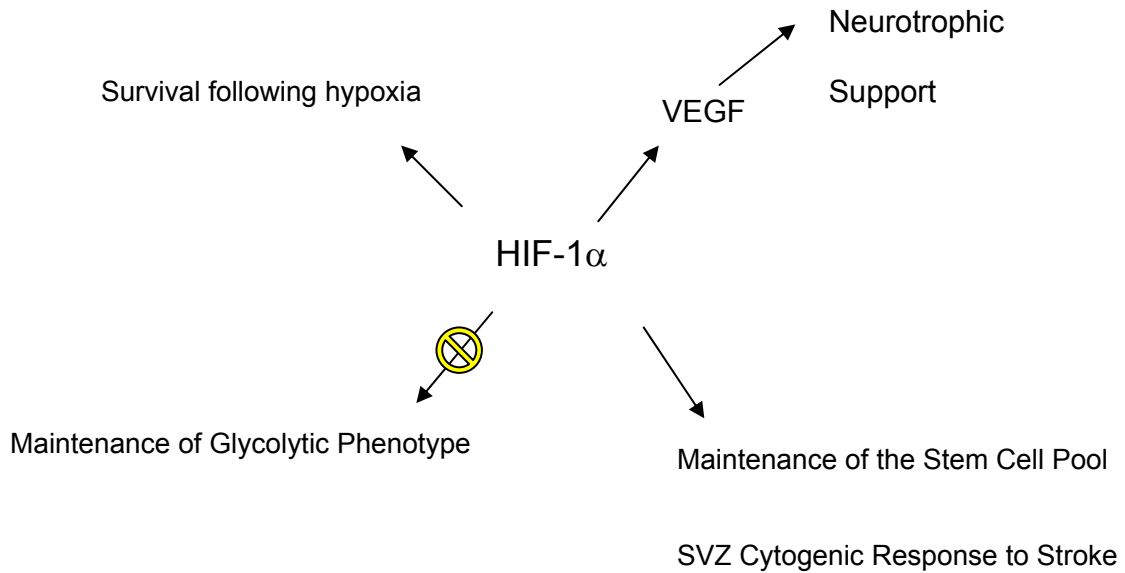
Figure 5.1: HIF-1α regulation of NSPC phenotype. This dissertation describes a role for NSPC-specific HIF-1α, including the regulation of survival during hypoxia, VEGF production and subsequent neuroprotection. Preliminary data (Appendix) suggests HIF-1α maintains the neural stem cell pool following stroke *in vivo*. We found that HIF-1α does not regulate the metabolic phenotype of NSPCs in culture.

5.2 NSPC-mediated neuroprotection

We demonstrated that NSPCs protect cortical neurons against ischemic cell death via HIF-1α-regulated VEGF signaling *in vitro* using oxygen-glucose deprivation (OGD) as a model. *In vitro* modeling allowed us to compare the specific effects of hypoglycemia, hypoxia, and metabolic inhibition between neurons and NSPCs, and to thereby determine the cell-specific impact on viability and metabolic phenotype. These studies provide support to the hypothesis that the SVZ cytogenic response to stroke may be beneficial to the ischemic brain by protecting penumbral neurons against delayed neuronal cell death. Future studies will be aimed at understanding the implications of our *in vitro* findings to the *in vivo* environment of the ischemic brain.

The SVZ NSPC cytogenic response to stroke is delayed, with proliferation peaking at 2 weeks post-MCAO (Thored et al., 2006). Therefore, NSPC-mediated neuroprotection may occur in the immediate vicinity of the SVZ (medial striatum) during the early post-stroke event, but may also be important as NSPCs undergo migration into the injured penumbral regions. Furthermore, some evidence suggests a small population of resident parenchymal stem cells that may not originate from the SVZ, which could provide local neuroprotection if activated early (Shimada et al., 2010). It would be anticipated that both HIF-1α and VEGF would be upregulated *in vivo* following MCAO as we have shown *in vitro* following OGD and hypoxia, since the partial pressure of O_2 drops to <1.4% immediately following MCAO (Thored et al., 2007). Whether neural stem/progenitor cells express VEGF *in vivo* remains to be determined. To study the role of NSPC-specific VEGF *in vivo*, we could cross the *nestin*-Cre-ER^{T2}/R26R-YFP mouse to a VEGF floxed mouse. With this model, VEGF deletion from NSPCs would be induced with tamoxifen and the amount of ischemic damage could be measured.

5.3 NSPC bioenergetics

We demonstrated that NSPCs are primarily glycolytic and have low dependence on oxidative phosphorylation. The ability of NSPCs to survive severe hypoxia and mount a proliferative response to cerebral ischemia may result from their use of glycolysis under normoxic conditions. NSPCs closely associate with the vasculature (Mirzadeh et al., 2008; Shen et al., 2008; Tavazoie et al., 2008; Li et al., 2010), possibly due to their reliance on glucose metabolism and requirement for a glucose source. Use of glycolysis over mitochondrial respiration may aid in NSPC proliferation and migration capabilities, by avoiding flux through the electron transport chain. This would limit ROS production

that can lead to DNA damage and disruption of the maintainence of the stem cell phenotype.

We found that HIF-1α does not regulate the glycolytic phenotype of NSPCs. This was surprising given previous reports that HIF-1α regulates the transcription of genes that promote glycolysis (Seagroves et al., 2001). However, HIF-1α is not the only known regulator of the glycolytic phenotype. For example, c-Myc expression enhances the glycolytic pathway through upregulation of glycolytic enzymes including LDHA. HIF-1α negatively regulates c-Myc, so deletion of *Hif1a* may very well increase activity of c-Myc in our cultures (Gordan et al., 2007), and there is evidence that c-Myc regulates metabolism in cerebellar granule neural progenitor development (Wey et al., 2010). Conversely, p53 has been shown in cancer cells to suppress glycolysis and downregulate glucose transporters (Schwartzenberg-Bar-Yoseph et al., 2004; Kondoh et al., 2005; Matoba et al., 2006). Determining whether lack of p53 regulation in NSPCs determines the glycolytic phenotype we observe could be resolved by overexpression of p53.

We have shown that HIF-1α target genes appear to be essential for the cytogenic response mounted by NSPCs in the SVZ for both autocrine (NSPC survival under hypoxia) and paracrine (neuronal survival) signaling. How HIF-1α regulates the ability of NSPCs to survive prolonged anoxia remains to be determined. Genes transcriptionally regulated by HIF-1α include neuroprotective factors. We determined that autocrine signaling via VEGF production is not required for NSPC survival under OGD, nor do NSPCs produce BDNF in culture. Future studies could investigate whether cultured

NSPCs require expression of autocrine EPO production, a likely candidate for protection of NSPCs following anoxia.

5.4 Conditional-Inducible *Hif1a* knockout mice

We generated and have begun to characterize a unique triple transgenic mouse for conditional, inducible *Hif1a* gene deletion. We were able to isolate NSPCs from these mice and expanded them in culture without loss of viability. Our genomic analysis demonstrated homozygosity for the *Hif1a*$^{fl/fl}$ alleles as well as the R26R-YFP alleles, and at least one allele for *nestin*-CreER^{T2} in the mice we used for our experiments. PCR analysis has demonstrated gene deletion of exon 2 of *Hif1a* following *in vivo* tamoxifen administration, but Western blot analysis is still required to verify HIF-1α protein depletion.

Interestingly, *Hif1a* knockout NSPCs survive and expand normally in culture; however, preliminary data suggest that *Hif1a*-gene deletion results in NSPC depletion within the adult SVZ *in vivo* (Appendix). It may be that *in vivo* gene deletion occurs not only in nestin-positive transient amplifying progenitor cells but also in the primitive slowly dividing astrocytic stem cells. If the more primitive cell type is reliant on HIF-1α for normal survival *in vivo* this would result in eventual depletion of all NSPCs and their progeny. It will be important to determine whether the survival of GFAP+/nestin+ population is differentially impaired by *Hif1a* gene deletion *in vivo*. These mice also showed a decreased cytogenic response *in vivo*, which may have been due to a depleted NSPC pool and may involve limited proliferation or migration. Further studies will be

aimed at understanding how the properties of NSPCs we discovered in culture relate to their properties *in vivo*.

5.5 Critique of Research

5.5.1 *In vitro* modeling

Neural stem/progenitor cells exist in a niche where cell-cell interactions occur between neurons, astrocytes, ependymal cells, and the vasculature (Mirzadeh et al., 2008; Shen et al., 2008; Tavazoie et al., 2008). Ideally, researching NSPCs in their niche would provide the most insight as to how NSPCs interact in their environment *in vivo*. Our laboratory employs the transient middle cerebral artery occlusion (MCAO) model in mice to understand the *in vivo* effects of ischemic stroke. However, understanding cell-specific mechanisms is best studied using *in vitro* techniques. *In vitro* modeling allowed us to compare the specific effects of hypoglycemia, hypoxia, and metabolic inhibition between neurons and NSPCs, and determine the cell-specific impact on viability and metabolic phenotype. In addition, *in vitro* modeling helped us utilize fewer resources, such that many experiments were performed from fewer animals.

One way we investigated cell-cell interactions *in vitro* is to use a coculture system, where neurons and NSPCs were cultured together. However, in understanding the limitations of an *in vitro* system, we utilized a mouse model to study the effects of cerebral ischemia on nestin-positive stem cells and created a transgenic mouse model to determine how HIF-1α regulates those effects (Chapter 4 and Appendix). The combination of *in vitro* with *in vivo* techniques will provide a greater understanding of the role of NSPCs in brain repair following stroke.

5.5.2 Primary cell culture of cortical neurons and neural stem/progenitor cells

In order to study cell-specific mechanisms *in vitro*, neurons and NSPCs were isolated from mouse brain. Primary cortical neurons were consistently isolated from gestational day 15.5 embryonic mice. These cells were dissociated from the cerebral cortex after removal of the meninges, striatum, and hippocampal ridge from the telencephalon. Neurons were cultured in serum-free conditions to prevent the growth of astrocytes, which are also prevalent in the cortex at this gestational age. However, approximately 1-2% of cells in neuronal cultures are astrocytes (Wetzel et al., 2008) and the number of astrocytes from culture to culture could potentially vary between experiments. Because astrocytes and neurons exhibit differential properties (e.g. cellular metabolism), the presence of astrocytes in neuronal cultures could change the outcome of our experiments. The age of the cultured neurons could also impact our results. Cortical neurons are difficult to culture from adult brain, thus we utilize embryonic day 15.5 neurons. Whether post-mitotic neurons from embryonic brain display the same properties as adult neurons remains to be determined. One way to investigate the properties of a mature adult neuron would be to differentiate an adult NSPC into a post-mitotic neuron.

NSPCs were either cultured from embryonic day 14.5 mouse telencephalon or postnatal day 28 mouse SVZ. Dissection from either age results in the isolation of a variety of cell types within these brain regions. Use of the growth factors basic fibroblast growth factor (bFGF) and epidermal growth factor (EGF) selects for mitotically active stem and progenitor cells. The stem cell population is selected for using bFGF whereas the transient amplifying progenitor population is selected for using EGF (Doetsch et al., 1997; Riquelme et al., 2008), and serum-free conditions discourage differentiation and

the growth of astrocytes. However, the precise ratio of stem to progenitor cells could vary between cultures. In addition, NSPCs were used a different passage numbers for each experiment which could also change the ratio of stem cells to progenitors. Age appears to be a factor in NSPC cultures. We observed differences between embryonic and postnatal NSPCs, such as the ability of postnatal NSPCs to withstand higher doses of mitochondrial inhibitors. NSPCs from an aged brain, which may better mimic cells from a brain that would undergo stroke, may exhibit different properties than embryonic or postnatal NSPCs.

Cell culture in the presence of growth factors stimulates tyrosine kinase activity and PI3K/Akt signaling that drive glycolysis (Vander Heiden et al., 2009). It could therefore be argued that the glycolytic phenotype we observe in cultured NSPCs is an artifact of cell culture. This could be resolved *in vivo* using ^{18}F-deoxyglucose positron emission tomography where accumulation of this 2-DG analog in the SVZ could be compared to cortical tissue.

Both neurons and NSPCs were cultured in media containing 25 mM glucose. However, blood glucose levels *in vivo* range from 8 mM in the human (MacKay, 1932) to 10 mM in the rat (Sun et al., 2003). High glucose levels in cultured cells contributes to the Crabtree effect, where cells shift away from ATP production via the electron transport chain to ATP production via glycolysis due to an excess of substrate (Frezza and Gottlieb, 2009). Neurons require 25 mM glucose to survive in culture (Russell et al., 2002), and appeared to maintain oxidative metabolism in our studies. However, future studies to determine whether NPSCs display the Crabtree effect could be resolved by testing the metabolic phenotype of NSPCs under lower concentrations of glucose.

The ability of NSPCs to resist sudden onset hypoxia *in vivo,* together with the observation that many other stem cell types have low oxygen consumption rates under normoxic conditions, would argue against a culture artifact, but *in vivo* studies will be required to confirm this.

5.5.3 Oxygen-glucose deprivation as a model of cerebral ischemia

To model cerebral ischemia in neurons and NSPCs *in vitro*, we utilized oxygen-glucose deprivation (OGD). This model is a well-characterized and popular *in vitro* model used to study the effects of ischemia on cultured neurons (Goldberg and Choi, 1993; Martin-Villalba et al., 2001; Plesnila et al., 2001). Ischemic stroke occurs with the blockade of blood flow to brain tissue, preventing the delivery of oxygen and glucose to the core of the infarct by the vasculature. Neuronal cells in the ischemic penumbra surrounding the core of the infarct die by delayed programmed cell death (apoptosis), which is characterized by DNA fragmentation, membrane blebbing, and the formation of apoptotic bodies which are phagocytosed by surrounding microglia. This model mimics the programmed cell death that neurons undergo in the penumbral region (Martin-Villalba et al., 2001; Plesnila et al., 2001; Wetzel et al., 2008).

The OGD model was initially developed using Earle's Balanced Salt Solution (EBSS) to incubate the cells during the insult. EBSS is glucose- and pyruvate-free, and devoid of amino acids. For our studies performing 2 h OGD, we utilized EBSS as this technique has provided consistent results to model neuronal ischemia (Chapter 2). However, to study the effects of prolonged anoxia on NSPCs, we changed our protocol to use glucose- and pyruvate-free Neurobasal media with necessary supplementation (Chapter 3 and 4).

Our rationale for making this change was to ensure that we were studying the effects of oxygen-deprivation on our cultures, and not amino acid, growth factor, or antioxidant deprivation. Even still, this model does not mimic all of the events that follow ischemic stroke, and thus only allows us to study the effects of hypoglycemia and oxygen-deprivation on our chosen cell types.

5.5.4 MTT assay as a measure of cell viability

In order to measure cell viability *in vitro*, we utilized the MTT assay to measure viability of both neuronal and neural stem/progenitor cells. Methylthiazolyldiphenyl-tetrazolium bromide (MTT) is a tetrazolium salt that is reduced to a water-insoluble purple formazan by mitochondrial dehydrogenase enzymes. The amount of reduction that occurs can be measured by detection of a color change using a spectrophotometer (see Materials and Methods sections in Chapters 2, 3, and 4). Active dehydrogenases of living cells cause this conversion whereas dead cells cannot make this change. Therefore, the measurement of MTT reduction is widely used as a cell viability assay. The caveats to using the MTT assay include the inability to distinguish survival versus proliferation. In addition, MTT may be reduced by NADH and NADPH directly (Berridge et al., 2005), which are coenzymes that exist outside of mitochondrial metabolism. Verification of cell viability can be resolved by using other cell survival assays in parallel with MTT, such as calcein AM, or by immunocytochemistry analysis of healthy appearing nuclei using a nuclear stain such as DAPI. Distinguishing cell viability from survival can also be determined through the use of immunocytochemistry by staining for the cell cycle marker Ki67 or for the thymadine analog bromodeoxyuridine (BrdU).

5.6 Unresolved issues for the study

Whereas this dissertation describes a role for HIF-1α in NSPCs under conditions of hypoxia, questions still remain. Unanswered questions include those regarding NSPC age and their phenotypes *in vitro vs. in vivo*. For example, embryonic NSPCs appear to survive mitochondrial inhibition but their oxygen consumption rate plummits in the presence of rotenone. These data suggests that NSPCs have the capacity to consume oxygen via the electron transport chain. Therefore, while NSPCs appear to have functional electron transport it remains to be determined what role mitochondrial respiration plays under sudden-onset hypoxia. Oxygen consumption and extracellular acidification rates in postnatal NSPCs were not measured in this study, and it will be important to expose them to a mitochondrial stress test in order to determine whether they exhibit the same properties as embryonic NSPCs. It will also be important to take our studies into an animal model to determine whether NSPCs exhibit similar properties *in vivo*. For example, that NSPCs appear to utilize glycolysis in culture conditions should be confirmed by studying NSPCs in the SVZ of adult mice. In addition, our *nestin*-CreER^{T2}/R26R-YFP/*Hif1a*$^{fl/fl}$ triple transgenic mice could be used to determine whether the endogenous NSPC response to stroke is neuroprotective, and if HIF-1α regulates the neuroprotective effects of NSPCs *in vivo*.

5.7 Clinical Relevance and Conclusions

It has been well-realized that brain plasticity is critical in functional repair following stroke, and that the cytogenic response to stroke aids in this repair process (Maysami et al., 2008; Jin et al., 2010a). As reported in this dissertation, we found that the cytogenic response may be important to rescue at risk tissue. We describe a role for HIF-1α in

NSPC-mediated neuroprotection and the ability of NSPCs to survive severe hypoxia. Understanding the NSPC response to hypoxia will be required if these mechanisms are to be harnessed for therapeutic application.

The use of neural stem cells in therapy following stroke and other injuries is an attractive avenue of basic and clinical research, given their regenerative capabilities and differentiation potential. Even if cells that differentiate from neural stem cells do not incorporate into the existing cicuitry, their ability to provide protection to existing cells make them an intriguing candidate to assist in tissue repair. The neuroprotective properties of endogenous NSPCs may be important for limiting the expansion of the lesion area following stroke. Our studies suggest that HIF-1α-regulated VEGF may underlie beneficial effects of exogenously transplanted cells. However, therapeutic use of neural stem cells must proceed with caution. Their proliferative capacity makes them susceptible to graft overgrowth and tumor formation (Seminatore et al., 2010). However, given the limited treatment options for many diseases and injuries, understanding the therapeutic use of neural stem cells have the potential to advance their use into the clinic.

The clinical relevance of our work may include the future use of small molecule regulators of HIF-1α stability in the treatment of stroke. Inhibitors of prolyl hydroxlase activity have been developed for promoting angiogenesis for treating ischemic lesions (HIF-1α stabilizers) (Shen et al., 2009); various inhibitors of HIF-1α, both at the protein and mRNA levels, have been developed for treatment of cancers (Onnis et al., 2009). In the case of stroke, one might envision acute administration of a drug that would enhance HIF-1α stability in order to maximize the viability of the neural stem cell pool at early

post-stroke periods. However, at later times it may be important to inhibit HIF-1α function if it is demonstrated that HIF-1α overexpression impairs neuronal differentiation of NSPCs. Our transgenic mice will be very useful in delineating the role of HIF-1α during various phases of stroke injury.

Cytogenesis following stroke is a delayed response which results in long-term migration of progenitor cells to the lesion but incorporation of few (approximately 0.2%) post-mitotic neurons into the striatal circuitry (Arvidsson et al., 2002; Thored et al., 2006). That the brain mounts a neurogenic response involving hundreds of thousands of SVZ-derived NSPCs following stroke (Arvidsson et al., 2002) may be a mechanism to rescue surviving tissue rather than to regenerate it. Therapies using the endogenous NSPC response to stroke will most-likely target long-term rehabilitation rather than acute processes that result in immediate infarction. However, long-term rehabilitation may be improved by enhancement of NSPC function to promote stem cell migration, proliferative ability, or growth factor release.

Appendix A: Supplemental Data Chapter 3
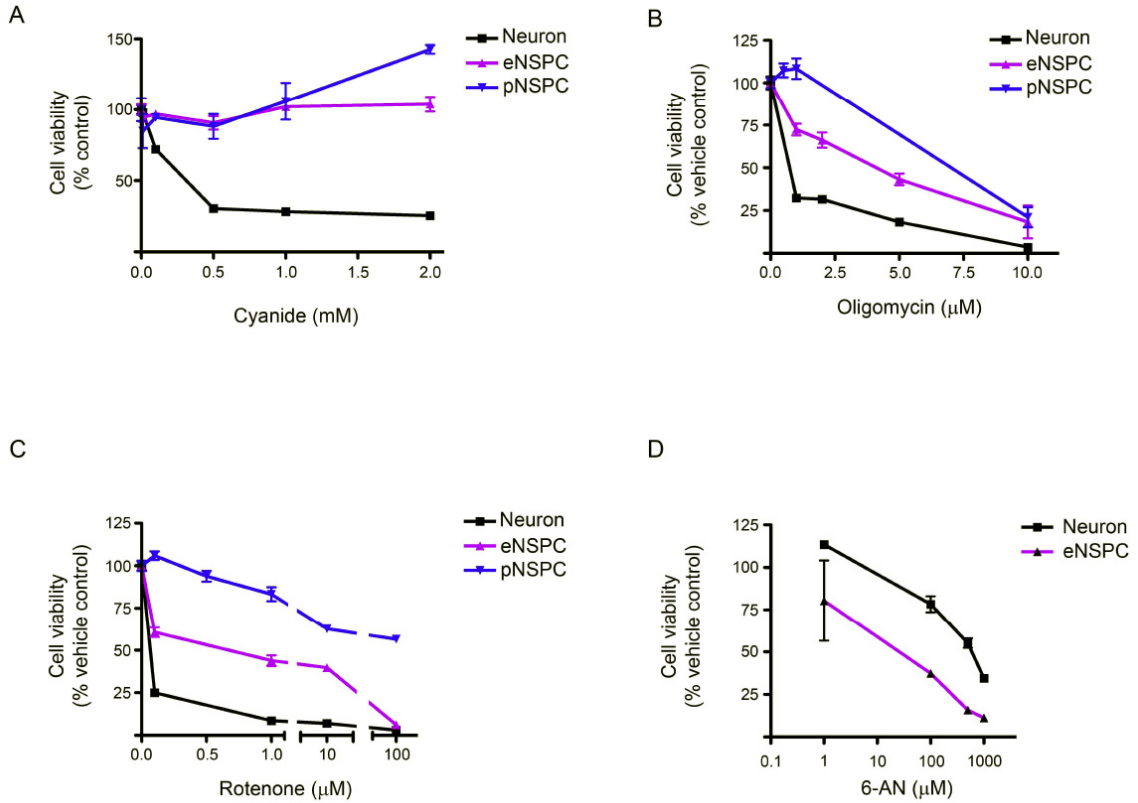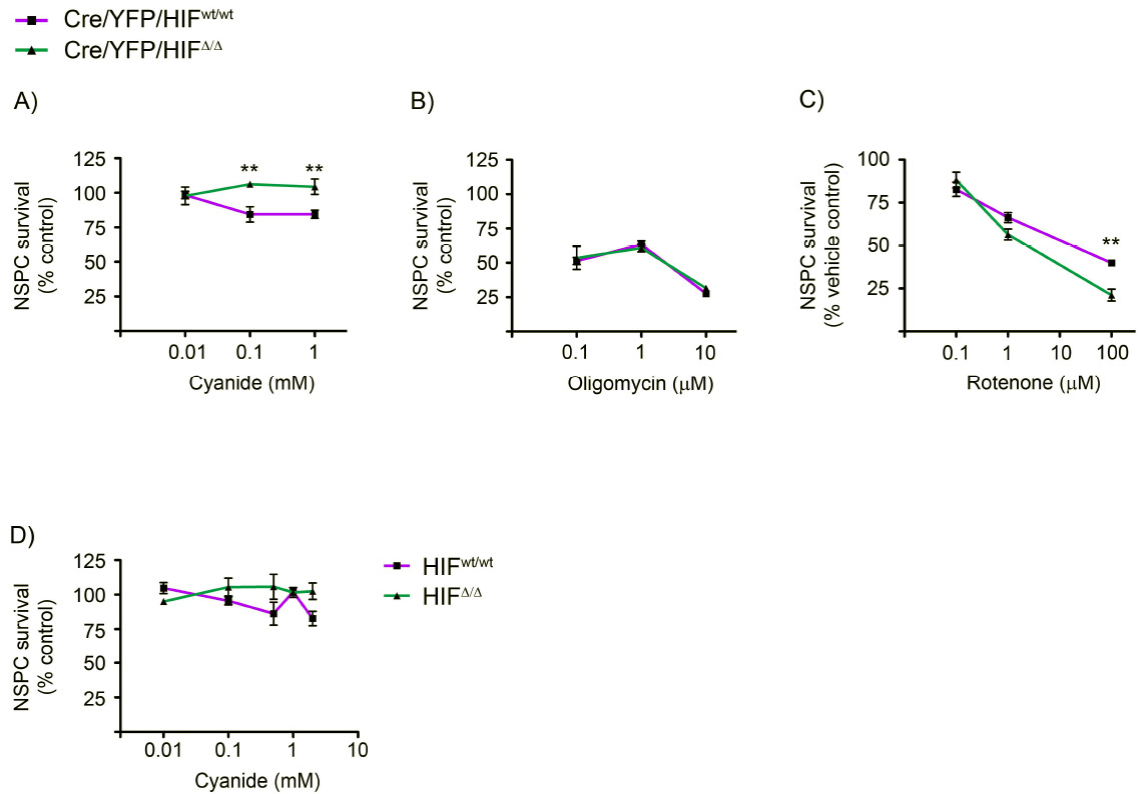
Figure A1: Dose-response curves of neurons and eNSPCs in the presence of cellular respiration inhibitors. (A) cyanide (0.1-2 mM), **(B)** oligomycin (1-10 μM), **(C)** rotenone (0.1-100 μM), and **(D)** 6-aminonicotinamide (6-AN; 1-1000 μM).

Figure A2: Visualization of mitochondria using **(A)** MitoTracker Red staining (60X image) or **(B)** transmission electron microscopy. For immunocytochemistry in (A), NSPCs were identified using an antibody against nestin (green). TEM scale bar = 250 nm.

Figure B1: Dose-response to mitochondrial inhibitors. **(A-C)** *Nestin*-CreER^{T2}/R26R-YFP/*Hif1a*$^{wt/wt}$ and *nestin*-CreER^{T2}/R26R-YFP/*Hif1a*$^{Δ/Δ}$ cultures were exposed to the following inhibitors for 24 h at normoxia: **(A)** cyanide (0.1-1 mM), **(B)** oligomycin (0.1-10 μM), and **(C)** rotenone (0.1-100 μM). **(D)** Dose-response of wild-type and *Hif1a*$^{Δ/Δ}$ embryonic NSPCs treated with Ad-CMV-Cre to cyanide (0.1-2 mM) for 24 h at normoxia.

Appendix C: Focal cerebral ischemia induces a multilineage cytogenic response from adult subventricular zone that is predominantly gliogenic

Lu Li[1], Kate M. Harms[1], P. Britten Ventura[1], Diane C. Lagace[2], Amelia J. Eisch[3], and Lee Anna Cunningham[1]

[1]Department of Neurosciences, University of New Mexico Health Sciences Center, Albuquerque, New Mexico 87131

[2]Department of Cellular and Molecular Medicine, University of Ottawa, Ottawa, Ontario Canada K1H 8M5

[3]Department of Psychiatry, University of Texas Southwestern Medical Center, Dallas, Texas 75390

C.1 Abstract

The purpose of this study was to ascertain the relative contribution of neural stem/progenitor cells (NSPCs) of the subventricular zone (SVZ) to lineages that repopulate the injured striatum following focal ischemia. We utilized a tamoxifen-inducible Cre/loxP system under control of the nestin promoter, which provides permanent YFP labeling of multipotent nestin$^+$ SVZ-NSPCs prior to ischemic injury and continued YFP expression in all subsequent progeny following stroke. YFP reporter expression was induced in adult male nestin-CreER^{T2}:R26R-YFP mice by tamoxifen administration (180 mg kg^{-1}, daily for 5 days). Fourteen days later, mice were subjected to 60-min transient middle cerebral artery occlusion (MCAO) and sacrificed at 2 days, 2 weeks, or 6 weeks post-MCAO for phenotypic fate mapping of YFP$^+$ cells using lineage-specific markers. Migration of YFP$^+$ cells from SVZ into the injured striatal parenchyma was apparent at 2 and 6 weeks, but not 2 days, post-MCAO. At 2 weeks post-MCAO, the average percent distribution of YFP$^+$ cells within the injured striatal parenchyma was as follows: 10% Dcx$^+$ neuroblasts, 15-20% oligodendrocyte progenitors, 59% GFAP$^+$ astrocytes, and only rare NeuN$^+$ postmitotic neurons. A similar phenotypic distribution was observed at 6 weeks, except for an increased average percentage of YFP$^+$ cells that expressed Dcx$^+$ (20%) or NeuN (5%). YFP$^+$ cells did not express endothelial markers, but displayed unique anatomical relationships with striatal vasculature. These results indicate that nestin$^+$ NSPCs within the SVZ mount a multilineage response to stroke that includes a gliogenic component more predominant than previously appreciated.

C.2 Introduction

A promising discovery in stroke research within the past decade is the SVZ response to cerebral ischemia, which may contribute importantly to recovery and repair processes. Focal cerebral ischemia stimulates a cytogenic response from SVZ of both adult rodent (Arvidsson et al., 2002) and human brain (Jin et al., 2006; Macas et al., 2006; Marti-Fabregas et al., 2010).This response is characterized by proliferation of neural stem/progenitor cells (NSPCs) within the SVZ and heterotypic migration of neuroblasts from SVZ into the ischemic brain parenchyma. Although most ectopic neuroblasts undergo cell death within the injured parenchyma, a small number survive and give rise to postmitotic neurons that replace ~0.2% of neurons that are lost to injury within the peri-infarct region (Arvidsson et al., 2002; Thored et al., 2006). In addition to neurogenesis, gliogenesis and angiogenesis contribute to brain repair following stroke, but the relative contribution of the SVZ to new glial or endothelial cell phenotypes following stroke has not been well characterized.

To ascertain the relative contribution of the SVZ-NSPCs to lineages that repopulate striatum following focal cerebral ischemia, we utilized a tamoxifen-inducible Cre/loxP system under control of the nestin promoter to genetically label a large cohort of nestin[+] NSPCs within the SVZ prior to the onset of ischemic injury. Administration of tamoxifen to nestin-CreER[T2]:R26R-YFP bitransgenic mice transiently activates Cre-mediated recombination, resulting in permanent excision of a floxed transcriptional stop sequence upstream of an YFP reporter gene sequence within nestin^{+} cells (Lagace et al., 2007). This leads to permanent YFP reporter gene expression by NSPCs and all subsequent progeny, thereby providing a genetic marker for tracking the migration of nestin

derivatives and for phenotypic fate mapping. Here, we describe the use of nestin-CreER^{T2}:R26R-YFP mice to fate map both neuronal and nonneuronal SVZ derivatives following focal cerebral ischemia induced by transient middle cerebral artery occlusion (MCAO). Our results indicate that the cytogenic response of nestin$^+$ NSPCs within the SVZ is primarily gliogenic following stroke.

C.3 Materials and Methods

C.3.1 Mice

Animal experiments were approved by the University of New Mexico Animal Care and Use Committee in accordance with the NIH Guide for the Care and Use of Laboratory Animals. The generation and characterization of the nestin-CreER^{T2}:R26R-YFP strain used in this study were previously described (Lagace et al., 2007). All mice were housed under a 12 h light: 12 h dark cycle with food and water available *ad libitum*.

C.3.2 Tamoxifen Administration

Male nestin-CreER^{T2}:R26R-YFP mice (6- to 8-weeks old) were administered tamoxifen dissolved in 10% EtOH/90% sunflower oil intraperitoneally (i.p) at the dose of 180 mg kg^{-1} daily for 5 consecutive days. Control mice received vehicle injections. This dosing regimen was previously demonstrated to provide maximal recombination with minimal mortality (Lagace et al., 2007).

C.3.3 Middle Cerebral Artery Occlusion (MCAO)

Two weeks following the final injection of tamoxifen or vehicle, nestin-CreER^{T2}:R26R-YFP mice received 60-min transient MCAO or sham MCAO by intraluminal filament as published previously (Kokovay et al., 2006).

C.3.4 Histology

Mice were overdosed with sodium pentobarbital (150 mg kg^{-1}, i.p.; Fort Dodge Animal Health, Fort Dodge, IA), and transcardially perfused with phosphate-buffered saline (PBS) containing 0.1% procaine and 2 U mL^{-1} heparin, followed by 4% paraformaldehyde (w/v) in 0.1 M PBS. The brains were postfixed overnight, cryoprotected with 30% sucrose (w/v) in 0.1 M PBS for 48 h at 4°C and sectioned at 30 μm thickness in the coronal plane using a freezing sliding knife mictrotome. Floating sections were processed for immunofluorescence as previously published (Roitbak et al., 2008) using the following primary antibodies: goat anti-doublecortin (Dcx; 1:200; Santa Cruz Biotechnology, Santa Cruz, CA), mouse anti-glial fibrillary acidic protein (GFAP; 1:500, Sigma, St. Louis, MO), rabbit anti-GLUT-1 (1:200, Abcam, Cambridge, MA), rabbit anti-NG2 (1:200; Millipore, Billerica, MA), rabbit anti-Olig2 (1:1,000; Millipore, Billerica, MA), rabbit anti-laminin (1:500; Sigma, St. Louis, MO), chicken anti-GFP (1:1,000; Invitrogen, Carlsbad, CA), rabbit anti-Iba-1 (1:500; Wako Chemicals USA, Richmond, VA). Immunofluorescence was visualized using FITC-, CY3-, or Cy5-conjugated secondary antibodies (1:250; Jackson ImmunoResearch Laboratories, West Grove, PA). YFP immunofluorescence was visualized using biotinylated donkey antichicken secondary antibody and Tyramide-Plus amplification (PerkinElmer Life Sciences, Boston, MA) as previously described(Lagace et al., 2007). For Fluoro-Jade

staining, histological sections were incubated with 0.05% potassium permanganate for 15 min, followed by 30 min in 0.001% Fluoro-Jade (Histo-Chem, Jefferson, AR).

Coexpression of YFP with lineage-specific markers was quantified by random sampling of at least 100 YFP$^+$ cells per mouse for each marker using a 40× oil objective on a Zeiss LSM510 confocal microscope, coupled with rapid z-axis analysis at 1 μm optical section thickness. YFP$^+$ cells were scored as positive or negative for coexpression of each marker. Data are presented as the mean percentage of YFP$^+$ cells coexpressing Dcx, NeuN, NG2, Olig2, or GFAP ± SEM. Statistical analysis was performed using Students t test, comparing data acquired from 2- vs. 6-week post-MCAO with $P < 0.05$ considered significant.

C.4 Results

C.4.1 Stroke Induces Delayed Migration of YFP Reporter$^+$ Cells from SVZ into Adjacent Striatal Parenchyma

We utilized a previously published protocol for achieving maximum Cre-mediated recombination in the nestin-CreER^{T2}:R26R-YFP mice by administration of tamoxifen (180 mg kg^{-1}, i.p.) daily for five consecutive days (Lagace, 2007 #88). Two weeks were allowed following the final injection for tamoxifen clearance, and the mice were then subjected to 60 min transient MCAO ($n = 12$) or sham MCAO ($n = 2$). Nestin-CreER^{T2}:R26R-YFP mice that received vehicle i.p. injections served as additional controls (see below). Mice were sacrificed after 2 days ($n = 4$), 2 weeks ($n = 4$), or 6 weeks ($n = 4$) post-MCAO, and brain tissue was processed for histological evaluation of

stroke-induced neurodegeneration, distribution of YFP$^+$ cells and phenotypic fate of YFP$^+$ cells using lineage-specific markers (see Fig. 1A for experimental design).

Neurodegeneration throughout the striatum was apparent as early as 2-days post-MCAO, as evidenced by positive Fluoro-Jade staining throughout the striatum and parietal cortex on the ischemic side (Fig. 1B), however, YFP$^+$ cells remained localized to the SVZ and were not observed within the adjacent striatal parenchyma at this early postinjury time point (Fig. 1C). By 2-week post-MCAO, the density of YFP reporter$^+$ cells was increased throughout the SVZ and adjacent ischemic striatum, heavily populating the striatal parenchyma on the ischemic side (Fig. 1D). A similar distribution and density of YFP$^+$ cells within the injured striatum was apparent at 6 weeks (Supp. Info. Fig. 1A). YFP reporter$^+$ cells were not present within the contralateral striatum of tamoxifen-induced nestin-CreER^{T2}:R26R-YFP MCAO mice (Supp. Info. Fig. 1B), or within the ipsilateral striatum of tamoxifen-induced mice that received sham MCAO surgery (Supp. Info. Fig. 1C).

C.4.2 YFP Reporter Fidelity is Maintained in Adult Nestin-CreER^{T2}:R26R-YFP Mice Following Stroke

Nestin-CreER^{T2}:R26R-YFP mice that received vehicle i.p. injections were used to verify the stringency of Cre-mediated recombination under conditions of cerebral ischemia. In contrast to tamoxifen-treated mice, YFP$^+$ cells were not observed within the SVZ or within the injured striatal parenchyma of vehicle-injected nestin-CreER^{T2}:R26R-YFP mice as assessed at 2-weeks post-MCAO. However, Dcx$^+$ migrating neuroblasts were readily detected in vehicle-treated mice at this time point, confirming a normal neurogenic response to stroke in this control group (Fig. 2A). Thus, Cre-mediated

recombination does not occur in the absence of tamoxifen and does not occur spontaneously in response to MCAO injury in vehicle-treated nestin-CreER^{T2}:R26R-YFP mice. In mice treated with tamoxifen 2 weeks prior to MCAO, YFP expression was also not observed within reactive astrocytes that upregulate nestin following MCAO (Fig. 2B), indicating that the 14-day washout interval between tamoxifen administration and MCAO was sufficient time to ensure that all recombination occurred prior to the onset of ischemic injury. Taken together, these results verify the fidelity of the nestin-CreER^{T2} system under conditions of focal cerebral ischemia induced by transient 60-min MCAO.

C.4.3 Multilineage Analysis of YFP Reporter$^+$ Cells

C.4.3.1 Neuronal lineage

To determine the relative proportion of YFP reporter$^+$ cells within the ischemic striatum that represent migratory neuroblasts and/or postmitotic neurons, histological sections from tamoxifen-treated mice were assessed for co-labeling of YFP with Dcx or NeuN immunofluorescence, respectively. Dcx$^+$ neuroblasts were observed throughout the ischemic striatum (Fig. 3A), but were not present within the contralateral striatum or within the striatum of sham-operated controls (data not shown). Dcx$^+$ cells comprised 10% ± 3% and 20% ± 1% of all YFP$^+$ cells within the injured striatum at 2 and 6 weeks post-MCAO, respectively (Fig. 3A-C). The majority of Dcx$^+$ cells within the injured straitum were negative for YFP reporter expression at both 2- and 6-weeks post-MCAO (80% ± 3% and 67% ± 17%, respectively). YFP$^+$ cells within the injured striatum that co-expressed the mature neuronal marker, NeuN, were only rarely observed at 2 weeks (<1 NeuN$^+$/YFP$^+$ colabeled cell per histological section, data not shown), but represented 5% ± 1% of all YFP$^+$ cells by 6-weeks post-MCAO (Fig. 3D,E).

C.4.3.2 Oligodendrocyte lineage

To determine the relative contribution of YFP$^+$ cells to the oligodendrocyte lineage we utilized NG2 proteoglycan and the transcription factor, Olig2, as markers of oligodendrocyte progenitors (Fig. 4A,B). Triple labeling revealed that 15% ± 2% and 19% ± 4% of all YFP$^+$ cells within injured striatum co-expressed both NG2 and Olig2 markers at 2 and 6 weeks post-MCAO, respectively (Fig. 4D). Only a small percentage of YFP$^+$ cells were Olig2$^+$/NG2$^-$ (5% ± 2% and 5% ± 1% at 2 and 6 weeks, respectively). YFP$^+$ oligodendrocyte progenitors were abundant throughout the penumbral region that spanned from lateral ventricle to infarct boundary, but were sparse within the SVZ in both lesioned and unlesioned hemispheres (Fig. S2A, online). YFP$^+$ oligodendrocyte progenitors displayed a multiprocessed morphology and were negative for the microglial marker, Iba1 (Fig. 4C). YFP$^+$ cells immunofluorescent for the mature oligodendrocyte markers, CC1 or RIP, were not observed at 2- or 6-weeks post-MCAO, although YFP$^+$ cells with morphology reminiscent of mature oligodendrocytes were observed within the corpus callosum (Supp. Info. Fig. 2B).

C.4.3.3 Astrocyte lineage

YFP reporter$^+$ cells that co-expressed the astrocytic marker, GFAP, were abundant within the penumbral regions between lateral ventricle and ischemic core; 58% ± 4% and 45% ± 7% of all YFP$^+$ cells were co-labeled with GFAP at 2 and 6 weeks, respectively (see Fig. 5). GFAP$^+$/YFP$^+$ co-labeled cells displayed diverse morphologies ranging from multipolar highly branched hypertrophied astrocytes (Fig. 5A) to radial glia-like morphologies characterized by long slender sparsely branched processes (Fig. 5B).

C.4.3.4 YFP$^+$ Cells Display Unique Anatomical Relationships with Striatal Vasculature

Previous studies have demonstrated that exposure of isolated neural stem cells to endothelial cells in co-culture can induce neural stem cell expression of endothelial lineage markers(Roitbak et al., 2008). Since stroke-induced neurogenesis is thought to occur within an angiogenic niche, we assessed vascular phenotype in YFP$^+$ cells in the MCAO paradigm using laminin and the high affinity Glut-1 glucose transporter. Although we did not observe YFP$^+$ cells that adopted an endothelial cell fate, co-labeling with endothelial markers revealed a striking relationship of YFP$^+$ cells with microvasculature, both within the SVZ and within the ischemic striatum. As shown in Fig. 6, YFP reporter$^+$ cells within the SVZ were found to extend long radial processes from the SVZ into the surrounding brain parenchyma to terminate an endfoot-like terminal on capillaries (Fig. 6B). These cells likely represent B1 type astrocytic stem cells(Doetsch, 2003a). These cells were observed within the base of the SVZ at the level of medial septum, near the nucleus accumbens on both injured and uninjured hemispheres, and extended processes up to 180 μm in length to terminate on blood vessels. Most SVZ-derived YFP reporter$^+$ cells that had migrated into ischemic striatum were found in close physical contact with vasculature, with soma either directly juxtaposed to blood vessels or contacting blood vessels via endfoot-like processes (Fig. 6C,D). In some cases, YFP+ cells were closely associated with fine endothelial extensions that connected adjacent capillaries reminiscent of angiogenic microvasculature (Fig. 6D).

In the present study, we utilized tamoxifen inducible nestin-CreER^{T2}:R26R-YFP mice to label a large cohort of NSPCs within the adult subventricular zone prior to injury and followed migration and lineage fate of the NSPCs out to 6-weeks post-MCAO. This genetic fate-mapping approach permits long-term evaluation of a large cohort of SVZ NSPCs using an irreversible YFP reporter system, thereby enabling a comprehensive examination of lineage fate following stroke.

We found that Dcx$^+$ neuroblasts accounted for up to 20% of all YFP$^+$ cells within the ischemic striatal parenchyma by 6-weeks post-MCAO. In mouse, transgenic ablation of Dcx-expressing cells worsens stroke outcome (Jin et al., 2010a) indicating that these cells may be an important therapeutic target. Although NeuN$^+$/YFP$^+$ co-labeled cells were only sparsely represented at 2 weeks, their numbers increased to 5% of all YFP$^+$ cells by 6-weeks post-MCAO. Since ~80% of migrating neuroblasts were YFP$^-$ in our study, it is likely that up to 20% of all neuroblasts survive to become NeuN$^+$ postmitotic neurons by 6-weeks post-MCAO, which is consistent with previous estimates (Arvidsson et al., 2002). The presence of Dcx$^+$/YFP$^-$ cells may reflect suboptimal labeling efficiency within SVZ, since previous studies have demonstrated that Dcx$^+$ neuroblasts within ischemic striatum arise primarily from SVZ astrocytic stem cells of the nestin lineage (Yamashita et al., 2006). A previous study by Burns et al. (Burns et al., 2007)using a different strain of tamoxifen-inducible nestin-CreER:GFP bitransgenic mice reported only very few GFP-positive cells outside the SVZ following MCAO. Ectopic migration of Dcx$^+$ neuroblasts into the ipsilateral striatum was negligible in that study, possibly due to the

early time point of analysis at 1-week post-MCAO or due to less effective MCAO-induced injury.

We found that 18-21% of all YFP reporter^{+} cells within the injured striatal parenchyma at 6-weeks post-MCAO represent NG2^{+}/Olig2^{+} oligodendrocyte progenitor cells. NG2 is a chondroitin sulfate proteoglycan expressed on the surface of oligodendrocyte progenitors (Nishiyama et al., 2009), and Olig2 is a transcription factor necessary for the development of the oligodendrocyte lineage (Takebayashi et al., 2002). In adult brain, the majority of Olig2^{+} progenitor cells within the white matter transiently co-express NG2 and eventually give rise to NG2^{-} oligodendrocytes, whereas in grey matter most Olig2^{+} cells remain as nonproliferating Olig2^{+}/NG2^{+} progenitors (Dimou et al., 2008). Our study suggests that the latter population of oligodendrocyte progenitors is partially replaced by SVZ-NSPCs following stroke, since we did not observe co-labeling for mature oligodendrocyte markers within the ischemic parenchyma, even by 6 weeks.

GFAP[+] astrocytes comprise the largest fraction of all YFP reporter^{+} cells within the ischemic striatum at both 2 weeks (59%) and 6 weeks (45%) post-MCAO. Astrocytes are a heterogeneous population of cells within the CNS that play both beneficial and detrimental roles following injury (Sofroniew, 2009). Glial scarring within the CNS is recognized as a major impediment to neurite outgrowth and regeneration(Silver and Miller, 2004). In contrast, ablation of reactive astrocytes in adult mice (Bush et al., 1999) or disruption of cytokine signaling in reactive astrocytes (Okada et al., 2006; Herrmann et al., 2008) leads to spread of inflammation and increased injury responses. Furthermore, GFAP-null mice demonstrate increased kainate excitoxicity (Otani et al., 2006).

Pharmacological inhibition of reactive astrocytes with fluorocitrate retards neurovascular remodeling and recovery after focal cerebral ischemia (Hayakawa et al., 2010). Recent studies have shown that neural stem cells within the spinal cord give rise to a functionally distinct subset of astrocytes following injury, which do not produce axonal growth inhibitory chondroitin sulfate proteoglycans (CSPGs) and appear to promote axonal sprouting (Meletis et al., 2008). Buffo et al. recently reported that mature astrocytes have the capacity to re-enter the cell cycle, dedifferentiate and resume multipotency in response to brain injury (Buffo et al., 2008). Future studies will be required to determine the extent to which SVZ-derived astrocytes within the ischemic parenchyma promote regenerative processes vs. contribute to glial scarring and inhibition of neurite outgrowth following focal ischemia.

YFP reporter^{+} cells displayed unique anatomical association with microvasculature within the SVZ and ischemic striatal parenchyma. Many YFP^{+} cells within the SVZ were found to extend a long basal process from the SVZ into the brain parenchyma to make contact with blood vessels through an endfoot-like structure. Mirzadeh et al. recently demonstrated that >95% of type B1 astrocytes within the SVZ have an apical ciliated process that is in contact with the ventricle, and a long basal process that extends several hundred microns into the brain parenchyma to contact a blood vessel via an endfoot (Mirzadeh et al., 2008). The functional significance of vascular contact of neural stem cells may reflect the need for vascular-derived factors important in maintaining the stem-cell phenotype (Shen et al., 2004), or allow signals from CSF and bloodstream to be integrated (Tavazoie et al., 2008). Neural stem cells within the SVZ are also associated with extravascular basal lamina unique to the subependymal layer, termed fractones,

purported to provide a specialized extracellular matrix within the neural stem cell niche (Mercier et al., 2002).

YFP^{+} cells were also found in close association with the microvasculature throughout the injured striatum. This anatomical relationship likely reflects the use of vascular basal lamina as a migratory substrate (Ohab et al., 2006), and/or the importance of reciprocal signaling between SVZ derivatives and nascent vasculature during the repair process (Louissaint et al., 2002; Roitbak et al., 2008). The migration of neuroblasts along nonstereotypical routes toward the injured area occurs in response to chemotactic growth factors and chemokines that also signal angiogenesis, including stromal cell-derived growth factor (SDF-1) (Imitola et al., 2004), vascular endothelial growth factor (VEGF) (Zhang et al., 2003a) and angiopoietin 2 (Liu et al., 2009). SDF-1- and VEGF-induced migration of adult NSPCs in culture is mediated by matrix metalloproteinase (MMP)-3 and MMP-9 expression and activation in NSPCs (Barkho et al., 2008). Pharmacological inhibition of MMP activity also impairs stroke-induced neurogenesis *in vivo* (Lee et al., 2006). Thus, the angiogenic and neurogenic responses to stroke are tightly linked.

In conclusion, our genetic-lineage tracing study shows that stroke induces a multilineage cytogenic response in which nestin[+] neural stem cells of the SVZ produce neuroblasts, postmitotic neurons, oligodendrocyte progenitor cells, and astrocytic cells that repopulate the striatal parenchyma out to at least 6 weeks following the ischemic event. These studies are important in light of recent evidence for increased proliferation of GFAP^{+} cells within the ribbon layer of human ipsilateral SVZ at early times following stroke (Marti-Fabregas et al., 2010) and subsequent appearance of cells expressing markers of

143

newborn neurons (PSA-NCAM and Dcx) within the infarct penumbra of human brain weeks following the onset of stroke symptoms (Jin et al., 2006; Macas et al., 2006). A recent study by (Ohira et al., 2010), provides evidence for cortical neurogenesis from nonnestin derivatives within subpial regions of the neocortex in response to global forebrain ischemia in mice (Ohira et al., 2010). In addition, induced repetitive cortical spreading depression, an epiphenomenon of stroke injury in humans and rodents, has recently been reported to stimulate hippocampal neurogenesis and subpial cortical neurogenesis (Yanamoto et al., 2005; Urbach et al., 2008). However, we did not observe contribution of YFP$^+$ cells to superficial gliosis or evidence for cellular migration from subpial regions of cortex following MCAO.

An important finding of the current study is the percent distribution of YFP$^+$ SVZ derivatives; in which glia represent ~67-78% of all YFP reporter$^+$ cells, indicating a significant gliogenic component. It is currently unclear whether YFP$^+$ SVZ cells adopt a glial fate prior to migration or after they arrive within the striatal parenchyma. Previous studies have shown that transplantation of multipotent SVZ cells directly into nonneurogenic brain regions limits neurogenic potential and promotes astrocyte differentiation (Alvarez-Buylla and Lim, 2004; Zheng et al., 2006), underscoring the importance of microenvironment in determining NSPC lineage fate. The current studies provide a baseline for the use of nestin-CreER^{T2} transgenic mice to study the molecular regulation of migration and differentiation of NSPCs following ischemic injury through selective knockout or overexpression of genes within nestin$^+$ NSPCs and their progeny. Understanding the molecular regulation of lineage fate of NSPCs following injury should lead to improved strategies for facilitating structural and functional recovery.

C.6 Figure Legends

Figure C.1. (**A**) Experimental design. (**B**) Fluoro-Jade at Day 2 post-MCAO. (**C**) YFP immunofluorescence 2-days post-MCAO. (**D**) YFP immunofluorescence at 2-weeks post-MCAO. LV (lateral ventricle), ST (Striatum). Scale Bars = 100 μm.

Figure C.2. (**A**) Dcx (red) and YFP (green) immunofluorescence in vehicle-injected control Nestin-CreER^{T2}:R26R-YFP mice. (**B**) Nestin (red), GFAP (blue), and YFP (green) immunofluorescence in tamoxifen-treated Nestin-CreER^{T2}:R26R-YFP mice at Day-14 post-MCAO. LV (lateral ventricle). Scale bar = 100 μm.

Figure C.3. (**A**) Doublecortin (red) and YFP (green) immunofluorescence at 2-weeks post-MCAO. (**B**) Higher power images with orthogonal view of confocal z-stack. DCX$^+$/YFP$^+$ cells (arrows) and DCX$^-$/YFP$^+$ cells (arrowheads). (**C,E**) Percentage of YFP reporter$^+$ cells that co-express Dcx (C) or NeuN (E). (**D**) NeuN+ (red) and YFP (green) immunofluorescence at 6-weeks post-MCAO. ND = <1 cell per section. *$P < 0.05$. Scale bars = 100 μm (A), 10 μm (B), or 20 μm (D).

Figure C.4. Dual immunofluorescence for YFP (green) with (**A**) NG2 (red) (**B**) Olig2 (red) and (**C**) Iba-1 (red) at 2-weeks post-MCAO. (**D**) Percentage of YFP$^+$ cells that express Olig2 and NG2 at 2- and 6-weeks post-MCAO. Scale bars = 20 μm (A,C) or 10 μm (B).

Figure C.5. Dual immunofluorescence for YFP (green) with GFAP (red or blue) at 2-weeks post-MCAO. Graph depicts the percentage of YFP$^+$ cells that express GFAP at 2- and 6-weeks post-MCAO. Scale bars = 20 μm.

Figure C.6. (A) Boxed images on histological section are shown in higher power in **B-D**. Solid area represents region of ischemic damage. (B) Dual immunofluorescence for YFP (green) and GLUT-1 (red) demonstrating YFP$^+$ processes from radial glial-like cells in the SVZ with endothelial end-feet. (C) YFP reporter$^+$ cells (green) that have migrated into the ischemic border zone and are associated with laminin$^+$ (red) cerebral blood vessels. (D) YFP reporter$^+$ cells (green) within the ischemic striatum associated with processes of laminin+ (red) angiogenic blood vessels. Scale bars = 10 μm (B-D).

Supporting Information Figure 1. **A)** YFP+ cells within the ischemic striatum at 6 weeks post-MCAO. **B)** YFP immunofluorescence on the non-ischemic hemisphere of a tamoxifen-injected mouse at 2 weeks post-MCAO. **C)** YFP (green) and NeuN (red) immunofluorescence of ipsilateral hemisphere 2 weeks after sham MCAO surgery. CTX (cortex), STM (striatum). Scale bars = 100 μm (A) or 20 μm (B,C).

Supporting Information Figure 2. A) YFP and Olig2 (left) or NG2 (right) immunofluorescence within the subventricular zone. **B)** YFP+ cells within the corpus callosum (CC); higher power shown on right panel. LV (lateral ventricle). Scale bars = 10 μm.

Figure C.1 Experimental design.
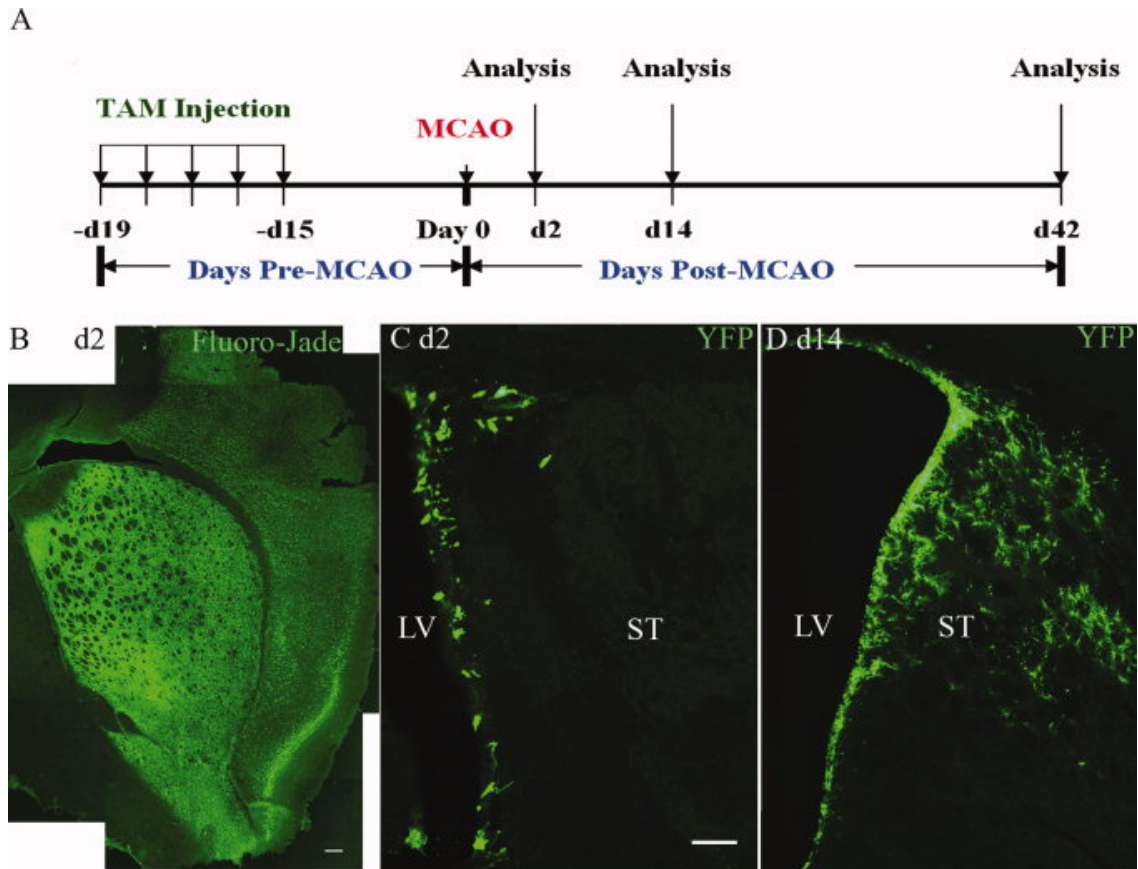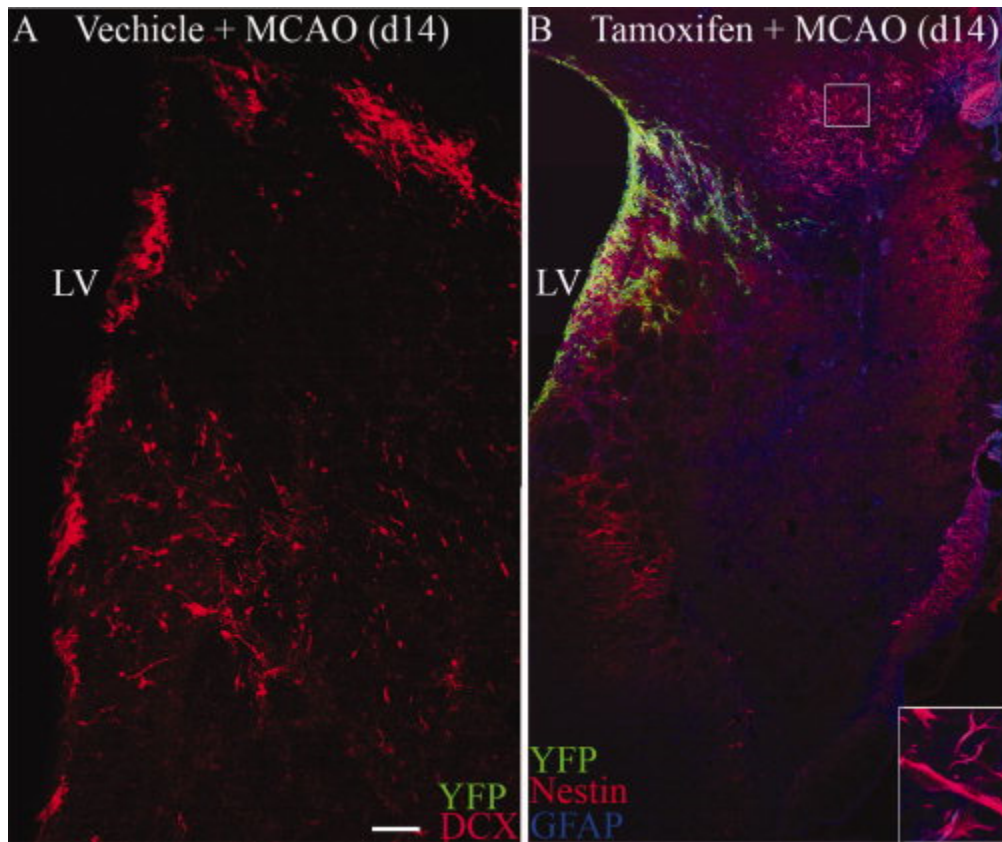
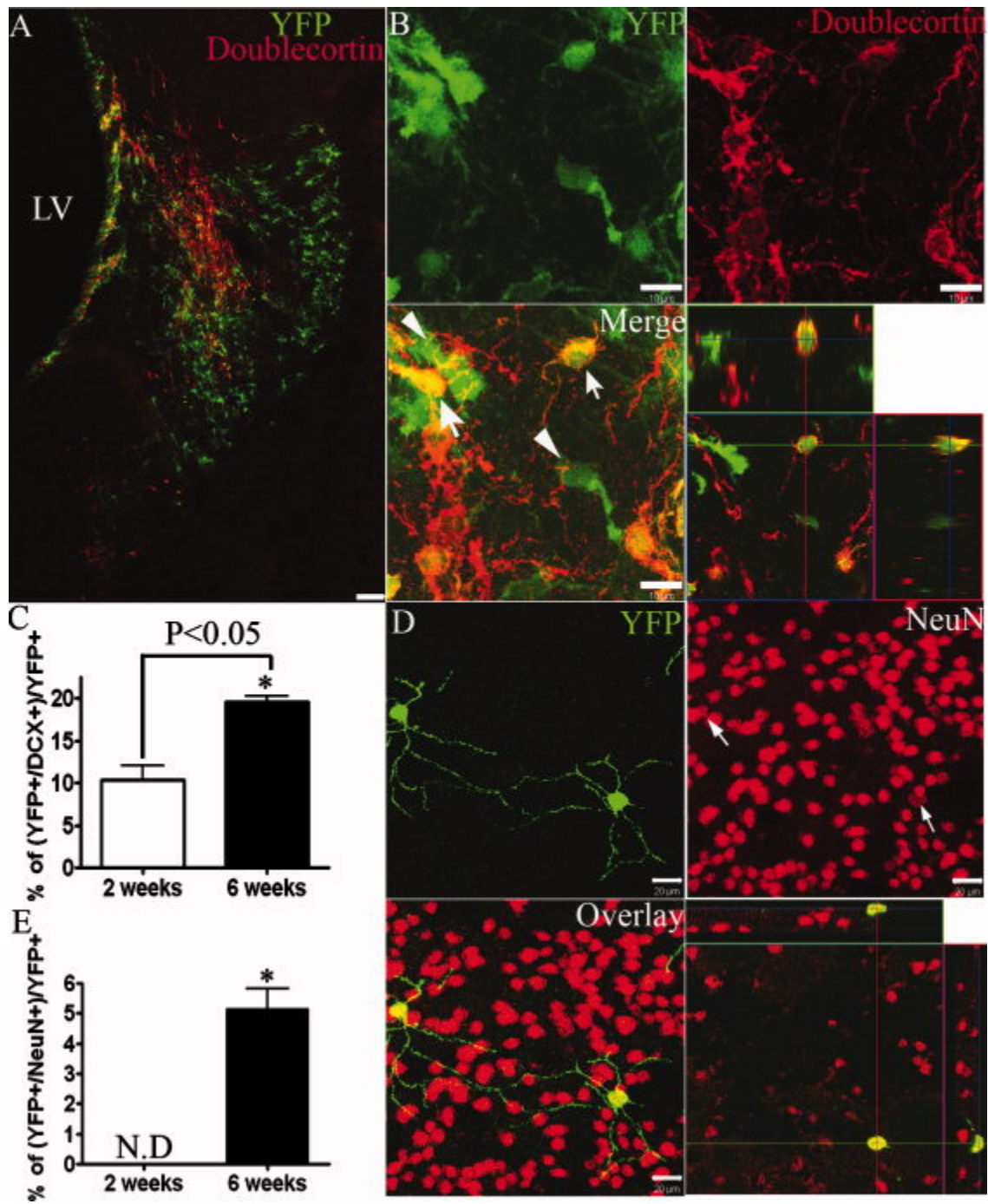**Figure C.2 Dcx and YFP immunofluorescence following MCAO**

Figure C.3 Dcx and NeuN immunofluorescence 2 weeks post-MCAO
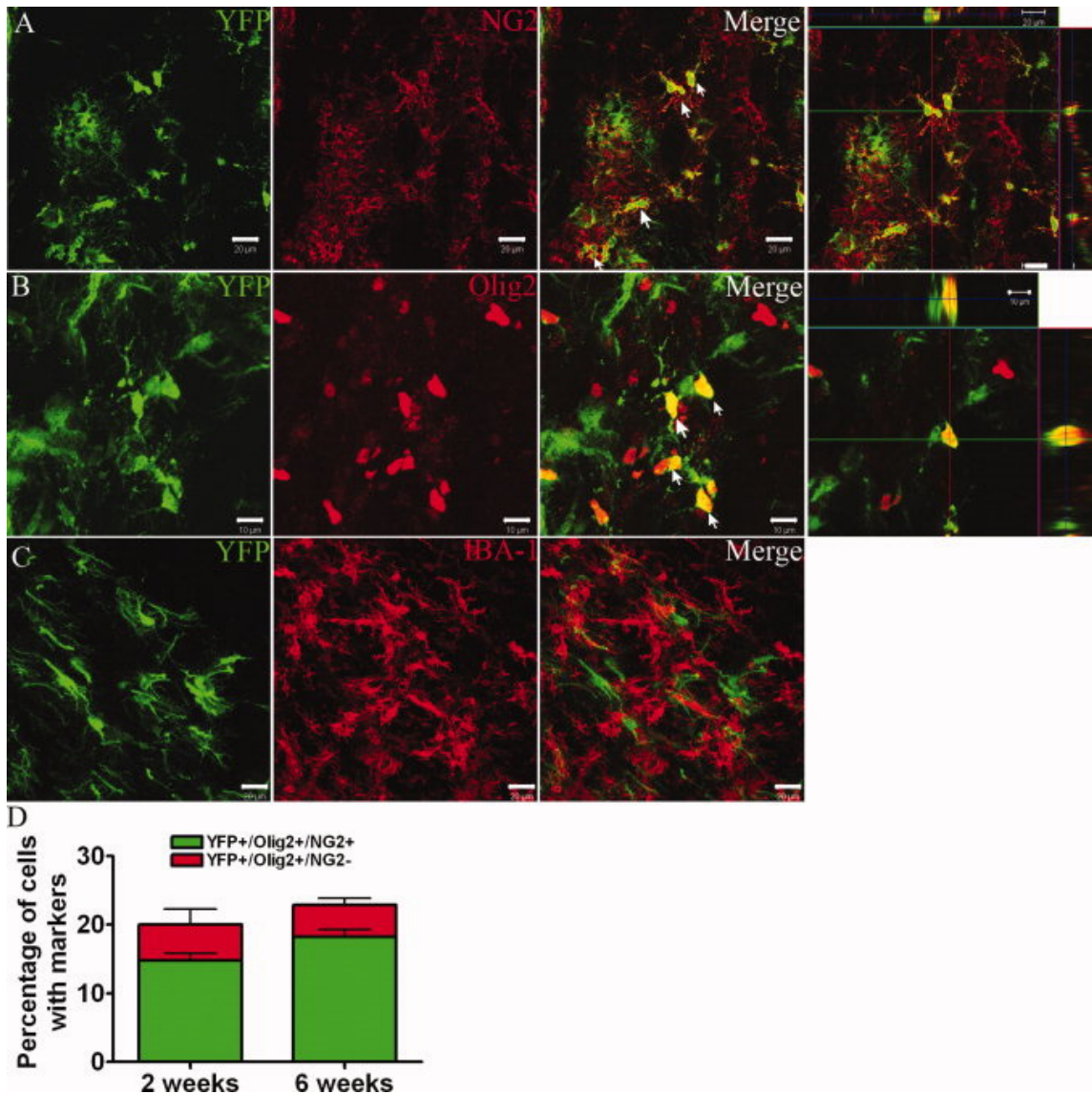
Figure C.4 NG2, Olig2, and Iba-1 immunofluorescence 2 weeks post-MCAO
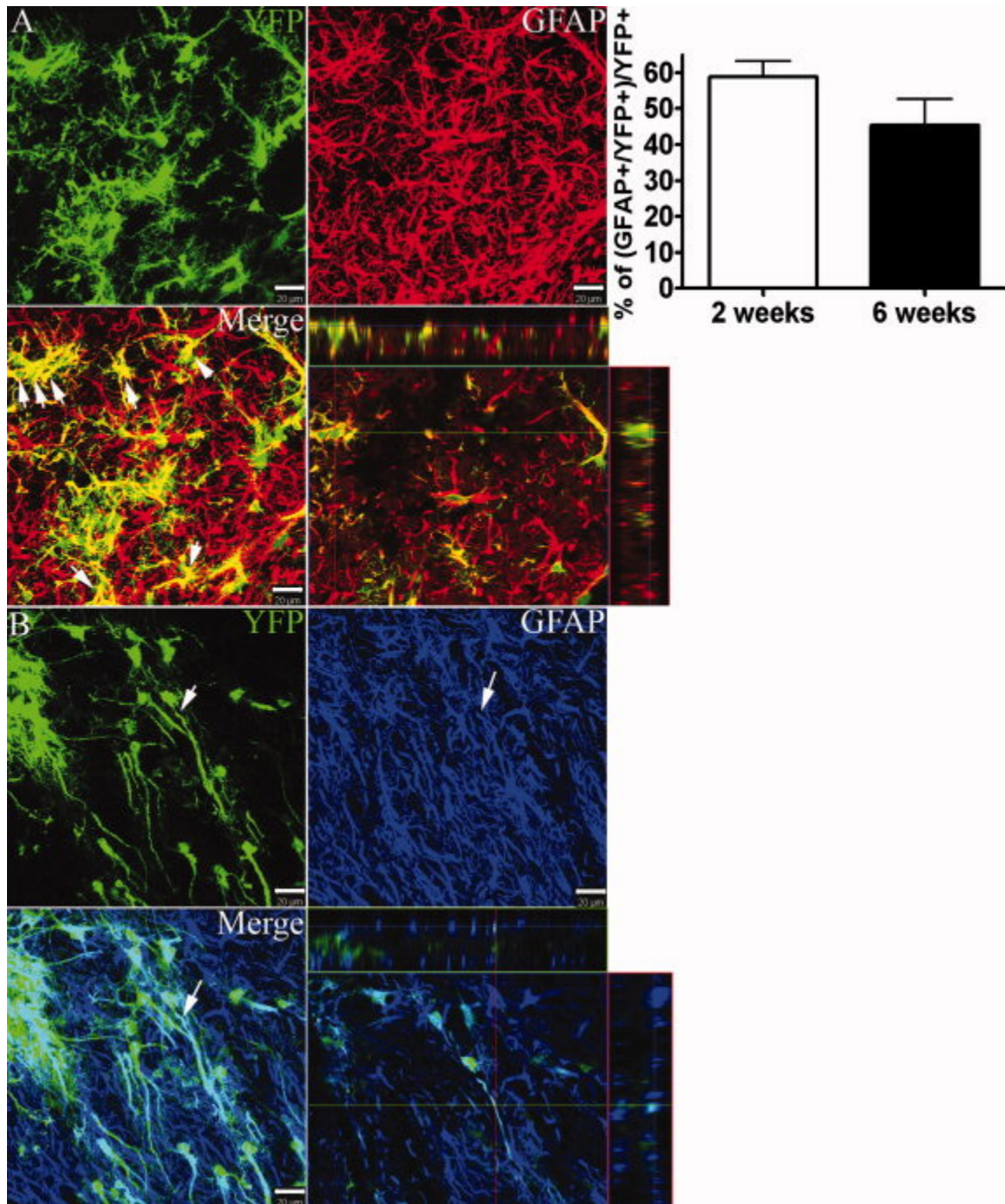
Figure C.5 GFAP immunofluorescence 2 and 6 weeks post-MCAO
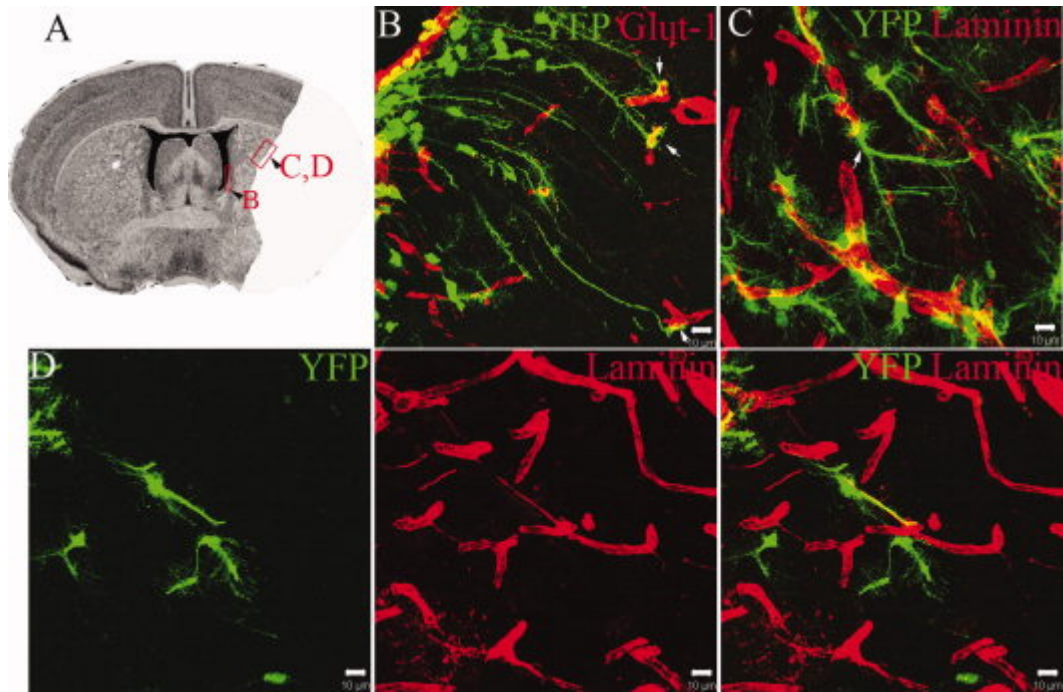
Figure C.6 Glut-1 and laminin immunofluorescence
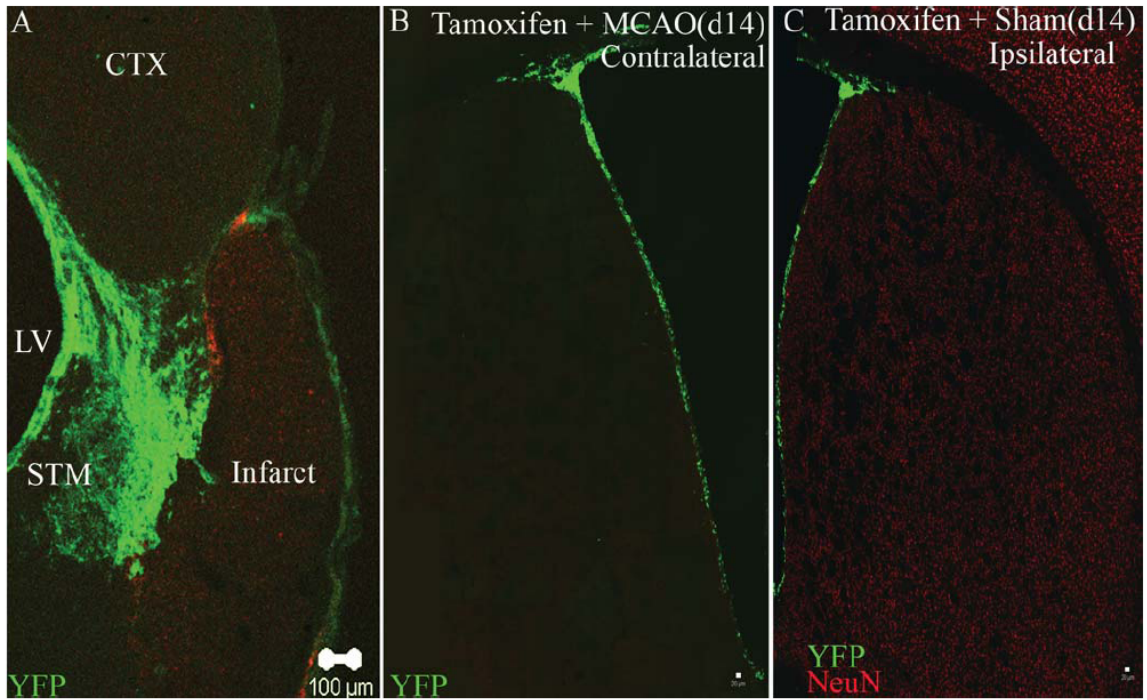
Supporting Information Figure C.1
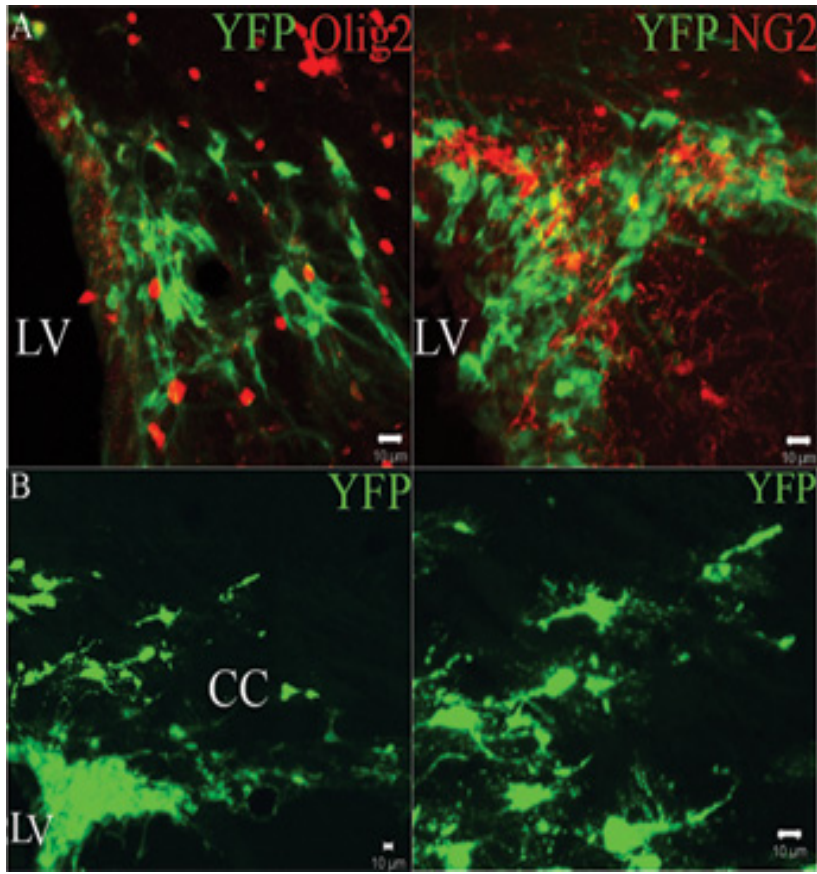
Supporting Information Figure C.2

Appendix D: Use of *nestin*-CreER^{T2}/R26R-YFP/*Hif1a*$^{fl/fl}$ mice to characterize NSPC response to MCAO

Lu Li^{1*}, Kate M. Candelario^{1*}, Kelsey Thomas^{1}, Diane C. Lagace^{2}, Amelia J. Eisch^{3}, and Lee Anna Cunningham^{1}

^{1}Department of Neurosciences, University of New Mexico Health Sciences Center, Albuquerque, New Mexico 87131

^{2}Department of Cellular and Molecular Medicine, University of Ottawa, Ottawa, Ontario Canada K1H 8M5

^{3}Department of Psychiatry, University of Texas Southwestern Medical Center, Dallas, Texas 75390

*Denotes equal authorship.

Work presented in this appendix was performed by Lu Li.

D.1 NSPC-HIF-1α gene deletion results in cell autonomous NSPC depletion in SVZ and SGZ under non-pathological conditions

To determine the effect of NSPC-HIF-1α gene deletion *in vivo*, tamoxifen was administered to triple transgenic mice (*nestin*-CreER^{T2}/R26R-YFP/*Hif1a*$^{fl/fl}$) and the mice were sacrificed 2 weeks later. In the triple transgenic mice, tamoxifen induces simultaneous and irreversible Cre-mediated recombination at the R26R-YFP and *Hif1a*$^{fl/fl}$ loci yielding *nestin*-CreER^{T2}/R26R-YFP/*Hif1a*$^{Δ/Δ}$ NSPCs in which YFP reporter expression is activated and HIF-1α exon 2 is deleted from genomic DNA in the same cells. *Nestin*-CreER^{T2}/R26R-YFP double transgenics that do not harbor floxed *Hif1a* exon 2 received the same tamoxifen dosing regimen and served as controls (*nestin*-CreER^{T2}/R26R-YFP/*Hif1a*$^{wt/wt}$). As shown in **Figure D1**, *Hif1a* gene deletion resulted in depletion of YFP$^+$ cells throughout the SVZ (compare **A** *vs.* **B**). YFP+ NSPC depletion was even more pronounced within the SGZ, where only sparse YFP+ cells were observed two weeks following *in vivo* recombination (compare **C** *vs.* **D**). Noticeably, the negative impact of *Hif1a* gene deletion on the NSPC pool appears to be a cell-autonomous effect, since Dcx+ neuroblasts were observed throughout the SGZ in the *nestin*-CreER^{T2}/R26R-YFP/*Hif1a*$^{Δ/Δ}$ mice, indicating that *Hif1a* gene deletion did not impair neurogenesis in non-recombined cells. These results also suggest the possibility of suboptimal recombination efficiency, or that Dcx+ neuroblasts observed in **D** represent those existing prior to TM induction. Future dosing regimens will be tested for optimized recombination efficiency, by increasing the number of dosing cycles or by providing tamoxifen orally through drinking water or gavage. In the interim, we propose a focuses series of experiments to elucidate the *in vivo* mechanisms that underlie HIF-1α regulation

of stem cell pool and subsequent phenotypic fate by restricting analysis to YFP reporter cells.

D.2 NSPC-*Hif1a* gene deletion impairs the cytogenic response to stroke

To determine the effects of NSPC-*Hif1a* gene deletion on the SVZ cytogenic response to stroke, triple or double transgenic mice received tamoxifen injections as described above and were subjected to 60 minute transient MCAO 14 days following the final injection. The mice were sacrificed at 2 weeks post-MCAO. As anticipated, fewer YFP+ cells were observed within the injured striatum of *nestin*-CreER^{T2}/R26R-YFP/*Hif1a*$^{\Delta/\Delta}$ mice compared to tamoxifen treated control mice (**Fig. D2**). This is likely due to decreased numbers of YFP+ cells in the stem cell pool prior to injury as described above, coupled with reduced survival and/or proliferation of *Hif1a*$^{\Delta/\Delta}$ NSPCs following stroke. Nevertheless, some YFP^{+} *Hif1a*$^{\Delta/\Delta}$ NSPCs survived the injury and migrated into the ischemic striatum. Preliminary phenotypic analysis suggests that *Hif1a* gene deletion, while decreasing the total number of YFP+ cells within the ischemic striatum, increases the percentage of YFP+ cells that express the neuroblasts marker Dcx at 2 weeks post-MCAO (**Fig. D3**).
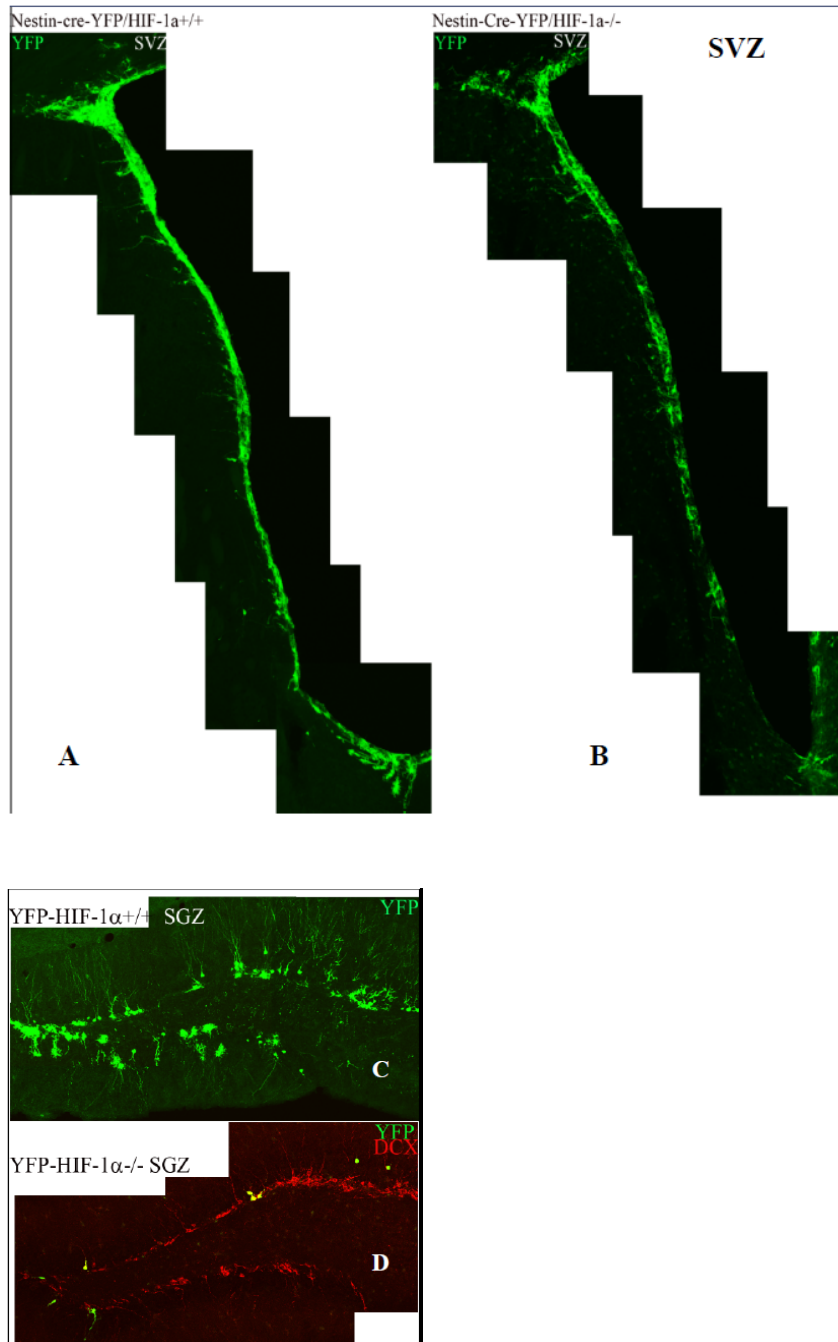
Figure D1. YFP+ reporter expression in SVZ (left) and SGZ (above) 2 weeks following TM injections to *nestin*-CreER[T2]/R26R-YFP/*Hif1a*[wt/w]t (**A,C**) or *nestin*-CreER[T2]/R26R-YFP/*Hif1a*^{fl/fl} mice (**B,D**). Note that *Hif1a* gene deletion resulted in depletion of YFP+ cells throughout the SVZ and SGZ. Dual labeling for YFP and DCX in **D** revealed many non-YFP+ neuroblasts indicating that *Hif1a* gene deletion resulted in NSC autonomous depletion and did impair neurogenesis in non-recombined cells.
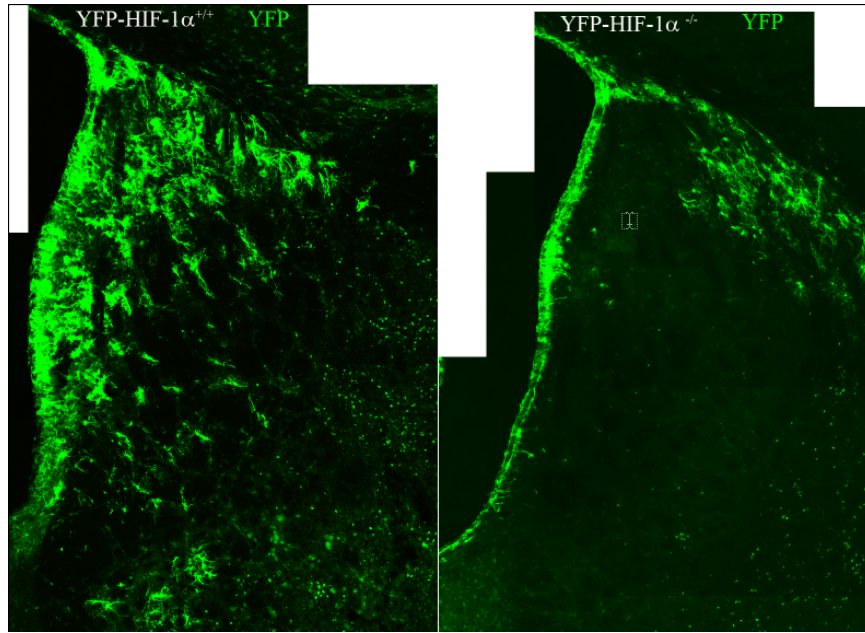
Figure D2.   YFP reporter expression within the ischemic striatum in *nestin*-CreER^{T2}/R26R-YFP/*Hif1a*+/+ (left) and *nestin*-CreER^{T2}/R26R-YFP/*Hif1a*$^{\Delta/\Delta}$ (right) mice at 2 weeks post-MCAO.
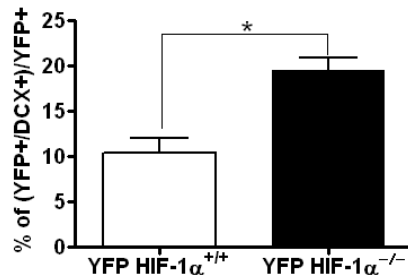
Figure D3. Percentage of YFP+ cells that co-express DCX within ischemic striatum at 2 weeks following MCAO.

Abbreviations Used

2-DG	2-deoxy-D-glucose
4-OH-TM	4-hydroxy-tamoxifen
6-AN	6-aminonicotinamide
ADP	Adenosine diphosphate
ANOVA	Analysis of variance
ARNT	Aryl hydrocarbon receptor nuclear translocator
ATP	Adenosine triphosphate
BDNF	Brain derived neurotrophic factor
bFGF	Basic fibroblast growth factor
BrdU	Bromodeoxyuridine
CCA	Common carotid artery
CMV	Cytomegalovirus
CN	Cyanide
Cy	Cyanine
DAPI	4',6-diamidino-2-phenylindole
DCA	Dichloroacetate
Dcx	Doublecortin
DIV	Days in vitro
DNA	Deoxyribonucleic acid
EGF	Epidermal growth factor
EPO	Erythropoietin
GFAP	Glial fibrillary acidic protein
GFP	Green fluorescent protein
EBSS	Earle's balanced salt solution

ECAR	Extracellular acidification rate
EGFP	Enhanced green fluorescent protein
FITC	Fluorescein isothiocyanate
FCCP	Carbonyl cyanide-4-(trifluoromethoxy)phenylhydrazone
HIF	Hypoxia-inducible factor
HRE	Hypoxia response element
HSP	Heat shock protein
ICD	Intracellular domain
LDH	Lactate dehydrogenase
MCAO	Middle cerebral artery occlusion
MCT	Monocarboxylate transporter
MOI	Multiplicities of infection
MPO	Myeloperoxidase
NAD(P)H	Nicotinamide adenine dinucleotide (phosphate)
NIH	National Institutes of Health
NSPC	Neural stem/progenitor cell
OCR	Oxygen consumption rate
OGD	Oxygen-glucose deprivation
PBS	Phosphate buffered saline
PCR	Polymerase chain reaction
PDH	Pyruvate dehydrogenase
PDK	Pyruvate dehydrogenase kinase
PSA-NCAM	Polysialylated neural cell adhesion molecule
ROS	Reactive oxygen species
SDF	Stromal derived factor

SGZ	Subgranular zone
SVZ	Subventricular zone
TCA	Tricarboxylic acid cycle
TEM	Transmission electron microscopy
TM	Tamoxifen
tPA	Tissue plasminogen activator
Tuj1	Neuron-specific class III beta-tubulin
TUNEL	Terminal deoxynucleotidyl transferase dUTP nick end labeling
VEGF	Vascular Endothelial Growth Factor
VHL	von Hippel-Lindau
YFP	Yellow fluorescent protein

References

Abrous DN, Koehl M, Le Moal M (2005) Adult neurogenesis: from precursors to network and physiology. Physiol Rev 85:523-569.

Alvarez-Buylla A, Lim DA (2004) For the long run: maintaining germinal niches in the adult brain. Neuron 41:683-686.

Arany Z, Foo SY, Ma Y, Ruas JL, Bommi-Reddy A, Girnun G, Cooper M, Laznik D, Chinsomboon J, Rangwala SM, Baek KH, Rosenzweig A, Spiegelman BM (2008) HIF-independent regulation of VEGF and angiogenesis by the transcriptional coactivator PGC-1alpha. Nature 451:1008-1012.

Arvidsson A, Collin T, Kirik D, Kokaia Z, Lindvall O (2002) Neuronal replacement from endogenous precursors in the adult brain after stroke. Nat Med 8:963-970.

Babu H, Cheung G, Kettenmann H, Palmer TD, Kempermann G (2007) Enriched monolayer precursor cell cultures from micro-dissected adult mouse dentate gyrus yield functional granule cell-like neurons. PLoS One 2:e388.

Barkho BZ, Munoz AE, Li X, Li L, Cunningham LA, Zhao X (2008) Endogenous matrix metalloproteinase (MMP)-3 and MMP-9 promote the differentiation and migration of adult neural progenitor cells in response to chemokines. Stem Cells 26:3139-3149.

Battiste J, Helms AW, Kim EJ, Savage TK, Lagace DC, Mandyam CD, Eisch AJ, Miyoshi G, Johnson JE (2007) Ascl1 defines sequentially generated lineage-restricted neuronal and oligodendrocyte precursor cells in the spinal cord. Development 134:285-293.

Bergeron M, Yu AY, Solway KE, Semenza GL, Sharp FR (1999) Induction of hypoxia-inducible factor-1 (HIF-1) and its target genes following focal ischaemia in rat brain. Eur J Neurosci 11:4159-4170.

Bernaudin M, Marti HH, Roussel S, Divoux D, Nouvelot A, MacKenzie ET, Petit E (1999) A potential role for erythropoietin in focal permanent cerebral ischemia in mice. J Cereb Blood Flow Metab 19:643-651.

Berridge MV, Herst PM, Tan AS (2005) Tetrazolium dyes as tools in cell biology: new insights into their cellular reduction. Biotechnol Annu Rev 11:127-152.

Birk DM, Barbato J, Mureebe L, Chaer RA (2008) Current insights on the biology and clinical aspects of VEGF regulation. Vasc Endovascular Surg 42:517-530.

Bonnet S, Archer SL, Allalunis-Turner J, Haromy A, Beaulieu C, Thompson R, Lee CT, Lopaschuk GD, Puttagunta L, Bonnet S, Harry G, Hashimoto K, Porter CJ,

Andrade MA, Thebaud B, Michelakis ED (2007) A mitochondria-K+ channel axis is suppressed in cancer and its normalization promotes apoptosis and inhibits cancer growth. Cancer Cell 11:37-51.

Bouzier-Sore AK, Voisin P, Canioni P, Magistretti PJ, Pellerin L (2003) Lactate is a preferential oxidative energy substrate over glucose for neurons in culture. J Cereb Blood Flow Metab 23:1298-1306.

Buffo A, Rite I, Tripathi P, Lepier A, Colak D, Horn AP, Mori T, Gotz M (2008) Origin and progeny of reactive gliosis: A source of multipotent cells in the injured brain. Proc Natl Acad Sci U S A 105:3581-3586.

Burgers HF, Schelshorn DW, Wagner W, Kuschinsky W, Maurer MH (2008) Acute anoxia stimulates proliferation in adult neural stem cells from the rat brain. Exp Brain Res 188:33-43.

Burns KA, Ayoub AE, Breunig JJ, Adhami F, Weng WL, Colbert MC, Rakic P, Kuan CY (2007) Nestin-CreER Mice Reveal DNA Synthesis by Nonapoptotic Neurons following Cerebral Ischemia-Hypoxia. Cereb Cortex. 17:2585-2592.

Burns TC, Verfaillie CM, Low WC (2009) Stem cells for ischemic brain injury: a critical review. J Comp Neurol 515:125-144.

Bush TG, Puvanachandra N, Horner CH, Polito A, Ostenfeld T, Svendsen CN, Mucke L, Johnson MH, Sofroniew MV (1999) Leukocyte infiltration, neuronal degeneration, and neurite outgrowth after ablation of scar-forming, reactive astrocytes in adult transgenic mice. Neuron 23:297-308.

Carmeliet P, Storkebaum E (2002) Vascular and neuronal effects of VEGF in the nervous system: implications for neurological disorders. Semin Cell Dev Biol 13:39-53.

Chen CT, Shih YR, Kuo TK, Lee OK, Wei YH (2008) Coordinated changes of mitochondrial biogenesis and antioxidant enzymes during osteogenic differentiation of human mesenchymal stem cells. Stem Cells 26:960-968.

Chen HL, Pistollato F, Hoeppner DJ, Ni HT, McKay RD, Panchision DM (2007a) Oxygen tension regulates survival and fate of mouse central nervous system precursors at multiple levels. Stem Cells 25:2291-2301.

Chen N, Chen X, Huang R, Zeng H, Gong J, Meng W, Lu Y, Zhao F, Wang L, Zhou Q (2009) BCL-xL is a target gene regulated by hypoxia-inducible factor-1{alpha}. J Biol Chem 284:10004-10012.

Chen ZY, Asavaritikrai P, Prchal JT, Noguchi CT (2007b) Endogenous erythropoietin signaling is required for normal neural progenitor cell proliferation. J Biol Chem 282:25875-25883.

Chu K, Jung KH, Kim SJ, Lee ST, Kim J, Park HK, Song EC, Kim SU, Kim M, Lee SK, Roh JK (2008) Transplantation of human neural stem cells protect against ischemia in a preventive mode via hypoxia-inducible factor-1alpha stabilization in the host brain. Brain Res 1207:182-192.

Chung S, Dzeja PP, Faustino RS, Perez-Terzic C, Behfar A, Terzic A (2007) Mitochondrial oxidative metabolism is required for the cardiac differentiation of stem cells. Nat Clin Pract Cardiovasc Med 4 Suppl 1:S60-67.

Coezy E, Borgna JL, Rochefort H (1982) Tamoxifen and metabolites in MCF7 cells: correlation between binding to estrogen receptor and inhibition of cell growth. Cancer Res 42:317-323.

Connolly DT, Heuvelman DM, Nelson R, Olander JV, Eppley BL, Delfino JJ, Siegel NR, Leimgruber RM, Feder J (1989) Tumor vascular permeability factor stimulates endothelial cell growth and angiogenesis. J Clin Invest 84:1470-1478.

Csete M (2005) Oxygen in the cultivation of stem cells. Ann N Y Acad Sci 1049:1-8.

Curtis MA, Kam M, Nannmark U, Anderson MF, Axell MZ, Wikkelso C, Holtas S, van Roon-Mom WM, Bjork-Eriksson T, Nordborg C, Frisen J, Dragunow M, Faull RL, Eriksson PS (2007) Human neuroblasts migrate to the olfactory bulb via a lateral ventricular extension. Science 315:1243-1249.

Diehn M, Cho RW, Lobo NA, Kalisky T, Dorie MJ, Kulp AN, Qian D, Lam JS, Ailles LE, Wong M, Joshua B, Kaplan MJ, Wapnir I, Dirbas FM, Somlo G, Garberoglio C, Paz B, Shen J, Lau SK, Quake SR, Brown JM, Weissman IL, Clarke MF (2009) Association of reactive oxygen species levels and radioresistance in cancer stem cells. Nature 458:780-783.

Dimou L, Simon C, Kirchhoff F, Takebayashi H, Gotz M (2008) Progeny of Olig2-expressing progenitors in the gray and white matter of the adult mouse cerebral cortex. J Neurosci 28:10434-10442.

Dirnagl U, Iadecola C, Moskowitz MA (1999) Pathobiology of ischaemic stroke: an integrated view. Trends Neurosci 22:391-397.

Doetsch F (2003a) A niche for adult neural stem cells. Curr Opin Genet Dev 13:543-550.

Doetsch F (2003b) The glial identity of neural stem cells. Nat Neurosci 6:1127-1134.

Doetsch F, Garcia-Verdugo JM, Alvarez-Buylla A (1997) Cellular composition and three-dimensional organization of the subventricular germinal zone in the adult mammalian brain. J Neurosci 17:5046-5061.

Eriksson PS, Perfilieva E, Bjork-Eriksson T, Alborn AM, Nordborg C, Peterson DA, Gage FH (1998) Neurogenesis in the adult human hippocampus. Nat Med 4:1313-1317.

Feigin VL, Lawes CM, Bennett DA, Anderson CS (2003) Stroke epidemiology: a review of population-based studies of incidence, prevalence, and case-fatality in the late 20th century. Lancet Neurol 2:43-53.

Ferrara N (2004) Vascular endothelial growth factor: basic science and clinical progress. Endocr Rev 25:581-611.

Ferriero DM (2005) Protecting neurons. Epilepsia 46 Suppl 7:45-51.

Fischer B, Bavister BD (1993) Oxygen tension in the oviduct and uterus of rhesus monkeys, hamsters and rabbits. J Reprod Fertil 99:673-679.

Forsythe JA, Jiang BH, Iyer NV, Agani F, Leung SW, Koos RD, Semenza GL (1996) Activation of vascular endothelial growth factor gene transcription by hypoxia-inducible factor 1. Mol Cell Biol 16:4604-4613.

Freeman RS, Hasbani DM, Lipscomb EA, Straub JA, Xie L (2003) SM-20, EGL-9, and the EGLN family of hypoxia-inducible factor prolyl hydroxylases. Mol Cells 16:1-12.

Frezza C, Gottlieb E (2009) Mitochondria in cancer: not just innocent bystanders. Semin Cancer Biol 19:4-11.

Fulzele K, DiGirolamo DJ, Liu Z, Xu J, Messina JL, Clemens TL (2007) Disruption of the insulin-like growth factor type 1 receptor in osteoblasts enhances insulin signaling and action. J Biol Chem 282:25649-25658.

Gage FH (2000) Mammalian neural stem cells. Science 287:1433-1438.

Gao Z, Ure K, Ables JL, Lagace DC, Nave KA, Goebbels S, Eisch AJ, Hsieh J (2009) Neurod1 is essential for the survival and maturation of adult-born neurons. Nat Neurosci 12:1090-1092.

Gatenby RA, Gillies RJ (2004) Why do cancers have high aerobic glycolysis? Nat Rev Cancer 4:891-899.

Germano I, Swiss V, Casaccia P (2010) Primary brain tumors, neural stem cell, and brain tumor cancer cells: where is the link? Neuropharmacology 58:903-910.

Goldberg MP, Choi DW (1993) Combined oxygen and glucose deprivation in cortical cell culture: calcium-dependent and calcium-independent mechanisms of neuronal injury. J Neurosci 13:3510-3524.

Gordan JD, Thompson CB, Simon MC (2007) HIF and c-Myc: sibling rivals for control of cancer cell metabolism and proliferation. Cancer Cell 12:108-113.

Gould E, Gross CG (2002) Neurogenesis in adult mammals: some progress and problems. J Neurosci 22:619-623.

Greenberg DA, Jin K (2005) From angiogenesis to neuropathology. Nature 438:954-959.

Gustafsson MV, Zheng X, Pereira T, Gradin K, Jin S, Lundkvist J, Ruas JL, Poellinger L, Lendahl U, Bondesson M (2005) Hypoxia requires notch signaling to maintain the undifferentiated cell state. Dev Cell 9:617-628.

Hansen TM, Moss AJ, Brindle NP (2008) Vascular endothelial growth factor and angiopoietins in neurovascular regeneration and protection following stroke. Curr Neurovasc Res 5:236-245.

Harms KM, Li L, Cunningham LA (2010) Murine Neural Stem/Progenitor Cells Protect Neurons against Ischemia by HIF-1alpha-Regulated VEGF Signaling. PLoS One 5:e9767.

Hayakawa K, Nakano T, Irie K, Higuchi S, Fujioka M, Orito K, Iwasaki K, Jin G, Lo EH, Mishima K, Fujiwara M (2010) Inhibition of reactive astrocytes with fluorocitrate retards neurovascular remodeling and recovery after focal cerebral ischemia in mice. J Cereb Blood Flow Metab 30:871-882.

Hayashi J, Takagi Y, Fukuda H, Imazato T, Nishimura M, Fujimoto M, Takahashi J, Hashimoto N, Nozaki K (2006) Primate embryonic stem cell-derived neuronal progenitors transplanted into ischemic brain. J Cereb Blood Flow Metab 26:906-914.

Hayashi S, McMahon AP (2002) Efficient recombination in diverse tissues by a tamoxifen-inducible form of Cre: a tool for temporally regulated gene activation/inactivation in the mouse. Dev Biol 244:305-318.

Herrera DG, Garcia-Verdugo JM, Alvarez-Buylla A (1999) Adult-derived neural precursors transplanted into multiple regions in the adult brain. Ann Neurol 46:867-877.

Herrmann JE, Imura T, Song B, Qi J, Ao Y, Nguyen TK, Korsak RA, Takeda K, Akira S, Sofroniew MV (2008) STAT3 is a critical regulator of astrogliosis and scar formation after spinal cord injury. J Neurosci 28:7231-7243.

Higgins DF, Kimura K, Bernhardt WM, Shrimanker N, Akai Y, Hohenstein B, Saito Y, Johnson RS, Kretzler M, Cohen CD, Eckardt KU, Iwano M, Haase VH (2007)

Hypoxia promotes fibrogenesis in vivo via HIF-1 stimulation of epithelial-to-mesenchymal transition. J Clin Invest 117:3810-3820.

Horie N, So K, Moriya T, Kitagawa N, Tsutsumi K, Nagata I, Shinohara K (2008) Effects of Oxygen Concentration on the Proliferation and Differentiation of Mouse Neural Stem Cells In Vitro. Cell Mol Neurobiol. 28:833-845.

Hua Z, Lv Q, Ye W, Wong CK, Cai G, Gu D, Ji Y, Zhao C, Wang J, Yang BB, Zhang Y (2006) MiRNA-directed regulation of VEGF and other angiogenic factors under hypoxia. PLoS One 1:e116.

Imitola J, Raddassi K, Park KI, Mueller FJ, Nieto M, Teng YD, Frenkel D, Li J, Sidman RL, Walsh CA, Snyder EY, Khoury SJ (2004) Directed migration of neural stem cells to sites of CNS injury by the stromal cell-derived factor 1alpha/CXC chemokine receptor 4 pathway. Proc Natl Acad Sci U S A 101:18117-18122.

Indra AK, Warot X, Brocard J, Bornert JM, Xiao JH, Chambon P, Metzger D (1999) Temporally-controlled site-specific mutagenesis in the basal layer of the epidermis: comparison of the recombinase activity of the tamoxifen-inducible Cre-ER(T) and Cre-ER(T2) recombinases. Nucleic Acids Res 27:4324-4327.

Ivanova NB, Dimos JT, Schaniel C, Hackney JA, Moore KA, Lemischka IR (2002) A stem cell molecular signature. Science 298:601-604.

Iwai M, Sato K, Kamada H, Omori N, Nagano I, Shoji M, Abe K (2003) Temporal profile of stem cell division, migration, and differentiation from subventricular zone to olfactory bulb after transient forebrain ischemia in gerbils. J Cereb Blood Flow Metab 23:331-341.

Iyer NV, Kotch LE, Agani F, Leung SW, Laughner E, Wenger RH, Gassmann M, Gearhart JD, Lawler AM, Yu AY, Semenza GL (1998) Cellular and developmental control of O2 homeostasis by hypoxia-inducible factor 1 alpha. Genes Dev 12:149-162.

Jin K, Wang X, Xie L, Mao XO, Greenberg DA (2010a) Transgenic ablation of doublecortin-expressing cells suppresses adult neurogenesis and worsens stroke outcome in mice. Proc Natl Acad Sci U S A 107:7993-7998.

Jin K, Mao XO, Batteur SP, McEachron E, Leahy A, Greenberg DA (2001a) Caspase-3 and the regulation of hypoxic neuronal death by vascular endothelial growth factor. Neuroscience 108:351-358.

Jin K, Zhu Y, Sun Y, Mao XO, Xie L, Greenberg DA (2002) Vascular endothelial growth factor (VEGF) stimulates neurogenesis in vitro and in vivo. Proc Natl Acad Sci U S A 99:11946-11950.

Jin K, Minami M, Lan JQ, Mao XO, Batteur S, Simon RP, Greenberg DA (2001b) Neurogenesis in dentate subgranular zone and rostral subventricular zone after focal cerebral ischemia in the rat. Proc Natl Acad Sci U S A 98:4710-4715.

Jin K, Mao X, Xie L, Galvan V, Lai B, Wang Y, Gorostiza O, Wang X, Greenberg DA (2010b) Transplantation of human neural precursor cells in Matrigel scaffolding improves outcome from focal cerebral ischemia after delayed postischemic treatment in rats. J Cereb Blood Flow Metab 30:534-544.

Jin K, Wang X, Xie L, Mao XO, Zhu W, Wang Y, Shen J, Mao Y, Banwait S, Greenberg DA (2006) Evidence for stroke-induced neurogenesis in the human brain. Proc Natl Acad Sci U S A 103:13198-13202.

Jin KL, Mao XO, Greenberg DA (2000) Vascular endothelial growth factor: direct neuroprotective effect in in vitro ischemia. Proc Natl Acad Sci U S A 97:10242-10247.

Kaidi A, Williams AC, Paraskeva C (2007) Interaction between beta-catenin and HIF-1 promotes cellular adaptation to hypoxia. Nat Cell Biol 9:210-217.

Kang J, Shakya A, Tantin D (2009) Stem cells, stress, metabolism and cancer: a drama in two Octs. Trends Biochem Sci 34:491-499.

Kilic E, Kilic U, Wang Y, Bassetti CL, Marti HH, Hermann DM (2006) The phosphatidylinositol-3 kinase/Akt pathway mediates VEGF's neuroprotective activity and induces blood brain barrier permeability after focal cerebral ischemia. Faseb J 20:1185-1187.

Kim JW, Tchernyshyov I, Semenza GL, Dang CV (2006) HIF-1-mediated expression of pyruvate dehydrogenase kinase: a metabolic switch required for cellular adaptation to hypoxia. Cell Metab 3:177-185.

Kokaia Z, Thored P, Arvidsson A, Lindvall O (2006) Regulation of stroke-induced neurogenesis in adult brain--recent scientific progress. Cereb Cortex 16 Suppl 1:i162-167.

Kokovay E, Li L, Cunningham LA (2006) Angiogenic recruitment of pericytes from bone marrow after stroke. J Cereb Blood Flow Metab 26:545-555.

Kokovay E, Shen Q, Temple S (2008) The incredible elastic brain: how neural stem cells expand our minds. Neuron 60:420-429.

Kokovay E, Goderie S, Wang Y, Lotz S, Lin G, Sun Y, Roysam B, Shen Q, Temple S (2010) Adult SVZ Lineage Cells Home to and Leave the Vascular Niche via Differential Responses to SDF1/CXCR4 Signaling. Cell Stem Cell 7:163-173.

Kondoh H, Lleonart ME, Gil J, Wang J, Degan P, Peters G, Martinez D, Carnero A, Beach D (2005) Glycolytic enzymes can modulate cellular life span. Cancer Res 65:177-185.

Kondziolka D, Wechsler L, Goldstein S, Meltzer C, Thulborn KR, Gebel J, Jannetta P, DeCesare S, Elder EM, McGrogan M, Reitman MA, Bynum L (2000) Transplantation of cultured human neuronal cells for patients with stroke. Neurology 55:565-569.

Kotch LE, Iyer NV, Laughner E, Semenza GL (1999) Defective vascularization of HIF-1alpha-null embryos is not associated with VEGF deficiency but with mesenchymal cell death. Dev Biol 209:254-267.

Kovacs Z, Ikezaki K, Samoto K, Inamura T, Fukui M (1996) VEGF and flt. Expression time kinetics in rat brain infarct. Stroke 27:1865-1873.

Kriegstein A, Alvarez-Buylla A (2009) The glial nature of embryonic and adult neural stem cells. Annu Rev Neurosci 32:149-184.

Krum JM, Rosenstein JM (1998) VEGF mRNA and its receptor flt-1 are expressed in reactive astrocytes following neural grafting and tumor cell implantation in the adult CNS. Exp Neurol 154:57-65.

Krupinski J, Kaluza J, Kumar P, Kumar S, Wang JM (1994) Role of angiogenesis in patients with cerebral ischemic stroke. Stroke 25:1794-1798.

Kuwabara T, Hsieh J, Muotri A, Yeo G, Warashina M, Lie DC, Moore L, Nakashima K, Asashima M, Gage FH (2009) Wnt-mediated activation of NeuroD1 and retro-elements during adult neurogenesis. Nat Neurosci 12:1097-1105.

Lagace DC, Benavides DR, Kansy JW, Mapelli M, Greengard P, Bibb JA, Eisch AJ (2008) Cdk5 is essential for adult hippocampal neurogenesis. Proc Natl Acad Sci U S A 105:18567-18571.

Lagace DC, Whitman MC, Noonan MA, Ables JL, DeCarolis NA, Arguello AA, Donovan MH, Fischer SJ, Farnbauch LA, Beech RD, DiLeone RJ, Greer CA, Mandyam CD, Eisch AJ (2007) Dynamic contribution of nestin-expressing stem cells to adult neurogenesis. J Neurosci 27:12623-12629.

Lee HC, Wei YH (2005) Mitochondrial biogenesis and mitochondrial DNA maintenance of mammalian cells under oxidative stress. Int J Biochem Cell Biol 37:822-834.

Lee SR, Kim HY, Rogowska J, Zhao BQ, Bhide P, Parent JM, Lo EH (2006) Involvement of matrix metalloproteinase in neuroblast cell migration from the subventricular zone after stroke. J Neurosci 26:3491-3495.

Leventhal C, Rafii S, Rafii D, Shahar A, Goldman SA (1999) Endothelial trophic support of neuronal production and recruitment from the adult mammalian subependyma. Mol Cell Neurosci 13:450-464.

Li L, Harms KM, Ventura PB, Lagace DC, Eisch AJ, Cunningham LA (2010) Focal cerebral ischemia induces a multilineage cytogenic response from adult subventricular zone that is predominantly gliogenic. Glia 58:1610-1619.

Li X, Barkho BZ, Luo Y, Smrt RD, Santistevan NJ, Liu C, Kuwabara T, Gage FH, Zhao X (2008) Epigenetic regulation of the stem cell mitogen Fgf-2 by Mbd1 in adult neural stem/progenitor cells. J Biol Chem 283:27644-27652.

Lichtenwalner RJ, Parent JM (2006) Adult neurogenesis and the ischemic forebrain. J Cereb Blood Flow Metab 26:1-20.

Lie DC, Colamarino SA, Song HJ, Desire L, Mira H, Consiglio A, Lein ES, Jessberger S, Lansford H, Dearie AR, Gage FH (2005) Wnt signalling regulates adult hippocampal neurogenesis. Nature 437:1370-1375.

Liu J, Solway K, Messing RO, Sharp FR (1998) Increased neurogenesis in the dentate gyrus after transient global ischemia in gerbils. J Neurosci 18:7768-7778.

Liu XS, Chopp M, Zhang RL, Hozeska-Solgot A, Gregg SC, Buller B, Lu M, Zhang ZG (2009) Angiopoietin 2 mediates the differentiation and migration of neural progenitor cells in the subventricular zone after stroke. J Biol Chem 284:22680-22689.

Lonergan T, Bavister B, Brenner C (2007) Mitochondria in stem cells. Mitochondrion 7:289-296.

Louissaint A, Jr., Rao S, Leventhal C, Goldman SA (2002) Coordinated interaction of neurogenesis and angiogenesis in the adult songbird brain. Neuron 34:945-960.

Lum JJ, Bui T, Gruber M, Gordan JD, DeBerardinis RJ, Covello KL, Simon MC, Thompson CB (2007) The transcription factor HIF-1alpha plays a critical role in the growth factor-dependent regulation of both aerobic and anaerobic glycolysis. Genes Dev 21:1037-1049.

Macas J, Nern C, Plate KH, Momma S (2006) Increased generation of neuronal progenitors after ischemic injury in the aged adult human forebrain. J Neurosci 26:13114-13119.

Madhavan L, Ourednik V, Ourednik J (2008) Neural stem/progenitor cells initiate the formation of cellular networks that provide neuroprotection by growth factor-modulated antioxidant expression. Stem Cells 26:254-265.

Marti-Fabregas J, Romaguera-Ros M, Gomez-Pinedo U, Martinez-Ramirez S, Jimenez-Xarrie E, Marin R, Marti-Vilalta JL, Garcia-Verdugo JM (2010) Proliferation in the human ipsilateral subventricular zone after ischemic stroke. Neurology 74:357-365.

Marti HH, Risau W (1999) Angiogenesis in ischemic disease. Thromb Haemost 82 Suppl 1:44-52.

Martin-Villalba A, Hahne M, Kleber S, Vogel J, Falk W, Schenkel J, Krammer PH (2001) Therapeutic neutralization of CD95-ligand and TNF attenuates brain damage in stroke. Cell Death Differ 8:679-686.

Martino G, Pluchino S (2006) The therapeutic potential of neural stem cells. Nat Rev Neurosci 7:395-406.

Matoba S, Kang JG, Patino WD, Wragg A, Boehm M, Gavrilova O, Hurley PJ, Bunz F, Hwang PM (2006) p53 regulates mitochondrial respiration. Science 312:1650-1653.

Maysami S, Lan JQ, Minami M, Simon RP (2008) Proliferating progenitor cells: a required cellular element for induction of ischemic tolerance in the brain. J Cereb Blood Flow Metab 28:1104-1113.

McColl BK, Stacker SA, Achen MG (2004) Molecular regulation of the VEGF family -- inducers of angiogenesis and lymphangiogenesis. Apmis 112:463-480.

McFate T, Mohyeldin A, Lu H, Thakar J, Henriques J, Halim ND, Wu H, Schell MJ, Tsang TM, Teahan O, Zhou S, Califano JA, Jeoung NH, Harris RA, Verma A (2008) Pyruvate dehydrogenase complex activity controls metabolic and malignant phenotype in cancer cells. J Biol Chem 283:22700-22708.

McKay R (1997) Stem cells in the central nervous system. Science 276:66-71.

Meletis K, Barnabe-Heider F, Carlen M, Evergren E, Tomilin N, Shupliakov O, Frisen J (2008) Spinal cord injury reveals multilineage differentiation of ependymal cells. PLoS Biol 6:e182.

Mercier F, Kitasako JT, Hatton GI (2002) Anatomy of the brain neurogenic zones revisited: fractones and the fibroblast/macrophage network. J Comp Neurol 451:170-188.

Milosevic J, Maisel M, Wegner F, Leuchtenberger J, Wenger RH, Gerlach M, Storch A, Schwarz J (2007) Lack of hypoxia-inducible factor-1 alpha impairs midbrain neural precursor cells involving vascular endothelial growth factor signaling. J Neurosci 27:412-421.

Ming GL, Song H (2005) Adult neurogenesis in the mammalian central nervous system. Annu Rev Neurosci 28:223-250.

Mirzadeh Z, Merkle FT, Soriano-Navarro M, Garcia-Verdugo JM, Alvarez-Buylla A (2008) Neural stem cells confer unique pinwheel architecture to the ventricular surface in neurogenic regions of the adult brain. Cell Stem Cell 3:265-278.

Mitchell JA, Yochim JM (1968) Intrauterine oxygen tension during the estrous cycle in the rat: its relation to uterine respiration and vascular activity. Endocrinology 83:701-705.

Mizukami Y, Kohgo Y, Chung DC (2007) Hypoxia inducible factor-1 independent pathways in tumor angiogenesis. Clin Cancer Res 13:5670-5674.

Mohyeldin A, Garzon-Muvdi T, Quinones-Hinojosa A (2010) Oxygen in Stem Cell Biology: A Critical Component of the Stem Cell Niche. Cell Stem Cell 7:150-161.

Morrison SJ, Csete M, Groves AK, Melega W, Wold B, Anderson DJ (2000) Culture in reduced levels of oxygen promotes clonogenic sympathoadrenal differentiation by isolated neural crest stem cells. J Neurosci 20:7370-7376.

Moskowitz MA, Lo EH, Iadecola C (2010) The Science of Stroke: Mechanisms in Search of Treatments. Neuron 67:181-198.

Nagy A (2000) Cre recombinase: the universal reagent for genome tailoring. Genesis 26:99-109.

Nishiyama A, Komitova M, Suzuki R, Zhu X (2009) Polydendrocytes (NG2 cells): multifunctional cells with lineage plasticity. Nat Rev Neurosci 10:9-22.

Ogunshola OO, Antic A, Donoghue MJ, Fan SY, Kim H, Stewart WB, Madri JA, Ment LR (2002) Paracrine and autocrine functions of neuronal vascular endothelial growth factor (VEGF) in the central nervous system. J Biol Chem 277:11410-11415.

Ohab JJ, Fleming S, Blesch A, Carmichael ST (2006) A neurovascular niche for neurogenesis after stroke. J Neurosci 26:13007-13016.

Ohira K, Furuta T, Hioki H, Nakamura KC, Kuramoto E, Tanaka Y, Funatsu N, Shimizu K, Oishi T, Hayashi M, Miyakawa T, Kaneko T, Nakamura S (2010) Ischemia-induced neurogenesis of neocortical layer 1 progenitor cells. Nat Neurosci 13:173-179.

Okada S, Nakamura M, Katoh H, Miyao T, Shimazaki T, Ishii K, Yamane J, Yoshimura A, Iwamoto Y, Toyama Y, Okano H (2006) Conditional ablation of Stat3 or

Socs3 discloses a dual role for reactive astrocytes after spinal cord injury. Nat Med 12:829-834.

Onnis B, Rapisarda A, Melillo G (2009) Development of HIF-1 inhibitors for cancer therapy. J Cell Mol Med 13:2780-2786.

Otani N, Nawashiro H, Fukui S, Ooigawa H, Ohsumi A, Toyooka T, Shima K, Gomi H, Brenner M (2006) Enhanced hippocampal neurodegeneration after traumatic or kainate excitotoxicity in GFAP-null mice. J Clin Neurosci 13:934-938.

Panchision DM (2009) The role of oxygen in regulating neural stem cells in development and disease. J Cell Physiol 220:562-568.

Papandreou I, Cairns RA, Fontana L, Lim AL, Denko NC (2006) HIF-1 mediates adaptation to hypoxia by actively downregulating mitochondrial oxygen consumption. Cell Metab 3:187-197.

Parent JM, Vexler ZS, Gong C, Derugin N, Ferriero DM (2002) Rat forebrain neurogenesis and striatal neuron replacement after focal stroke. Ann Neurol 52:802-813.

Pelicano H, Martin DS, Xu RH, Huang P (2006) Glycolysis inhibition for anticancer treatment. Oncogene 25:4633-4646.

Pellerin L, Bonvento G, Chatton JY, Pierre K, Magistretti PJ (2002) Role of neuron-glia interaction in the regulation of brain glucose utilization. Diabetes Nutr Metab 15:268-273; discussion 273.

Perez-Terzic C, Behfar A, Mery A, van Deursen JM, Terzic A, Puceat M (2003) Structural adaptation of the nuclear pore complex in stem cell-derived cardiomyocytes. Circ Res 92:444-452.

Piccoli C, Ria R, Scrima R, Cela O, D'Aprile A, Boffoli D, Falzetti F, Tabilio A, Capitanio N (2005) Characterization of mitochondrial and extra-mitochondrial oxygen consuming reactions in human hematopoietic stem cells. Novel evidence of the occurrence of NAD(P)H oxidase activity. J Biol Chem 280:26467-26476.

Pistollato F, Chen HL, Schwartz PH, Basso G, Panchision DM (2007) Oxygen tension controls the expansion of human CNS precursors and the generation of astrocytes and oligodendrocytes. Mol Cell Neurosci 35:424-435.

Plesnila N, Zinkel S, Le DA, Amin-Hanjani S, Wu Y, Qiu J, Chiarugi A, Thomas SS, Kohane DS, Korsmeyer SJ, Moskowitz MA (2001) BID mediates neuronal cell death after oxygen/ glucose deprivation and focal cerebral ischemia. Proc Natl Acad Sci U S A 98:15318-15323.

Prigione A, Fauler B, Lurz R, Lehrach H, Adjaye J (2010) The senescence-related mitochondrial/oxidative stress pathway is repressed in human induced pluripotent stem cells. Stem Cells 28:721-733.

Puceat M (2005) Role of Rac-GTPase and reactive oxygen species in cardiac differentiation of stem cells. Antioxid Redox Signal 7:1435-1439.

Rakic P (2002) Adult neurogenesis in mammals: an identity crisis. J Neurosci 22:614-618.

Ray J, Peterson DA, Schinstine M, Gage FH (1993) Proliferation, differentiation, and long-term culture of primary hippocampal neurons. Proc Natl Acad Sci U S A 90:3602-3606.

Rempe D, Vangeison G, Hamilton J, Li Y, Jepson M, Federoff HJ (2006) Synapsin I Cre transgene expression in male mice produces germline recombination in progeny. Genesis 44:44-49.

Riquelme PA, Drapeau E, Doetsch F (2008) Brain micro-ecologies: neural stem cell niches in the adult mammalian brain. Philos Trans R Soc Lond B Biol Sci 363:123-137.

Rodesch F, Simon P, Donner C, Jauniaux E (1992) Oxygen measurements in endometrial and trophoblastic tissues during early pregnancy. Obstet Gynecol 80:283-285.

Roitbak T, Li L, Cunningham LA (2008) Neural stem/progenitor cells promote endothelial cell morphogenesis and protect endothelial cells against ischemia via HIF-1alpha-regulated VEGF signaling. J Cereb Blood Flow Metab 28:1530-1542.

Roitbak T, Surviladze Z, Cunningham LA (2010) Continuous Expression of HIF-1alpha in Neural Stem/Progenitor Cells. Cell Mol Neurobiol. In press.

Rosenstein JM, Mani N, Khaibullina A, Krum JM (2003) Neurotrophic effects of vascular endothelial growth factor on organotypic cortical explants and primary cortical neurons. J Neurosci 23:11036-11044.

Rossant J, Nagy A (1995) Genome engineering: the new mouse genetics. Nat Med 1:592-594.

Russell JW, Golovoy D, Vincent AM, Mahendru P, Olzmann JA, Mentzer A, Feldman EL (2002) High glucose-induced oxidative stress and mitochondrial dysfunction in neurons. Faseb J 16:1738-1748.

Ryan HE, Lo J, Johnson RS (1998) HIF-1 alpha is required for solid tumor formation and embryonic vascularization. Embo J 17:3005-3015.

Ryan HE, Poloni M, McNulty W, Elson D, Gassmann M, Arbeit JM, Johnson RS (2000) Hypoxia-inducible factor-1alpha is a positive factor in solid tumor growth. Cancer Res 60:4010-4015.

Santilli G, Lamorte G, Carlessi L, Ferrari D, Rota Nodari L, Binda E, Delia D, Vescovi AL, De Filippis L (2010) Mild hypoxia enhances proliferation and multipotency of human neural stem cells. PLoS One 5:e8575.

Saretzki G, Armstrong L, Leake A, Lako M, von Zglinicki T (2004) Stress defense in murine embryonic stem cells is superior to that of various differentiated murine cells. Stem Cells 22:962-971.

Sathananthan H, Pera M, Trounson A (2002) The fine structure of human embryonic stem cells. Reprod Biomed Online 4:56-61.

Schipani E, Ryan HE, Didrickson S, Kobayashi T, Knight M, Johnson RS (2001) Hypoxia in cartilage: HIF-1alpha is essential for chondrocyte growth arrest and survival. Genes Dev 15:2865-2876.

Schlappack OK, Zimmermann A, Hill RP (1991) Glucose starvation and acidosis: effect on experimental metastatic potential, DNA content and MTX resistance of murine tumour cells. Br J Cancer 64:663-670.

Schwartzenberg-Bar-Yoseph F, Armoni M, Karnieli E (2004) The tumor suppressor p53 down-regulates glucose transporters GLUT1 and GLUT4 gene expression. Cancer Res 64:2627-2633.

Seagroves TN, Ryan HE, Lu H, Wouters BG, Knapp M, Thibault P, Laderoute K, Johnson RS (2001) Transcription factor HIF-1 is a necessary mediator of the pasteur effect in mammalian cells. Mol Cell Biol 21:3436-3444.

Semenza GL (2003) Targeting HIF-1 for cancer therapy. Nat Rev Cancer 3:721-732.

Semenza GL (2010a) Defining the role of hypoxia-inducible factor 1 in cancer biology and therapeutics. Oncogene 29:625-634.

Semenza GL (2010b) HIF-1: upstream and downstream of cancer metabolism. Curr Opin Genet Dev 20:51-56.

Semenza GL, Wang GL (1992) A nuclear factor induced by hypoxia via de novo protein synthesis binds to the human erythropoietin gene enhancer at a site required for transcriptional activation. Mol Cell Biol 12:5447-5454.

Seminatore C, Polentes J, Ellman D, Kozubenko N, Itier V, Tine S, Tritschler L, Brenot M, Guidou E, Blondeau J, Lhuillier M, Bugi A, Aubry L, Jendelova P, Sykova E, Perrier AL, Finsen B, Onteniente B (2010) The postischemic environment

differentially impacts teratoma or tumor formation after transplantation of human embryonic stem cell-derived neural progenitors. Stroke 41:153-159.

Seyfried TN, Shelton LM (2010) Cancer as a metabolic disease. Nutr Metab (Lond) 7:7.

Sharp FR, Lu A, Tang Y, Millhorn DE (2000) Multiple molecular penumbras after focal cerebral ischemia. J Cereb Blood Flow Metab 20:1011-1032.

Sheldon RA, Osredkar D, Lee CL, Jiang X, Mu D, Ferriero DM (2009) HIF-1 alpha-deficient mice have increased brain injury after neonatal hypoxia-ischemia. Dev Neurosci 31:452-458.

Shen Q, Wang Y, Kokovay E, Lin G, Chuang SM, Goderie SK, Roysam B, Temple S (2008) Adult SVZ stem cells lie in a vascular niche: a quantitative analysis of niche cell-cell interactions. Cell Stem Cell 3:289-300.

Shen Q, Goderie SK, Jin L, Karanth N, Sun Y, Abramova N, Vincent P, Pumiglia K, Temple S (2004) Endothelial cells stimulate self-renewal and expand neurogenesis of neural stem cells. Science 304:1338-1340.

Shen X, Wan C, Ramaswamy G, Mavalli M, Wang Y, Duvall CL, Deng LF, Guldberg RE, Eberhart A, Clemens TL, Gilbert SR (2009) Prolyl hydroxylase inhibitors increase neoangiogenesis and callus formation following femur fracture in mice. J Orthop Res 27:1298-1305.

Shihabuddin LS, Horner PJ, Ray J, Gage FH (2000) Adult spinal cord stem cells generate neurons after transplantation in the adult dentate gyrus. J Neurosci 20:8727-8735.

Shimada IS, Peterson BM, Spees JL (2010) Isolation of Locally Derived Stem/Progenitor Cells From the Peri-Infarct Area That Do Not Migrate From the Lateral Ventricle After Cortical Stroke. Stroke. 41:e552-560.

Shingo T, Sorokan ST, Shimazaki T, Weiss S (2001) Erythropoietin regulates the in vitro and in vivo production of neuronal progenitors by mammalian forebrain neural stem cells. J Neurosci 21:9733-9743.

Shweiki D, Itin A, Soffer D, Keshet E (1992) Vascular endothelial growth factor induced by hypoxia may mediate hypoxia-initiated angiogenesis. Nature 359:843-845.

Silver J, Miller JH (2004) Regeneration beyond the glial scar. Nat Rev Neurosci 5:146-156.

Simon MC, Keith B (2008) The role of oxygen availability in embryonic development and stem cell function. Nat Rev Mol Cell Biol 9:285-296.

Smith J, Ladi E, Mayer-Proschel M, Noble M (2000) Redox state is a central modulator of the balance between self-renewal and differentiation in a dividing glial precursor cell. Proc Natl Acad Sci U S A 97:10032-10037.

Smrt RD, Eaves-Egenes J, Barkho BZ, Santistevan NJ, Zhao C, Aimone JB, Gage FH, Zhao X (2007) Mecp2 deficiency leads to delayed maturation and altered gene expression in hippocampal neurons. Neurobiol Dis 27:77-89.

Sofroniew MV (2009) Molecular dissection of reactive astrogliosis and glial scar formation. Trends Neurosci 32:638-647.

Soriano P (1999) Generalized lacZ expression with the ROSA26 Cre reporter strain. Nat Genet 21:70-71.

Soucek T, Cumming R, Dargusch R, Maher P, Schubert D (2003) The regulation of glucose metabolism by HIF-1 mediates a neuroprotective response to amyloid beta peptide. Neuron 39:43-56.

Studer L, Csete M, Lee SH, Kabbani N, Walikonis J, Wold B, McKay R (2000) Enhanced proliferation, survival, and dopaminergic differentiation of CNS precursors in lowered oxygen. J Neurosci 20:7377-7383.

Sturmey RG, Leese HJ (2003) Energy metabolism in pig oocytes and early embryos. Reproduction 126:197-204.

Sun Y, Jin K, Xie L, Childs J, Mao XO, Logvinova A, Greenberg DA (2003) VEGF-induced neuroprotection, neurogenesis, and angiogenesis after focal cerebral ischemia. J Clin Invest 111:1843-1851.

Takebayashi H, Nabeshima Y, Yoshida S, Chisaka O, Ikenaka K, Nabeshima Y (2002) The basic helix-loop-helix factor olig2 is essential for the development of motoneuron and oligodendrocyte lineages. Curr Biol 12:1157-1163.

Taoufik E, Petit E, Divoux D, Tseveleki V, Mengozzi M, Roberts ML, Valable S, Ghezzi P, Quackenbush J, Brines M, Cerami A, Probert L (2008) TNF receptor I sensitizes neurons to erythropoietin- and VEGF-mediated neuroprotection after ischemic and excitotoxic injury. Proc Natl Acad Sci U S A 105:6185-6190.

Taupin P (2006) Stroke-induced neurogenesis: physiopathology and mechanisms. Curr Neurovasc Res 3:67-72.

Taupin P (2007) BrdU immunohistochemistry for studying adult neurogenesis: paradigms, pitfalls, limitations, and validation. Brain Res Rev 53:198-214.

Tavazoie M, Van der Veken L, Silva-Vargas V, Louissaint M, Colonna L, Zaidi B, Garcia-Verdugo JM, Doetsch F (2008) A specialized vascular niche for adult neural stem cells. Cell Stem Cell 3:279-288.

Temple S (2001) The development of neural stem cells. Nature 414:112-117.

Teng H, Zhang ZG, Wang L, Zhang RL, Zhang L, Morris D, Gregg SR, Wu Z, Jiang A, Lu M, Zlokovic BV, Chopp M (2008) Coupling of angiogenesis and neurogenesis in cultured endothelial cells and neural progenitor cells after stroke. J Cereb Blood Flow Metab 28:764-771.

Theus MH, Wei L, Cui L, Francis K, Hu X, Keogh C, Yu SP (2008) In vitro hypoxic preconditioning of embryonic stem cells as a strategy of promoting cell survival and functional benefits after transplantation into the ischemic rat brain. Exp Neurol 210:656-670.

Thored P, Wood J, Arvidsson A, Cammenga J, Kokaia Z, Lindvall O (2007) Long-term neuroblast migration along blood vessels in an area with transient angiogenesis and increased vascularization after stroke. Stroke 38:3032-3039.

Thored P, Arvidsson A, Cacci E, Ahlenius H, Kallur T, Darsalia V, Ekdahl CT, Kokaia Z, Lindvall O (2006) Persistent production of neurons from adult brain stem cells during recovery after stroke. Stem Cells 24:739-747.

Toledo EM, Colombres M, Inestrosa NC (2008) Wnt signaling in neuroprotection and stem cell differentiation. Prog Neurobiol 86:281-296.

Tomita S, Ueno M, Sakamoto M, Kitahama Y, Ueki M, Maekawa N, Sakamoto H, Gassmann M, Kageyama R, Ueda N, Gonzalez FJ, Takahama Y (2003) Defective brain development in mice lacking the Hif-1alpha gene in neural cells. Mol Cell Biol 23:6739-6749.

Tsai PT, Ohab JJ, Kertesz N, Groszer M, Matter C, Gao J, Liu X, Wu H, Carmichael ST (2006) A critical role of erythropoietin receptor in neurogenesis and post-stroke recovery. J Neurosci 26:1269-1274.

Tsatmali M, Walcott EC, Crossin KL (2005) Newborn neurons acquire high levels of reactive oxygen species and increased mitochondrial proteins upon differentiation from progenitors. Brain Res 1040:137-150.

Tsatmali M, Walcott EC, Makarenkova H, Crossin KL (2006) Reactive oxygen species modulate the differentiation of neurons in clonal cortical cultures. Mol Cell Neurosci 33:345-357.

Urbach A, Redecker C, Witte OW (2008) Induction of neurogenesis in the adult dentate gyrus by cortical spreading depression. Stroke 39:3064-3072.

Vander Heiden MG, Cantley LC, Thompson CB (2009) Understanding the Warburg effect: the metabolic requirements of cell proliferation. Science 324:1029-1033.

Vangeison G, Carr D, Federoff HJ, Rempe DA (2008) The good, the bad, and the cell type-specific roles of hypoxia inducible factor-1 alpha in neurons and astrocytes. J Neurosci 28:1988-1993.

Wachs FP, Couillard-Despres S, Engelhardt M, Wilhelm D, Ploetz S, Vroemen M, Kaesbauer J, Uyanik G, Klucken J, Karl C, Tebbing J, Svendsen C, Weidner N, Kuhn HG, Winkler J, Aigner L (2003) High efficacy of clonal growth and expansion of adult neural stem cells. Lab Invest 83:949-962.

Wang L, Chopp M, Gregg SR, Zhang RL, Teng H, Jiang A, Feng Y, Zhang ZG (2008) Neural progenitor cells treated with EPO induce angiogenesis through the production of VEGF. J Cereb Blood Flow Metab 28:1361-1368.

Wang Y, Jin K, Mao XO, Xie L, Banwait S, Marti HH, Greenberg DA (2007) VEGF-overexpressing transgenic mice show enhanced post-ischemic neurogenesis and neuromigration. J Neurosci Res 85:740-747.

Weidemann A, Johnson RS (2008) Biology of HIF-1alpha. Cell Death Differ 15:621-627.

Weinberg F, Chandel NS (2009) Mitochondrial metabolism and cancer. Ann N Y Acad Sci 1177:66-73.

Wetzel M, Li L, Harms KM, Roitbak T, Ventura PB, Rosenberg GA, Khokha R, Cunningham LA (2008) Tissue inhibitor of metalloproteinases-3 facilitates Fas-mediated neuronal cell death following mild ischemia. Cell Death Differ 15:143-151.

Wey A, Cerdeno VM, Pleasure D, Knoepfler PS (2010) c- and N-myc Regulate Neural Precursor Cell Fate, Cell Cycle, and Metabolism to Direct Cerebellar Development. Cerebellum. In press.

Xiong L, Zhao T, Huang X, Liu ZH, Zhao H, Li MM, Wu LY, Shu HB, Zhu LL, Fan M (2009) Heat shock protein 90 is involved in regulation of hypoxia-driven proliferation of embryonic neural stem/progenitor cells. Cell Stress Chaperones 14:183-192.

Yamashita T, Ninomiya M, Hernandez Acosta P, Garcia-Verdugo JM, Sunabori T, Sakaguchi M, Adachi K, Kojima T, Hirota Y, Kawase T, Araki N, Abe K, Okano H, Sawamoto K (2006) Subventricular zone-derived neuroblasts migrate and differentiate into mature neurons in the post-stroke adult striatum. J Neurosci 26:6627-6636.

Yanamoto H, Miyamoto S, Tohnai N, Nagata I, Xue JH, Nakano Y, Nakajo Y, Kikuchi H (2005) Induced spreading depression activates persistent neurogenesis in the subventricular zone, generating cells with markers for divided and early committed neurons in the caudate putamen and cortex. Stroke 36:1544-1550.

Yang Z, Levison SW (2006) Hypoxia/ischemia expands the regenerative capacity of progenitors in the perinatal subventricular zone. Neuroscience 139:555-564.

Yang Z, Levison SW (2007) Perinatal hypoxic/ischemic brain injury induces persistent production of striatal neurons from subventricular zone progenitors. Dev Neurosci 29:331-340.

Yang ZJ, Bao WL, Qiu MH, Zhang LM, Lu SD, Huang YL, Sun FY (2002) Role of vascular endothelial growth factor in neuronal DNA damage and repair in rat brain following a transient cerebral ischemia. J Neurosci Res 70:140-149.

Yeo EJ, Chun YS, Park JW (2004) New anticancer strategies targeting HIF-1. Biochem Pharmacol 68:1061-1069.

Zhang H, Vutskits L, Pepper MS, Kiss JZ (2003a) VEGF is a chemoattractant for FGF-2-stimulated neural progenitors. J Cell Biol 163:1375-1384.

Zhang R, Zhang Z, Wang L, Wang Y, Gousev A, Zhang L, Ho KL, Morshead C, Chopp M (2004) Activated neural stem cells contribute to stroke-induced neurogenesis and neuroblast migration toward the infarct boundary in adult rats. J Cereb Blood Flow Metab 24:441-448.

Zhang RL, Zhang ZG, Chopp M (2005) Neurogenesis in the adult ischemic brain: generation, migration, survival, and restorative therapy. Neuroscientist 11:408-416.

Zhang RL, Zhang ZG, Zhang L, Chopp M (2001) Proliferation and differentiation of progenitor cells in the cortex and the subventricular zone in the adult rat after focal cerebral ischemia. Neuroscience 105:33-41.

Zhang ZG, Zhang L, Jiang Q, Zhang R, Davies K, Powers C, Bruggen N, Chopp M (2000) VEGF enhances angiogenesis and promotes blood-brain barrier leakage in the ischemic brain. J Clin Invest 106:829-838.

Zhang ZG, Jiang Q, Zhang R, Zhang L, Wang L, Zhang L, Arniego P, Ho KL, Chopp M (2003b) Magnetic resonance imaging and neurosphere therapy of stroke in rat. Ann Neurol 53:259-263.

Zhao C, Deng W, Gage FH (2008) Mechanisms and functional implications of adult neurogenesis. Cell 132:645-660.

Zheng T, Rossignol C, Leibovici A, Anderson KJ, Steindler DA, Weiss MD (2006) Transplantation of multipotent astrocytic stem cells into a rat model of neonatal hypoxic-ischemic encephalopathy. Brain Res 1112:99-105.

Zhu LL, Wu LY, Yew DT, Fan M (2005) Effects of hypoxia on the proliferation and differentiation of NSCs. Mol Neurobiol 31:231-242.